ARABIDOPSIS MUTANTS REVEALING NOVEL ASPECTS OF LEAF MORPHOGENESIS

by

CHOKCHAI KITTIWONGWATTANA

A dissertation submitted to the

Graduate School-New Brunswick

Rutgers, The State University of New Jersey

In partial fulfillment of the requirements

For the degree of

Doctor of Philosophy

Graduate Program in Plant Biology

Written under the direction of

Dr. Randall A. Kerstetter

And approved by

_____

_____

_____

_____

New Brunswick, New Jersey

October, 2010

ABSTRACT OF THE DISSERTATION

Arabidopsis Mutants Revealing Novel Aspects in Leaf Morphogenesis

By CHOKCHAI KITTIWONGWATTANA

Dissertation Director:

Dr. Randall A. Kerstetter

The establishment of dorsoventrality along the adaxial-abaxial axis is considered an early and crucial step of leaf development and proposed as a requirement for subsequent leaf blade expansion. Because photosynthesis mainly takes place in leaves, several key determinants are required to ensure the proper formation of mature leaves. Several efforts have been dedicated to elucidate the regulatory networks controlling leaf morphogenesis. In this thesis, characterization of novel regulators for both leaf polarity establishment and leaf blade expansion is described.

Several Arabidopsis leaf polarity mutants have been identified. However, none of the single, recessive mutants display polarity defects similar to *phantastica (phan)*, the first leaf polarity mutant in *Antirrhinum majus.* Characterization of *filliforme (flr)* indicates that *flr* may be the missing counterpart of *phan*. *flr* exhibited the abaxial features in the radialized organs as well as disturbed shoot apical meristem organization. Gene expression analysis revealed the alteration of expression levels of

several key regulatory genes. Remarkably, *FLR* encodes a plastid membrane protein, underlining the roles of plastids in Arabidopsis growth and development.

***sensitive to red light reduced (srr) 1-2* mutants displayed a narrow-leaf phenotype in addition to defects in light perception and circadian clock regulation. This suggests a connection between leaf blade expansion and the circadian clock. Due to the lack of recognizable functional domains, molecular functions of SRR1 remain unknown. However, genetic interactions between *srr1-2* and translational machinery mutants indicate the involvement of *SRR1* in the translational regulation of leaf morphogenesis.**

Previous studies have demonstrated the importance of a translational regulation during leaf morphogenesis in Arabidopsis. Mutations in several ribosomal protein genes similarly result in a pointed-leaf phenotype. Characterization of *pointed-first-leaves (pfl) 2-2* mutants, in which the ribosomal protein gene *RPS13* is disrupted, revealed perturbation in both adaxial and abaxial mesophyll layers. This mutation in *pfl2-2* also significantly enhanced polarity defects in several leaf polarity mutants. These results suggest that *RPS13* contributes along with other regulatory genes in establishing or maintaining leaf polarity. Together, genetic approaches present in this dissertation expose unexpected contribution of plastids, the circadian clock and translational machineries on leaf morphogenesis.

Acknowledgement

This Ph.D. study is supported by the Ph.D. scholarship of the Thailand Commission on Higher Education.

Dr. Irina Vvedenskaya conducted map-based cloning of the mutation in *flr* and transgenic complementation analysis.

Chokchai Kittiwongwattana performed phenotypic characterization of *flr*, histological studies, *GUS*-reporter gene analysis, AtBT1-RNAi phenotying and gene expression analysis.

Transgenic plants containing p*WUS::GUS* and p*CLV3::GUS* were kindly provided by Dr. Thomus Laux, University of Freiburg, Germany.

Appendix 2 is the manuscript that has been published in Plant Molecular Biology volume 64, page 137-143, February 2007.

Table of Contents

Abstract …… ii

Acknowledgement iv

Lists of Tables …….....……..... viii

Lists of Figures .....…… ix

Introduction .....…… 1

References .....…… 9

Chapter 1. Arabidopsis mutant *filliforme (flr)* suggests an interconnection between leaf polarity, shoot meristem maintenance and plastid functions…… 11

Introduction …….. 11

Results …….. 13

Discussion ……..……..... 33

Materials and Methods……. 38

References …...……... 42

Chapter 2. A novel regulator of leaf blade expansion and its potential connection with the translational regulation in leaf morphogenesis……. 45

Introduction …….. 45

Results …….. 47

Discussion ..……..... 63

Materials and Methods…….... 66

References …..……..... 70

Chapter 3.Ribosomal proteins RPS13 and its role in leaf polarity establishment 71

Introduction …… 71

Results …… 72

Discussion ..…….. 81

Materials and Methods…… 83

References ..……...…… 85

Chapter 4. Research Significance of the Dissertation 87

References 88

Appendices ……...……...……... 89

Introduction ……...…….. 89

Appendix 1 ……..……...……..... 90

Appendix 2 Plastid marker gene excision by the phiC31 phage site-specific recombinase

.....……..…...…… 92

Abstract ...…….. 92

Keywords …….…….... 93

Abbreviations …...…….. 93

Contributions ……...…….. 93

Introduction ……. 94

Materials and Methods…… 97

Results ……. 100

Discussion …..……... 106

Acknowledgment …….…….... 108

References ……...……... 109

Curriculum Vitae ……..... 111

List of Tables

Table A1: Sequences primer used for qRT-PCR analysis …...…… 90

Table A2: Sequences of primers used for plasmid construction ……. 91

Table A3: Sequences of primers used for IPCR and genotyping of *pfl2-2*..... 91

List of Figures

Fig. 1-1 Phenotypic characterization of *flr* 14

Fig. 1-2 Genetic interaction between *flr* and *as1* and *as2* mutants 17

Fig. 1-3 Expression patterns of p*KAN1:GUS* in *flr* 19

Fig. 1-4 Expression of leaf polarity genes in *flr* apices..... 19

Fig. 1-5 Disturbance in meristematic cell characteristics in *flr* apices..... 21

Fig. 1-6 Expression patterns and expression levels of shoot meristem regulatory genes 23

Fig. 1-7 Molecular characterization of *FLR* 25

Fig.1-8 Sugar hypersensitivity in *flr* seedlings and leaf and shoot morphological defects in the AtBT1-RNai No.3 line 28

Fig. 1-9 Environmental effects on *flr* leaf phenotypes 32

Fig. 2-1 Phenotypic characterization of *srr1-2*..... 48

Fig. 2-2 *srr1-2* leaf phenotypes were exacerbated by constant, high-intensity light..... 50

Fig. 2-3 Molecular characterization of *SRR1*..... 53

Fig. 2-4 Expression patterns of circadian clock regulatory genes in *srr1-2* 55

Fig. 2-5 Epistatic interaction of *srr1-2* over *arw1-1*..... 57

Fig. 2-6 Expression patterns of circadian clock regulatory genes in *arw1-1*mutants 58

Fig. 2-7 Synergistic interaction between *srr1-2* and *pfl2-2* 60

Fig. 2-8 Genetic interactions between *srr1-2* and leaf polarity mutants 62

Fig. 2-9 A proposed model of the key determinants of leaf morphogenesis 65

Fig. 3-1 Phenotypic characterization of *pfl2-2* compared to Col wild type 73

Fig.3-2 Isolation of the T-DNA insertion in *pfl2-2* 75

Fig. 3-3 Synergistic interactions between *pfl2-2* and *as1-1* and *as2-1* single mutants 77

Fig. 3-4 Synergistic interaction between *pfl2-2* and *rev* 79

Fig. 3-5 Synergistic interaction between *pfl2-2* single and *kan1 kan2* double mutants 80

Fig. 4-1 The proposed model of the regulatory network controlling leaf morphogenesis..... 88

Fig. A2-1 Plastid vectors pPRV111A*att* and pPRV111B*att* 100

Fig. A2-2 Plastid DNA maps to show Int-mediated marker excision..... 101

Fig. A2-3 DNA gel blot analyses to detect Int-mediated *aadA* excision in Nt-pCK2 plants..... 102

Fig. A2-4 Phenotypes of wild type, Nt-pCK2, and *aadA*-free Nt-pCK2-Int plants 104

Introduction

Leaf polarity establishments and its effects on leaf anatomical structures

Leaf primodia are initiated at the flanks of the shoot apical meristem. During the early stage, leaf patterning occurs along the pre-determined adaxial (dorsal)- abaxial (ventral) axis. {for review see [19]}. This developmental process largely contributes to proper morphological and anatomical structures of the mature leaf. The adaxial mesophyll layer is mainly composed of tightly packed palisade cells that promote light harvesting and photosynthesis. The abaxial mesophyll layer contains loosely packed spongy cells and is associated with large intercellular spaces that promote gas exchange. This difference leads to the appearance of the dark-green adaxial and light-green abaxial surfaces. As the vascular system is formed, xylem, water and soluble mineral transporting tissues, is located toward the adaxial side, whereas phloem, organic nutrient transporting tissues, is positioned toward the abaxial side. While leaves develop, proper leaf polarity must be established, maintained and propagated. This process is controlled by several regulatory genes.

Transcriptional regulation of leaf polarity establishment

The majority of leaf regulatory genes promoting dorsoventrality are transcription factors. *PHANTASTICA (PHAN)* was the first leaf polarity gene isolated from *A. majus* [23]. Single, recessive mutations in *PHAN* result in different degrees of defects in leaf morphogenesis. Cotyledons and the first three pairs of leaves are wider and adopt the heart shape as opposed to narrower, elliptic wild-type leaves. On the higher nodes, lateral

organs with proximal radialization and distal narrow leaf blades are produced. The most severe leaf phenotype of *phan* is the formation of radialized leaves displaying abaxial features, indicating its function in the determination of adaxial cell identity. The mutation in *PHAN* also increases the low-temperature hypersensitivity regarding leaf morphogenesis. When mutants are grown under low-temperature conditions, almost all of lateral organs are produced in the radialized form [23]. Cloning of the *PHAN* gene has shown that the encoded protein contains a myb domain [24]. Because *PHAN* is uniformly expressed in organ primordia, its function in the determination of adaxialization may depend on additional regulators [24].

In Arabidopsis, various regulators for leaf polarity have been extensively studied. Class III homeodomain-leucine zipper (HD-ZIP III) transcription factors, containing a conserved leucin-zipper domain, have been previously demonstrated to function in adaxialization of leaf primordia. These include PHABULOSA (PHB), PHAVOLUTA (PHV), REVOLUTA (REV) and CORONA (CNA) [3]. Consistent with their functions is restrictive expression of these regulators in leaf adaxial domains and shoot apical meristems [3, 13]. Due to the genetic redundancy among the members of the HD-ZIP III family, *phb* and *phv* single mutants are aphenotypic, whereas *rev* single mutants only display dramatic defects in floral meristems [3, 16, 20]. However, a dramatic loss of leaf polarity establishment has been observed in gain-of-function and combinatorial mutants [3, 12, 13, 16]. *phb phv rev* and *phb rev can* triple mutants produce radialized apical structures with abaxial features and fail to form the shoot apical meristem [3, 16]. Consistent with the gene function in adaxialization, the gain-of-function *phb-1d* allele

displays adaxial features on its radialized organs as well as the formation of ectopic meristem on the lower side of the leaves [12, 13].

Other transcription factors specifying adaxialization in Arabidopsis are *ASYMMETRIC LEAVES (AS) 1* and *AS2*. *AS1* encodes a myb-domain containing protein that is an Arabidopsis homolog of PHAN [2]. Mutations in *AS1* result in the formation of triangular-shaped, lobed, asymmetric leaves with downward-curling edges and a wavy surface [2]. *AS2* encodes a protein member of the LATERAL ORGAN BOUNDARIES (LOB) family [10]. Leaf phenotypes of *as2* are similar to those of *as1* mutants, but a unique formation of leaflet-like structures on the petioles has been observed only in *as2* mutants [17]. Furthermore, over-expression of *AS1* and *AS2* results in very distinctive phenotypes. Leaves of *AS2*-overexpressing plants are narrow and display adaxial features on the abaxial domain, whereas *AS1*-overexpressing plants only exhibits a reduced stature [28]. However, a direct protein-protein interaction between AS1 and AS2 protein indicates that both genes may function in the same pathway and are required for the determination of adaxial cell fates [28]. Molecular functions of *AS1* and *AS2* have also been implicated in rosette leaves to suppress expression of class I *KNOX* genes, involved in shoot apical meristem maintenance [2, 17].

The *KANADI* (*KAN*) gene family is responsible for promoting abaxialization [8, 14, 18]. Members of this gene family encode transcription factors containing a MYB-like GARP DNA-binding domain [7]. Similar to *HD-ZIP III* genes, *KAN* genes display genetic redundancy regarding their functions in leaf polarity establishment. A mutation in *KAN1* only results in mild leaf polarity [8]. Leaf blades of the first leaf pair curl upward and adopt the cup shape. The abaxial paradermal layer exhibits adaxial characteristics.

Abaxial trichomes increase in number and appear early in the second leaf pair as opposed to the third leaf pair in wild type. Similarly, leaves produce in wild type and *kan2* single mutants are alike [4]. However, leaf polarity defects are dramatically enhanced in higher-order mutants. *kan1 kan2* double mutants produce narrow, pointed leaves with ectopic abaxial outgrowths, whereas *kan1 kan2 kan3* triple mutant display radialized leaves and the absence of the abaxial outgrowths [5]. Consistent with their functions, expression of *KAN* genes is found restricted on the abaxial domain [5, 8].

AUXIN RESPONSE FACTORs (ARF) have previously been shown to be involved in abaxialization [14]. These transcription factors regulate plant responses to the phytohormone auxin [7]. Mutations in *ETTIN (ETT)/ARF3* result in adaxialization in epidermal cells of petals. Remarkably, *ARF* genes have been proposed to act downstream of *KAN* genes, due to the partial rescue of leaf defects in *KAN2*- overexpressing mutants by a mutation in *ETT/ARF3.* Functions of *ARF* genes may also overlap with those of *KAN* genes [14]. Similar to *kan1 kan2* double mutants, ectopic outgrowths are found on the abaxial sides of *ett arf4* double mutant leaves as well. Additionally, expression patterns of *ETT/ARF3* and *ARF4* are not altered in leaf primordia of *kan1 kan2* double mutants [14]. These observations indicate the discrepancy between interactions of *ARF* and *KAN* with other regulators in leaf polarity establishment.

Another group of transcription factors contributing to abaxialization is *YABBY (YAB)* [18]. *FILAMENTOUS FLOWER (FIL)* and *YAB3* are example of genes belonging to the *YAB* family. Due to this genetic redundancy, single mutants including *fil* and *yab3* only display phenotypes comparable to wild type [18]. However, a leaf polarity defect has been observed in *fil yab3* mutants [18]. Some abaxial epidermal cells of double

mutant leaves resemble those on the adaxial domain, indicating partial loss of leaf abaxial identity. *YAB* functions in abaxialization is linked to those of *KAN* genes. Ectopic expression of *KAN2* results in the uniform expression of *FIL* in leaf primordia [5]. Additionally, mutations in *YAB* genes enhance leaf morphological and polarity defects of *kan1 kan2* double mutants [5]. The first two leaves of *kan1 kan2 fil yab3* quadruple mutants appear radialized, and cells of the paradermal layers of subsequent leaves are uniformly adaxialized. Ectopic abaxial outgrowths also vanished in the quadruple mutants. Consistently, expression of *YAB* genes is found exclusively on the abaxial domain of leaf primordia of quadruple mutants [18].

The designation of boundaries between adaxial and abaxial domains has been largely attributed to antagonistic interactions of these regulatory transcription factors [7]. Expression of *PHV* and *REV* genes is restricted in the adaxial domain of wild-type leaf primordia but, in *kan1 kan2* double mutants, expands into the abaxial domain as well [4]. Additionally, a recent study has demonstrated KAN1 is able to directly suppress expression of the *AS2* gene on the abaxial domain, and AS2 is a potential suppressor of *KAN1* in the adaxial domain [27].

Regulations of leaf polarity beyond the transcriptional level

While most of the aforementioned key regulators are transcription factors, several lines of evidence have shown that the regulation of leaf polarity establishment also occurs at other different levels. Previous studies have demonstrated the roles of small RNA as adaxial and abaxial determinants. Trans-acting short-interfering RNA (tasiRNA) *tasiR-ARF* has been shown to target *ETT/ARF3* and *ARF4* transcripts for cleavage suggesting its involvement in adaxialization in leaf primordia [1]. Additionally, mutations in an

ARGONAUTE gene required for the production and/or stability of *tasiR-ARF* result in the up-regulation of *ETT/ARF3* and *ARF4* [6].

Abaxially expressed miRNA *miR165/166* targets transcripts of HD-ZIPIII transcription factors for cleavage, eliminating the generation of adaxial identity in the abaxial domain [11]. A dominant, gain-of-function allele of *phb* containing a mutation that alters the *miR165/166* complementary side exhibits the uniform expression of *PHB* in organ primordia [13]. Conversely, overexpression of *miR166* down-regulate the expression levels of *PHB* and *REV* in lateral organs [26].

At the translational level, two studies have recently demonstrated the contribution of ribosomal proteins toward leaf polarity establishment. Mutations in *RPL10, RPL5A, RPL24,* and *RPL28A* commonly result in a pointed leaf phenotype and are able to enhance leaf polarity defects in *as1, as2, rev* single, and *kan1 kan2* double mutants [15, 29]. These interactions indicate that translational regulation is important for leaf polarity.

The regulation of leaf polarity is also present at the post-translational stage mediated by LITTLE ZIPPER (ZPR) [9, 25]. *ZPR* genes encode small proteins containing a leucine-zipper domain that is similar to those specifically found on the HD-ZIP III transcription factors [25]. Based on an *in vitro* and a yeast-two-hybrid assay, ZPR is proposed to bind to HD-ZIP III transcription factors through this domain [9, 25]. This protein-protein interaction would in turn inhibit the dimerization of HD-ZIP III transcription factors that is required for their DNA binding activities and adaxialization signaling [9, 25]. Consistently, overexpression of *ZPR3* results in the formation of radialized organs displaying abaxial features [25]. Remarkably, the expression level of *ZPR3* is elevated by ectopic expression of *REV,* and its adaxially expression pattern also

coincides with *HD-ZIP III* [25]. This suggests the potential feedback regulation between *ZPR* and *HD-ZIP III* [25].

Leaf blade expansion and various regulatory genes

In addition to proper anatomical structures of leaves, the photosynthetic capacity of plants depends largely on the maximization of leaf blade area. Leaf blades expand along the width and length axes, and this developmental process has been proposed to depend on the establishment of adaxial-abaxial leaf polarity [23]. Several leaf polarity mutants including *kan1 kan2 kan3* triple, *phb1-D* and *jba1-D* single mutants produce radialized organs with a complete loss of leaf dorsoventrality and leaf blade expansion, suggesting an intimate link between the two developmental processes [5, 12]. Despite this relationship, whether proper establishment of leaf polarity could solely drive leaf blade expansion still remains unclear.

Defects in leaf blade expansion have been previously recognized in a few Arabidopsis mutants. *angustifolia (an),* in which a gene encoding a homolog of a human carboxy-terminal binding protein (CtBP) is mutated, produces leaves displaying a decrease in blade expansion along the width axis [21]. In contrast, mutations in *ROTUNDIFOLIA (ROT) 3,* encoding a cytochrome P450, result in a reduction in leaf blade expansion along the length axis [21]. Additionally, a reduction of leaf width has been shown to associate with mutations in the *PHYTOCHROME B* gene that mediates red light perception [22]. The presence of these mutants suggests that multiple genes are required for determining the proper shape of Arabidopsis leaves.

The following chapters in this dissertation focus on Arabidopsis mutants that displayed defects in leaf morphogenesis. These include *filliforme (flr), sensitive to red*

light reduced (srr) 1-2 and *pointed first leave (pfl) 2-2. FLR* is potentially required for leaf polarity establishment, whereas *SRR1* contributes to blade growth expansion along the width axis. Genetically, *pfl2-2,* where the ribosomal protein gene *RPS13* is disrupted, interacts with both leaf polarity mutants and *srr1-2.* This indicates that perturbing the translation machinery has a broad-range of effects in these two related developmental processes. Altogether, this study provides novel insights that advance our understanding of the complex regulatory network that determines proper leaf morphology.

References

1. Allen E, Xie Z, Gustafson AM, Carrington JC: microRNA-directed phasing during trans-acting siRNA biogenesis in plants. Cell 121: 207-21 (2005).
2. Byrne ME, Barley R, Curtis M, Arroyo JM, Dunham M, Hudson A, Martienssen RA: Asymmetric leaves1 mediates leaf patterning and stem cell function in Arabidopsis. Nature 408: 967-71 (2000).
3. Emery JF, Floyd SK, Alvarez J, Eshed Y, Hawker NP, Izhaki A, Baum SF, Bowman JL: Radial patterning of Arabidopsis shoots by class III HD-ZIP and KANADI genes. Curr Biol 13: 1768-74 (2003).
4. Eshed Y, Baum SF, Perea JV, Bowman JL: Establishment of polarity in lateral organs of plants. Curr Biol 11: 1251-60 (2001).
5. Eshed Y, Izhaki A, Baum SF, Floyd SK, Bowman JL: Asymmetric leaf development and blade expansion in Arabidopsis are mediated by KANADI and YABBY activities. Development 131: 2997-3006 (2004).
6. Hunter C, Willmann MR, Wu G, Yoshikawa M, de la Luz Gutierrez-Nava M, Poethig SR: Trans-acting siRNA-mediated repression of ETTIN and ARF4 regulates heteroblasty in Arabidopsis. Development 133: 2973-81 (2006).
7. Husbands AY, Chitwood DH, Plavskin Y, Timmermans MC: Signals and prepatterns: new insights into organ polarity in plants. Genes Dev 23: 1986-97 (2009).
8. Kerstetter RA, Bollman K, Taylor RA, Bomblies K, Poethig RS: KANADI regulates organ polarity in Arabidopsis. Nature 411: 706-9 (2001).
9. Kim YS, Kim SG, Lee M, Lee I, Park HY, Seo PJ, Jung JH, Kwon EJ, Suh SW, Paek KH, Park CM: HD-ZIP III activity is modulated by competitive inhibitors via a feedback loop in Arabidopsis shoot apical meristem development. Plant Cell 20: 920-33 (2008).
10. Lin WC, Shuai B, Springer PS: The Arabidopsis LATERAL ORGAN BOUNDARIES-domain gene ASYMMETRIC LEAVES2 functions in the repression of KNOX gene expression and in adaxial-abaxial patterning. Plant Cell 15: 2241-52 (2003).
11. Mallory AC, Reinhart BJ, Jones-Rhoades MW, Tang G, Zamore PD, Barton MK, Bartel DP: MicroRNA control of PHABULOSA in leaf development: importance of pairing to the microRNA 5' region. Embo J 23: 3356-64 (2004).
12. McConnell JR, Barton MK: Leaf polarity and meristem formation in Arabidopsis. Development 125: 2935-42 (1998).
13. McConnell JR, Emery J, Eshed Y, Bao N, Bowman J, Barton MK: Role of PHABULOSA and PHAVOLUTA in determining radial patterning in shoots. Nature 411: 709-13 (2001).
14. Pekker I, Alvarez JP, Eshed Y: Auxin response factors mediate Arabidopsis organ asymmetry via modulation of KANADI activity. Plant Cell 17: 2899-910 (2005).
15. Pinon V, Etchells JP, Rossignol P, Collier SA, Arroyo JM, Martienssen RA, Byrne ME: Three PIGGYBACK genes that specifically influence leaf patterning encode ribosomal proteins. Development 135: 1315-24 (2008).
16. Prigge MJ, Otsuga D, Alonso JM, Ecker JR, Drews GN, Clark SE: Class III homeodomain-leucine zipper gene family members have overlapping,

antagonistic, and distinct roles in Arabidopsis development. Plant Cell 17: 61-76 (2005).
17. Semiarti E, Ueno Y, Tsukaya H, Iwakawa H, Machida C, Machida Y: The ASYMMETRIC LEAVES2 gene of Arabidopsis thaliana regulates formation of a symmetric lamina, establishment of venation and repression of meristem-related homeobox genes in leaves. Development 128: 1771-83 (2001).
18. Siegfried KR, Eshed Y, Baum SF, Otsuga D, Drews GN, Bowman JL: Members of the YABBY gene family specify abaxial cell fate in Arabidopsis. Development 126: 4117-28 (1999).
19. Steeves RA, Sussex IM: Organogenesis in the shoot: later stages of leaf development. In: Steeves RA, Sussex IM (eds) Patterns in Plant Development, pp. 147-175. Cambridge University Press, New York (1989).
20. Talbert PB, Adler HT, Parks DW, Comai L: The REVOLUTA gene is necessary for apical meristem development and for limiting cell divisions in the leaves and stems of Arabidopsis thaliana. Development 121: 2723-35 (1995).
21. Tsuge T, Tsukaya H, Uchimiya H: Two independent and polarized processes of cell elongation regulate leaf blade expansion in Arabidopsis thaliana (L.) Heynh. Development 122: 1589-600 (1996).
22. Tsukaya H, Kozuka T, Kim GT: Genetic control of petiole length in Arabidopsis thaliana. Plant Cell Physiol 43: 1221-8 (2002).
23. Waites R, Hudson A: *phantastica*: a gene required for dorsoventrality of leaves in *Antirrhinum majus*. Development 121: 2143-2154 (1995).
24. Waites R, Selvadurai HR, Oliver IR, Hudson A: The PHANTASTICA gene encodes a MYB transcription factor involved in growth and dorsoventrality of lateral organs in Antirrhinum. Cell 93: 779-89 (1998).
25. Wenkel S, Emery J, Hou BH, Evans MM, Barton MK: A feedback regulatory module formed by LITTLE ZIPPER and HD-ZIPIII genes. Plant Cell 19: 3379-90 (2007).
26. Williams L, Grigg SP, Xie M, Christensen S, Fletcher JC: Regulation of Arabidopsis shoot apical meristem and lateral organ formation by microRNA miR166g and its AtHD-ZIP target genes. Development 132: 3657-68 (2005).
27. Wu G, Lin WC, Huang T, Poethig RS, Springer PS, Kerstetter RA: KANADI1 regulates adaxial-abaxial polarity in Arabidopsis by directly repressing the transcription of ASYMMETRIC LEAVES2. Proc Natl Acad Sci U S A 105: 16392-7 (2008).
28. Xu L, Xu Y, Dong A, Sun Y, Pi L, Huang H: Novel as1 and as2 defects in leaf adaxial-abaxial polarity reveal the requirement for ASYMMETRIC LEAVES1 and 2 and ERECTA functions in specifying leaf adaxial identity. Development 130: 4097-107 (2003).
29. Yao Y, Ling Q, Wang H, Huang H: Ribosomal proteins promote leaf adaxial identity. Development 135: 1325-34 (2008).

Chapter1

Arabidopsis mutant *filliforme (flr)* suggests an interconnection between leaf polarity, shoot meristem maintenance and plastid functions.

Introduction

Establishment of leaf polarity along the adaxial (dorsal)- abaxial (ventral) axis leads to anatomical distinctions between the adaxial and abaxial leaf domains. One of the early discoveries in leaf polarity was the isolation of the *PHANTASTICA (PHAN)* gene from *Antirrhinum majus* [36]. Single, recessive mutations in *PHAN* result in various forms of leaf defects including an alteration in the leaf shape, a reduction in leaf blade expansion and the formation of radialized leaves displaying abaxial features, suggesting it functions in the determination of adaxial cell identity [36]. Additionally, leaf polarity defects of *phan* mutants are enhanced by low-temperature conditions [36]. To our knowledge, there is no single, recessive Arabidopsis mutant displaying phenotypes equivalent to *PHAN.* Although AS1 is the Arabidopsis ortholog of PHAN, *as1* mutants only exhibit a mild leaf polarity defect in the petioles [4]. This discrepancy between *as1* and *phan* indicates that an additional piece in the regulatory network of Arabidopsis leaf polarity remains undiscovered. In this chapter, data obtained from the study of the Arabidopsis mutant *filliforme (flr)* is described. Phenotypic characterization of the mutants revealed the formation of radialized structures displaying abaxial identity. Other defects in leaf morphogenesis of *flr* were also observed. When the mutants were grown under low-temperature conditions, the mutant leaf polarity defects were increased.

Remarkably, *flr* characteristics are similar to *phan.* Additionally, as *flr* seedlings developed, they showed disturbance in shoot apical meristem organization and stem fasciation. These defects during the vegetative state were associated with alterations in expression of known regulatory genes. Furthermore, the severity of mutant leaf phenotypes was modified by various light intensities and day-lengths suggesting an influence of environmental signals over leaf morphogenesis. Map-based cloning revealed a base transition in the first exon of At4g32400, previously described as a plastid adenine-nucleotide uniporter Arabidopsis BRITTLE (AtBT) 1 [17]. Together, this study of *flr* emphasizes the role of plastids in plant growth and development.

Results

flr exhibited severe leaf polarity defects

An *flr* mutant line was obtained from the Arabidopsis Stock Center (www.arabidopsis.org). The mutant was previously recognized by the formation of needle-shaped structures and the conical-shaped first two leaves [33]. Further characterization of the mutant was carried out in this study. *flr* exhibited a growth delay compared to Enkheim-2 (En-2) wild type (Fig. 1-1A-B). Variation in leaf morphological defects was observed among mutant individuals. The first pair of leaves often appeared rounded and occasionally adopted a triangular shape (Fig. 1-1B). Subsequent leaves displayed a wide range of leaf malformation including narrow leaves, pointed tips, abaxial outgrowths and asymmetric leaf blades (Fig. 1-1E-F). In contrast, all wild-type leaves were well-expanded, round to elliptical and symmetric (Fig. 1-1C-D). However, the most recognizable phenotype observed in all mutants was the formation of radially symmetric, needle-like organs (Fig. 1-1G). Wild-type and *flr* non-radialized leaves formed xylem adaxial to phloem in the midvein (Fig. 1-1H-I). In contrast, the vascular systems in the midvein of *flr* radialized organs were composed of xylem surrounded by phloem (Fig. 1-1J). To examine the inheritance of the mutation, *flr* was test-crossed with wild type. The segregation of wild type and mutant plants in the F2 population was close to the 3:1 ratio. This suggests the mutation was transmitted as a single, recessive locus. These results displayed the resemblance between *flr* and *phan* including the single-recessive inheritance, a variety of leaf malformation and the formation of radialized leaves displaying abaxial features.[36].

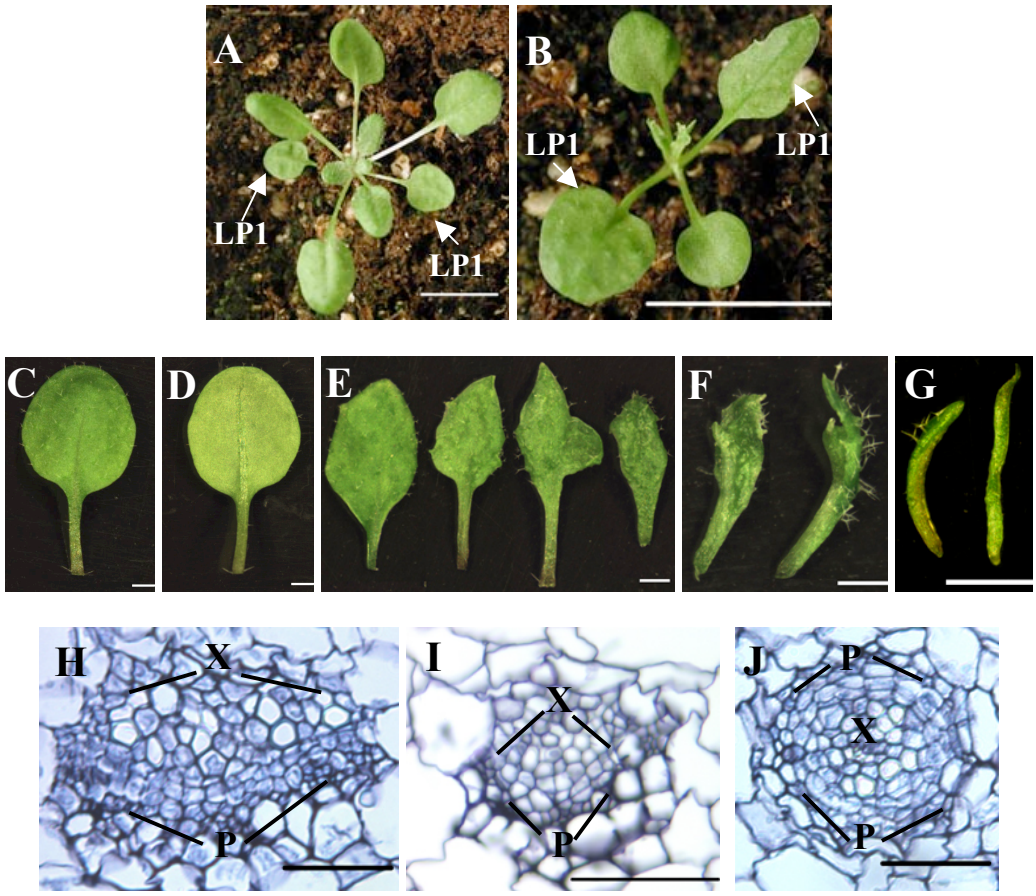

Fig. 1-1 Phenotypic characterization of *flr*. (A) Wild type En-2 and (B) *flr* seedlings 26 day-after-germination. Leaf 3 and 4 of wild-type (C-D) were rounded and well-expanded with dark green on the adaxial side (C) and light green on the abaxial side (D). Various types of leaf morphological defects were observed in leaf 3 and 4 of *flr* individuals including pointed tips, narrow leaves, asymmetry (E) and ectopic abaxial outgrowths (F). All *flr* mutants displayed the formation of radialized leaves (G) that could be observed as early as at the third leaf pair. The midvein in the middle part of the leaves was examined. Midvein of wild type (H) and *flr* (I) first two leaves contained xylem forming adaxial to phloem, whereas the midvein of *flr* radialized organs (J) displayed xylem surrounded by phloem. (Bars in A-B = 1 cm; Bars in C- G =1 mm; Bars in H-J = 0.5μm) (LP1= first leaf pair, X= xylem, P= phloem)

Synergistic interactions between *flr* and *as1* and *as2* single mutants

AS1 and *AS2* have previously been demonstrated to interact with each other and form a protein complex that potentially promotes adaxial cell identity [39]. Since *FLR* was required for leaf adaxialization, a genetic study was performed to investigate the genetic relationships between *flr* and *as1* and *as2*. Leaf morphological defects were analyzed in *flr as1-1* and *flr as2-1* double mutants. The single mutants were crossed, and double mutants were analyzed in the F3 generation obtained from *as1-1* and *as2-1* F2 plants segregating for the *flr* mutation. *as1-1* and *as2-1* single mutants have previously been reported to exhibit similar leaf phenotypes (Fig.1-2A and E) [4, 32]. These include the formation of triangular-shaped, lobed, asymmetric leaves with the wavy surface [4, 32]. Nonetheless, the formation of leaflet-like structures on the petioles was described only in *as2-1* [32]. Additionally, as shown in Fig. 1-2A and E, the distinction between leaf blades and petioles was relatively more prominent in *as2-1* than in *as1-1*.

In combinatorial *flr as1-1* and *flr as2-1* double mutants, leaf morphological defects appeared early in the first leaf pair (LP1) and generally resulted in the formation of narrow leaves. The most severe forms of *flr as1-1* and *flr as2-1* double mutants wereshown in Fig. 1-2B and F, respectively. Unlike expanded first leaf pairs of parental mutants, the first two leaves of *flr as1-1* displayed an extreme reduction in leaf blade expansion and pointed tips (Fig. 1-2B). Similarly, the first leaf pair of *flr as2-1* was extremely narrow with the proximal portion displaying a small degree of expansion (Fig. 1-2F). The variation among double mutants may be the effect of the *flr* mutant background that also occasionally exhibited the conical shape in this leaf pair (Fig. 1-1B).

Despite the production of extremely narrow leaves in *flr* single mutants, this phenotype only appeared in leaf 3 and 4 (Fig. 1-1E).

To examine the vascular systems in the midvein, the first leaf pairs of single and double mutant were cross-sectioned. In the midvein of the first two leaves of *flr, as1-1* and *as2-1* single mutants, the vasculature system was composed of xylem appearing adaxial to phloem (Fig. 1-1I, 1-2C and G). In contrast, the midvein of the first two leaves of *flr as1-1* and *flr as2-1* double mutants contained only a group of small cells. These cells were squamous-shaped resembling phloem as opposed to the polygonal shapes of cells in xylem, indicating the increased degree in abaxialization (Fig. 1-2D and H). The synergistic interactions in the double mutants suggest the interacting, independent pathways of *FLR* and *AS1* and *AS2*.

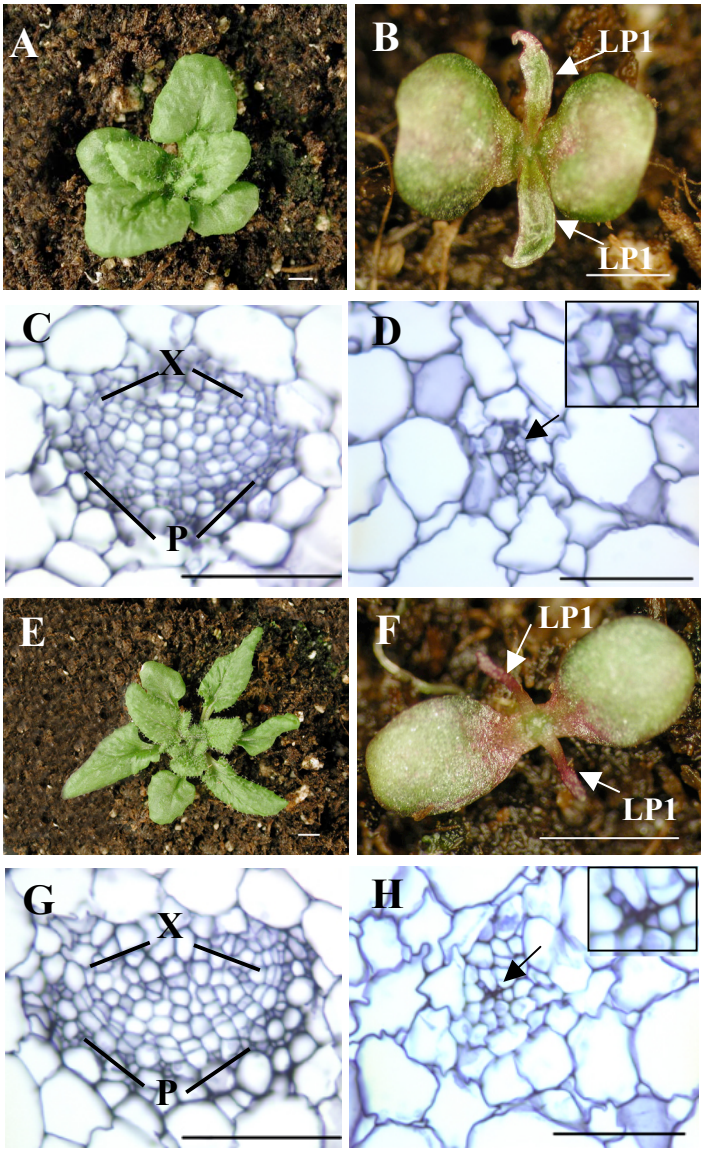

Fig. 1-2 Genetic interaction between *flr* and *as1* and *as2* mutants. *as1-1* (A) and *as2-1* (E) single mutants exhibited wavy-surfaced, triangular-shaped, lobed, asymmetric leaves. Leaf morphological defects of *flr* were dramatically enhanced in *flr as1-1* (B) and *flr as2-1* (F) double mutants as demonstrated by the early formation of extremely narrow first two leaves. The midvein of the first two leaves of *as1-1* (C) and *as2-1* (G) single mutants contained xylem positioned adaxial to phloem. Leaves of *flr as1-1* (D) and *flr as2-1* (H) double mutants displayed the formation of small, differentiated cells resembling phloem in the midveins (arrows). Insets showed the magnified views of double mutant midveins. (Bars in A, B, E, and F = 2mm; Bars in C, D, G, H, and I = 0.5μm) (LP1= first leaf pair, X = xylem, P = phloem)

Expression of leaf polarity genes in *flr* mutants

A number of leaf polarity mutants display changes in the expression patterns of genes that regulate adaxial or abaxial cell fate. For example, *AS2* expression is restricted to the adaxial domain in wild type and expands throughout leaf primordia in *kan1 kan2* double mutants [38]. Conversely, *KAN1* expression, normally exclusive to the abaxial side, expands into the adaxial side in *as2-1* single mutants [38]. To examine the *KAN1* expression pattern in *flr,* a GUS reporter gene fused to the *KAN1* promoter (p*KAN1:GUS*) was genetically introduced into the *flr* mutant. At 3 and 5 day-after-germination, abaxial expression of p*KAN1:GUS* in the *flr* background were not significantly different from those observed in wild type (Fig. 1-3A-D). The relatively high intensity of the blue precipitate in *flr* primordia 3-day-after-germination may result from the growth delay in *flr* leading to a higher cell density than wild type. Additionally, quantitative reverse-transcription-PCR (qRT-PCR) was performed to determine expression levels of several key determinants of leaf polarity in wild-type and *flr* apices at 4 day-after-germination. These included abaxial markers *KAN1, KAN2, YAB2, YAB3, ARF3,* and *ARF4* and adaxial markers *AS1, AS2, PHB, PHV,* and *REV* (Fig. 1-4A-B). Consistent with the GUS expression analysis, the expression level of *KAN1* in *flr* was unchanged compared to wild type (Fig. 4A). This was also reflected on expression of *AS2* that is negatively controlled by *KAN1*. As shown in Fig. 1-4B, *AS2* expression levels were not significantly different between wild type and *flr*. The same trends were found in *YAB2, YAB3, ARF3, ARF4,* and *PHV*. However, consistent with the abaxialization phenotype in *flr*, *KAN2,* promoting abaxialization, was up-regulated, whereas *AS1, PHB and REV*, promoting adaxialization, were down-regulated in mutant apices. These results suggest the alteration of the

expression levels in *KAN2, AS1, PHB* and *PHV* may be the early cause of abaxialization in *flr*.

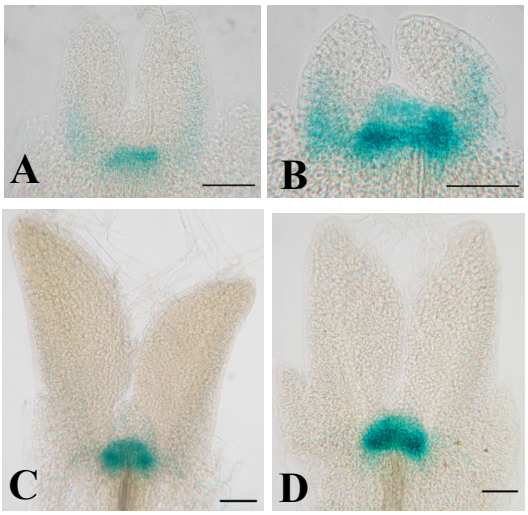

Fig. 1-3 Expression patterns of p*KAN1:GUS* in *flr* leaf primordia. Expression patterns of *pKAN1::GUS* were similar in 3-DAG wild type (A) and *flr* (B), despite the higher intensity of blue precipitate in mutants (see text). The expression patterns also remained similar in 5-DAG wild type (C) and *flr* (D). (Bars = 0.5μm)

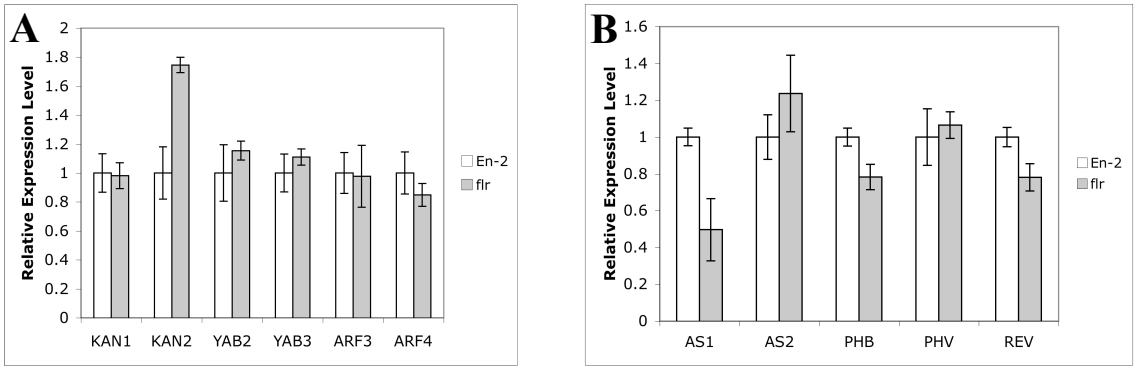

Fig. 1-4 Expression levels of leaf polarity genes in *flr* apices. Relative expression levels of abaxialization (A) and adaxialization (B) genes in wild-type (white bars) and *flr* (grey bars) apices were quantified by using qRT-PCR. Expression of *ACTIN2* was used for normalization.

Disturbance of meristematic cell organization in *flr* apices

Several previous studies have shown the close relationship between leaf polarity and shoot apical meristems [15, 25, 27, 35]. Separation of young leaf primorida from the connected shoot apical meristem results in the formation of abaxialized radialized organs [27, 35]. The loss of shoot apical meristem formation has also been shown in *phb phv rev* triple mutants and *KAN1*-overexpressing plants [15, 25]. Consistently, a disturbance in shoot apical meristems was observed in *flr* apices. At 18 days-after-germination, *flr* seedlings exhibited enlarged apices (Fig. 1-5A-B). Longitudinal sectioning of wild-type and *flr* seedlings at this stage revealed that mutant primary apices were indeed enlarged, compared to wild-type (Fig. 1-5C-D). At this stage, mutant primary apices lost the apical dominance as indicated by the early formation of axillary buds (Fig. 1-5C-D). The organization of the L2 and L3 layers in the primary apices was also affected in *flr*, compared to wild type. As shown in Fig 1-5E, the distinction of the L2 and L3 layers was clear in wild type apices. This distinction was distorted in *flr* as indicated by the loss of consistency of the layers from the central to peripheral portions. This distortion suggests perturbation in planes of cell division (Fig. 1-5E-F). Additionally, while wild-type meristematic cells were uniform, small and dark-toluidine-blue-stained, *flr* primary meristems contained irregular-shaped, enlarged, light-toluidine-blue-stained cells (Fig. 1-5E-F). These changes reflected the disturbance in meristematic cell characteristics. The enlargement of the primary shoot meristem in *flr* also resulted in the stem fasciation, the formation of horizontally enlarged, flattened, ribbon-like stems, whereas wild-type stems were round and radially symmetric (Fig. 1-5G-H). Remarkably, mutant axillary buds were typically unaffected and produced only normal fluorescence stems

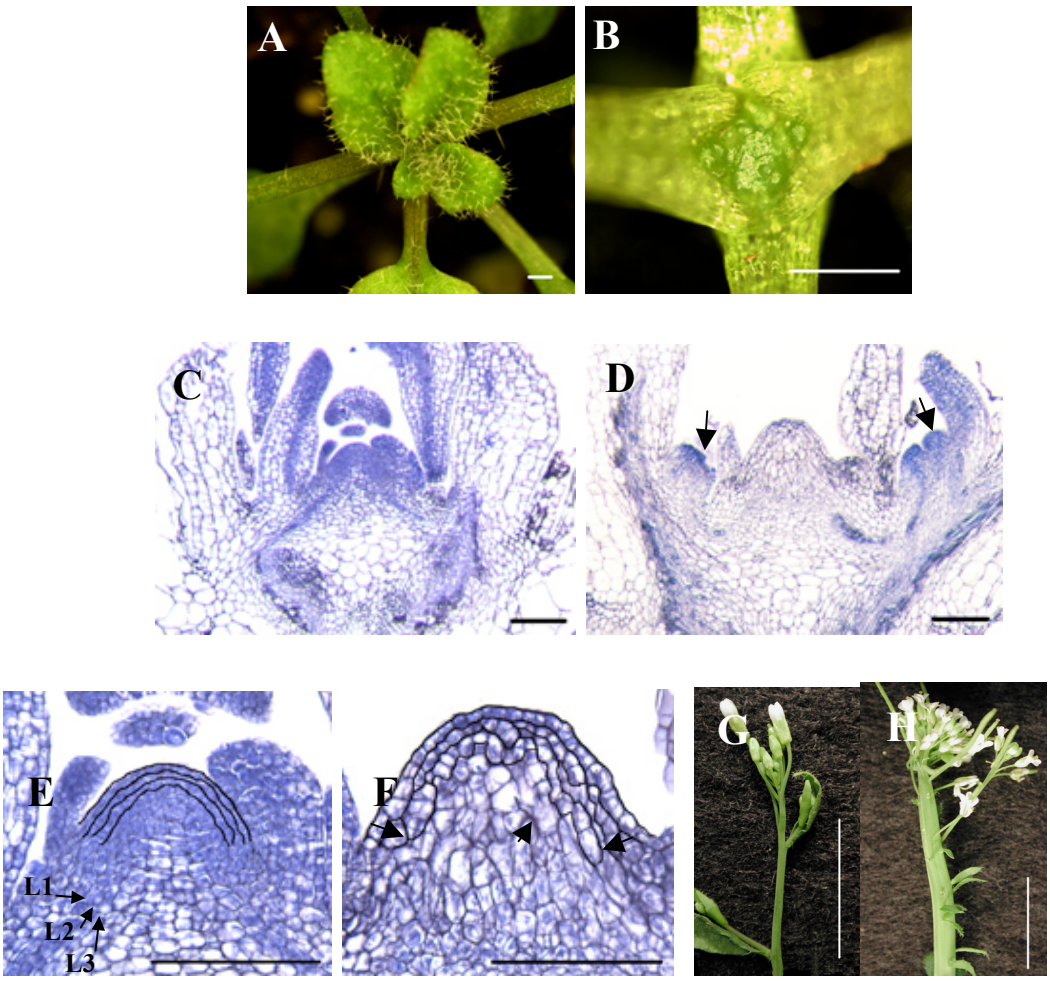

Fig. 1-5 Disturbance in meristematic cell characteristics in *flr* apices. At 18 day-after-germination, wild-type apices (A) produced several rosette leaves, whereas *flr* apices (B) became enlarged. Longitudinal sections of 18-day-after-germination seedlings wild type (C) and *flr* (D) apices. The early formation of axillary buds (arrows) was also observed in *flr* (D). Wild-type primary meristems (E) displayed normal meristematic cell characteristics and cell division planes. *flr* primary meristems (F) contained disturbed meristematic cells and exhibited distorted cell division planes in the L2 and L3 layers (arrows). Radially symmetric inflorescence stems were observed in wild type (G), while *flr* primary inflorescence stems (H) displayed fasciation (Bars in A-B = 5mm; Bars in C-F= 1 μm; Bars in G and H= 1cm)

A number of regulatory genes are required for the maintenance of meristematic activities. In wild type shoots, *CLAVATA (CLV) 3* is expressed in the stem cells, while *WUSCHEL (WUS)* expression is confined to the central domain underlying the stem cell region [10, 24]. *WUS* induces expression of *CLV3* in stem cells and promote stem cell formation, while proteins encoded by *CLV3* are transported to the central domain triggering the inhibition of *WUS* expression [3, 31]. This negative regulatory feedback loop confers and controls the size of the stem cell niche in the shoot meristem. On the other hand, class I *KNOX* gene family is expressed throughout the meristem and required for meristem initiation and maintenance [2, 13]. For example, a mutation in *SHOOTMERISTEMLESS*, a member of class I *KNOX,* result in the absence of the shoot apical meristem in mutant seedlings [2, 9]. Due to the presence of the shoot meristem defects in *flr,* the expression of *CLV3* and *WUS* were examined using the *GUS* reporter lines p*CLV3:GUS* and p*WUS:GUS.* The expression domains of *CLV3* and *WUS* in *flr* primary meristems were not significantly perturbed compared to those of wild type (Fig 1-6A-D). Expression of p*CLV3:GUS* and p*WUS:GUS* was also found in the early-formed axillary buds of the mutants (Fig. 6B and E). Additionally, the expression levels of *WUS, CLV3,* and class I *KNOX,* including *STM, KNAT1* and *KNAT2,* in wild-type and mutant apices were determined by qRT-PCR (Fig. 1-6F). *CLV3* and class I *KNOX* genes in wild type and *flr* were expressed at similar levels. Remarkably, expression of *WUS* in mutant apices was significantly lower than in wild type. *WUS* has previously been shown to be a positive regulator of stem cell identity, and *wus* mutants display the failure of shoot apical meristem organization [20]. *flr* meristem defects may be attributed to a reduction of *WUS* expression.

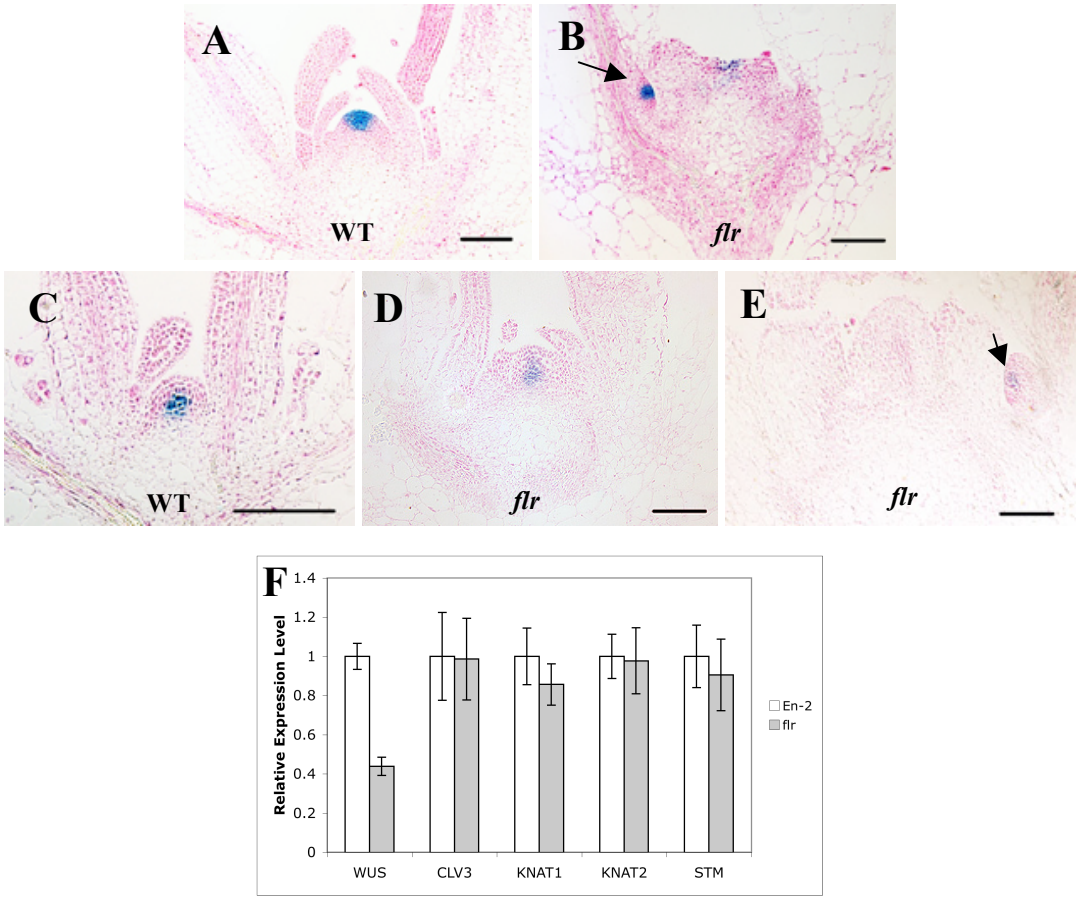

Fig. 1-6 Expression patterns and expression levels of shoot meristem regulatory genes. Longitudinal-sections and GUS staining assay displayed similar expression of p*CLV3:GUS* (A and B) and *pWUS:GUS* (C-E) in 18-days-after-germination wild-type (A and C) and *flr* (B, D and E) shoot meristems. Expression of *CLV3* and *WUS* was observed in mutant axillary buds (arrows) as well (B, E). (F) The expression levels of the regulatory genes were quantified in 4-day-after-germination wild-type (white bars) and *flr* (grey bars) apices by qRT-PCR. (Bars in A-E= 1μm)

***FLR* encodes a plastid nucleotide uniporter.**

Map-based cloning indicated the *FLR* mutation was located on a 90 kilobase (kb) region on the long arm of chromosome 4. This region is composed of 20 annotated genes. Several T-DNA insertion lines obtained from the Arabidopsis stock center were screened for *flr* phenotypes. However, *flr*-like mutant plants were not recovered in this screen. Subsequently, sequencing of the candidate genes was performed. A single base

substitution was identified at the position 479 base-pair (bp) downstream of the predicted ATG start codon in the first exon of At4g32400. This resulted in the conversion of the tryptophan-encoding codon TGG to a premature stop codon TGA (Fig. 1-7A). To confirm the mutation was responsible for the *flr* phenotypes, a 3.9 kb of the wild type At4g32400 genomic fragment encompassing the promoter, coding region, and terminator was transformed into *flr* mutants. Fifteen T1-transgenic *flr* mutants displayed phenotypes indistinguishable from wild type (Fig. 1-7B). This result indicated that At4g32400 was indeed *FLR.* Additionally, the accumulation of At4g32400 transcripts was dramatically reduced in *flr,* compared to wild type (Fig. 1-7C). As determined by qRT-PCR, expression of At4g32400 was detected in various parts of wild-type seedlings including shoot apices, cotyledons, and roots (Fig. 1-7D). The expression level of At4g32400 in roots was approximately 3.2-fold higher than those in shoot apices and cotyledons when normalized to *ACT2* expression. To confirm this observation, a 1.7 kb promoter fragment of At4g32400 was fused to the *GUS* reporter gene and transformed into wild type. Among the 14 independent T2 transgenic lines tested, 11 lines displayed similar differential *GUS* expression as determined by the incubation times for the assays (Fig. 1-7E-G). The incubation times required for the detection of GUS activity in primary roots, hypocotyls, and primary shoots including cotyledons were 30 minutes, one hour and 12 hours, respectively.

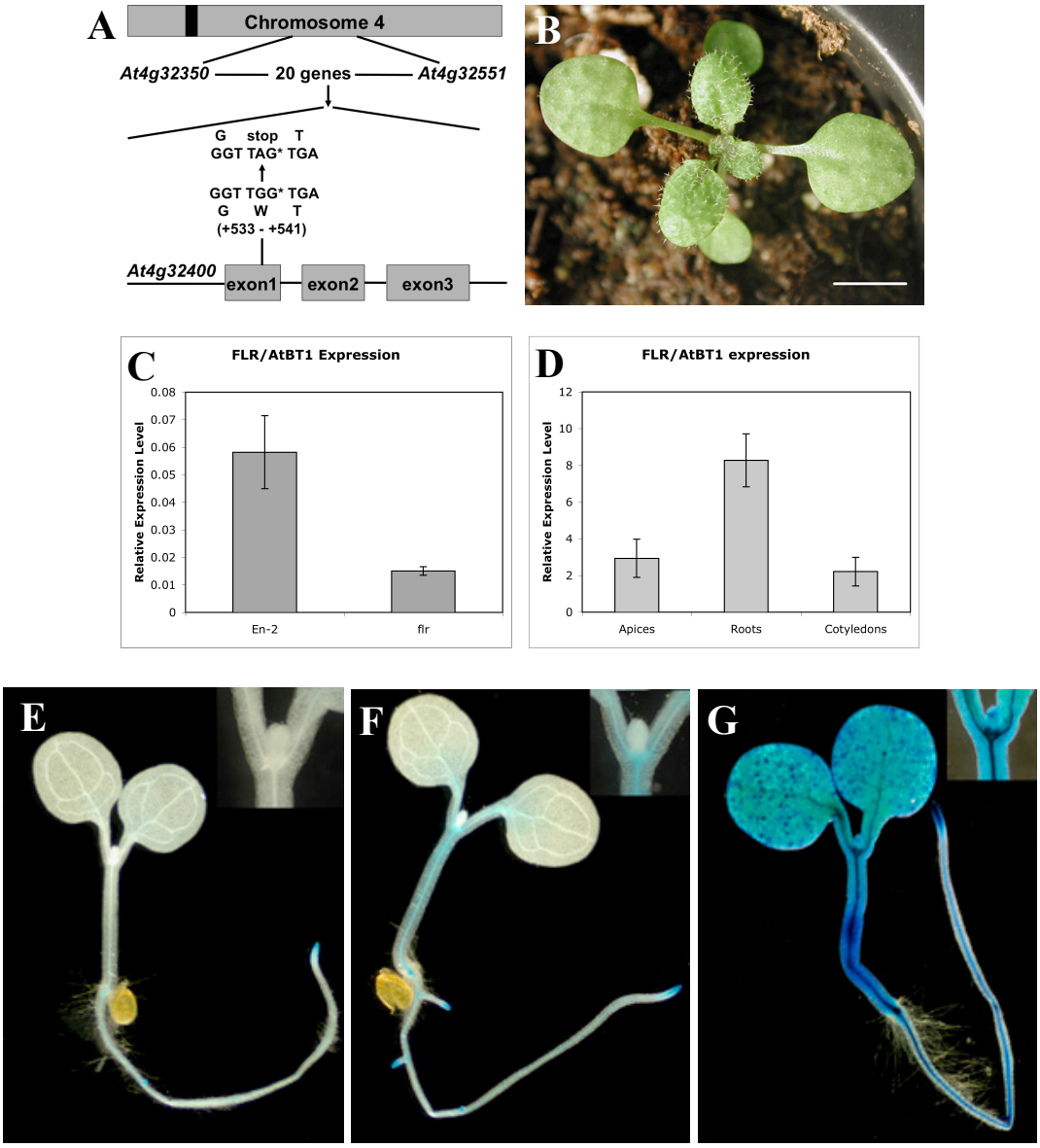

Fig. 1-7 Molecular characterization of *FLR*. Map-based cloning of *FLR* revealed a non-sense mutation in the first exon of At4g32400 (A). (B) 14-days-after-germination transgenic *flr* harboring the wild-type At4g32400 genomic fragment displayed phenotypes comparable to wild type and confirmed *FLR* was indeed At4g32400. (C) Normalized against *ACT2* expression, the expression level of *FLR* transcripts in mutant seedlings was significantly lower than wild type. (D) Expression of *FLR* was detected in roots, apices, and cotyledons at different levels. Analysis of *FLR* promoter activities confirmed this differential expression in various parts of seedlings. GUS activities were detected in roots after 30-minute incubation (E), in hypocotyls after one-hour incubation (F), and in shoot as well as cotyledons after 12-hour incubation (G). Insets (E-G) displayed the magnified views of the shoots. (Bar = 1 cm)

A mutation in At4g32400 has previously been described as *salt hypersensitive (shs) 1* that enhances the salt-hypersensitivity of *salt overly sensitive (sos) 3* mutants [12]. *shs1* mutants display cold and sugar hypersensitivity as well as abscisic insensitivity [12]. Additionally, vegetative growth defects including overall growth reduction, short roots and malformation in leaf shapes have been observed [12]. Similarly, *flr* displayed hypersensitivities toward high-concentration of glucose and sucrose. As shown in Fig. 1-8A-D, the first pair of leaves of wild type was well expanded, despite the presence of 200 mM glucose, sucrose or mannitol. *flr* seedlings produced expanded first leaf pairs in the absence of sugar (Fig. 1-8E), whereas leaf development was inhibited by glucose and sucrose (Fig. 1-8F-G). That osmotic effect that may cause this inhibition was ruled out, as non-metabolizable mannitol did not affect leaf expansion of the mutants (Fig. 1-8H). Together with *flr* phenotypes, the sugar-signaling pathway may be involved in the maintenance of Arabidopsis growth and development.

The protein encoded by At4g32400 has been annotated as a plastid-targeted Arabidopsis BRITTLE (AtBT) 1, a homolog of maize BT1 [22]. Maize BT1 is responsible for the transport of ADP-glucose, a substrate for ADP-glucosepyrophosphorylase (AGPase) for starch biosynthesis in amyloplasts of endosperm [16, 23, 34]. Different from maize BT1, a recent study has demonstrated AtBT1 may function in the transport of adenine nucleotides including AMP, ADP and ATP [17]. Unexpectedly, there were no leaf morphological defects reported in either the T-DNA insertion or AtBT1-RNAi lines in the study [17]. Thus, the leaf morphology of the three reported AtBT1-RNAi lines were re-examined. Under a close observation, progenies of one of the reported AtBT1-RNAi line (AtBT1-RNAi No.3) displayed leaf developmental

defects including ectopic abaxial outgrowths and radialized leaves (Fig. 1-8I-J). Additionally, the enlargement of meristematic cells and a slight distortion of cell division planes were observed in the primary meristems of these *FLR/AtBT1* knock-down mutants (Fig. 1-8K). These similarities between *flr, shs1* and AtBT1-RNAi mutants confirmed the identification of *FLR* as *AtBT1* and its involvement in leaf morphogenesis and shoot meristem maintenance.

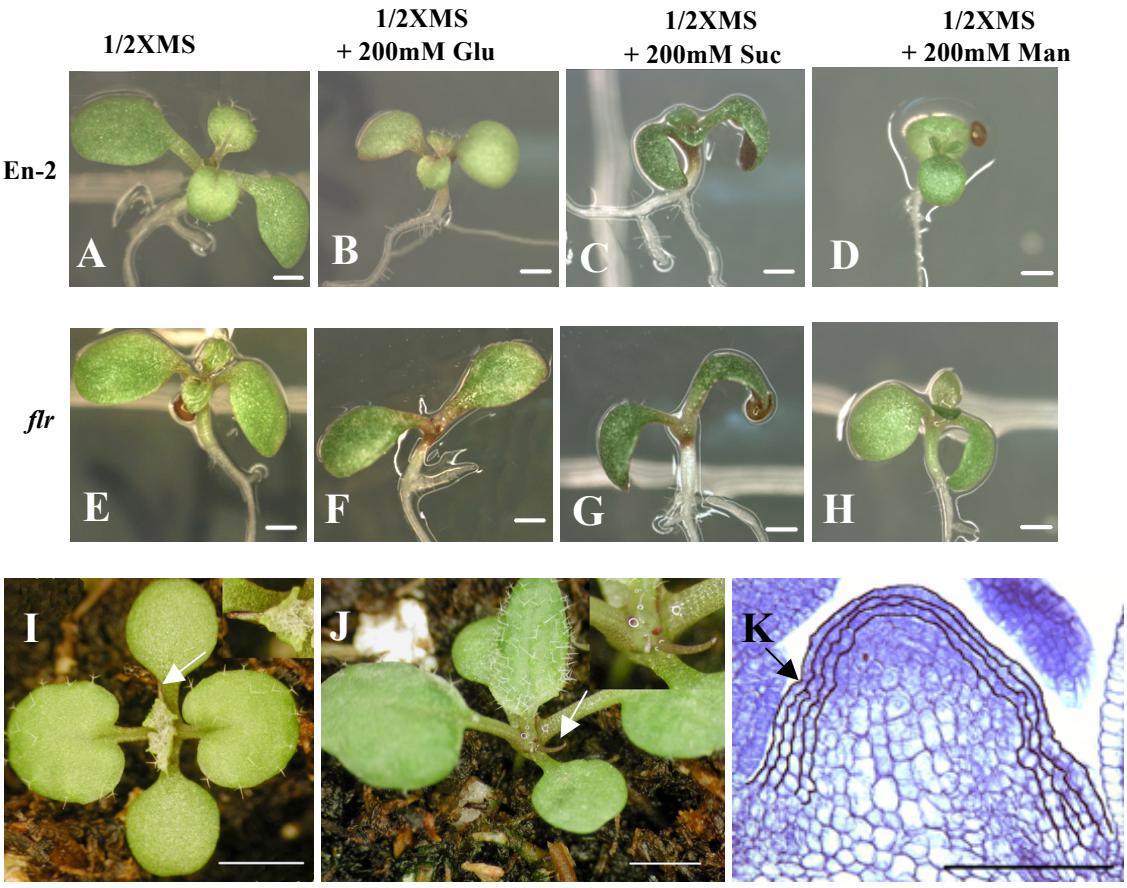

Fig.1-8 Sugar hypersensitivity in *flr* seedlings and leaf and shoot morphological defects in the AtBT1-RNai No.3 line. When germinated on 1/2X MS media (A,E) and 1/2X MS media plus 200 mM mannitol (Man) (D, H), the first pairs of leaves were well expanded in wild type (A, D) and *flr* (E,H) at 9 day-after-germination. 200 mM glucose (Glu) (B, F) and sucrose (Suc) (C, G) had no effects on 9-day-after-getmination wild-type seedlings (B, C) but inhibited leaf development in *flr* at the same age (F, G). Abaxial outgrowths (J, arrow) and radialized organs (I, arrow) were observed in 15- and 18-day-after-germination AtBT1-RNai No.3 seedlings, respectively (insets: magnified views of the aforementioned structures). (K) Longitudinal-sections of 18-day-after-germination AtBT-RNAi No.3 seedlings revealed disturbance in meristematic cell identity and the slight distortion in cell division planes in the L2 and L3 layers. (Bars in A-H = 1mm, Bars in I-J = 2mm, Bar in K = 1μm)

Modifications of *flr* phenotypes by environmental conditions

As a plastid nucleotide uniporter, FLR/AtBT1 is potentially required for properly functional plastids [17]. Recently, a study has shown that light hypersensitivity is increased in mutants where plastid-signaling pathways are disrupted [28]. To investigate the impact of light intensity and photoperiod, a set of experiments was carried out. For day length effects, wild-type and mutants plants were grown under long-day (16/8: light/dark, 35 μmol m^{-2} s^{-1}) and continuous-light (23 μmol m^{-2} s^{-1}) conditions for 26 days. Light intensities (μmol m^{-2} s^{-1}) were adjusted accordingly to deliver equal numbers of photons to plants each day under the different day-length conditions. Wild-type plants grown under the long-day conditions were slightly pale green compared to those under the constant-light conditions (Fig. 1-9A-B). In contrast, the severity of the mutant leaf defects progressed along with the increase of the day length (Fig. 1-9G-H). Under the tested long-day conditions, *flr* displayed only mild leaf morphological defects including crumpled leaves and pointed tips after the formation of the first leaf pair (Fig. 1-9G). Continuous light conditions caused tissue necrosis and severe reduction of leaf blade expansion in the second leaf pair of mutant seedlings (Fig. 1-9H). To determine the effects of light intensities, wild type and *flr* were grown under long day conditions with 113 and 180 μmol m^{-2} s^{-1} light intensities. High light intensity enhanced the leaf morphological defects in *flr* as indicated by the formation of several radialized leaves (Fig. 1-9I), while leaves of *flr* grown under the low light intensity only exhibited a reduction of leaf blade expansion (Fig. 1-9J). Leaf shapes of wild-type seedlings grown under these conditions were not significantly different, whereas an elongation of leaf petioles was more pronounced under the lower light intensity (Fig. 1-9C-D).

Additionally, to examine whether photoperiod or light intensity were more influential on *flr* leaf morphological defects, wild type and mutants were grown under short-day conditions with a high light intensity (8/16 light/dark, 270 μmol.m^{-2}.s^{-1}). While wild type grew normally under these conditions (Fig. 1-9E), *flr* seedlings still displayed the complete loss of leaf polarity as indicated by the second leaf pair that appeared radialized (Fig. 1-9K). This result suggests *flr* may be more sensitive to light intensity than to photoperiod.

phan mutants of *A. majus* displayed a low-temperature hypersensitivity [36]. When grown under at permissive temperature (25 ^{o}C), *phan* mutants are relatively similar to wild type [36]. Remarkably, *phan* mutants formed large cotyledons with ectopic abaxialization at 17^{o}C. Furthermore, subsequent leaves were almost exclusively radialized [36]. Based on the superficial resemblance of *flr* leaf polarity defects to *phan*, *flr* mutants were tested for the effects of the low temperature conditions (16/8 light/dark, 113 μmol m^{-2} s^{-1}, 16 ^{o}C). Similar to *phan*, *flr* exhibited the low-temperature hypersensitivity. While wild type grew normally (Fig. 1-9F), leaf polarity defects of *flr* were exacerbated (Fig. 1-9L), compared to mutants grown under optimal temperature (22 ^{o}C) and similar light conditions (Fig. 1-9I). The expansion of the first two leaves was greatly reduced, and photo-bleaching was observed. All subsequent leaves displayed a complete loss of leaf polarity as indicated by their thread-like appearance. This low-temperature hypersensitivity of *flr* was similar to *phan* and supported the speculation that *FLR/AtBT1* may be functionally similar to *PHAN* regarding leaf polarity establishment. These modifications of *flr* leaf phenotypes by environmental factors also suggests

FLR/AtBT1 may directly or indirectly play an important role in the perception of environmental cues to ensure proper leaf morphogenesis.

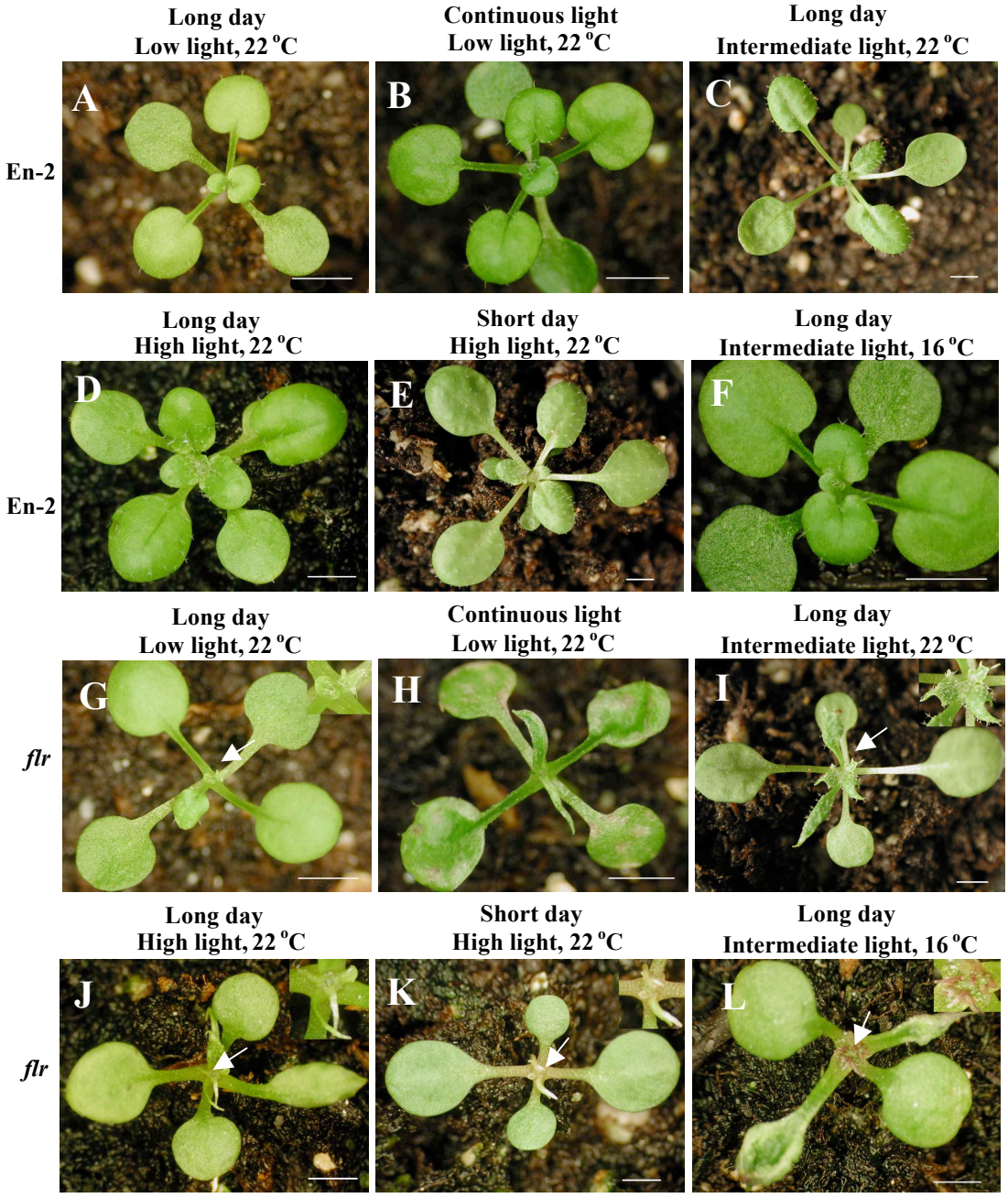

Fig. 1-9 Environmental effects on *flr* leaf phenotypes (see text). 26-day-after-germination wild type (A, B, C, D, E, and F) and *flr* (G, H, I, J, K, and L) grown under various growth conditions. (A and G) 16/8: light/dark, 35 μmol.m^{-2}.s^{-1}, 22 °C. (B and H) Continuous light, 23 μmol.m^{-2}.s^{-1}, 22 °C. (C and I) 16/8: light/dark, 113 μmol.m^{-2}.s^{-1}, 22 °C. (D and J) 16/8: light/dark, 180 μmol.m^{-2}.s^{-1}, 22 °C. (E and K) 8/16 light/dark, 270 μmol.m^{-2}.s^{-1} 22 °C. (F and L) 16/8: light/dark, 113 μmol.m^{-2}.s^{-1}, 16 °C. Insets displayed the magnified views of the apices (arrows). (Bars = 2mm)

Discussion

Mutations in *FLR/AtBT1* cause leaf abaxialization similar to *phan*.

flr holds a particular significance for the study of leaf polarity. Despite the presence of several leaf-polarity mutants in Arabidopsis, a single recessive mutant with leaf polarity defects resembling *phan* phenotypes has never been described. *AS1* encodes a myb-domain containing transcription factor that is the Arabidopsis ortholog of PHAN in Antirrhinum [4]. Previous studies have demonstrated *PHAN* and *AS1* are able to suppress expression of *KNOX* genes in organ primordia [4, 37]. However, *as1* mutant plants only displayed triangular-shaped, asymmetric leaves with a mild leaf polarity defect on petioles [4]. The phenotype differences between *as1* and *phan* mutants could be attributed to functional redundancy or the presence of modifiers in Arabidopsis that are not present in Antirrhinum. To date, these functionally redundant factors or modifiers have remained unknown in Arabidopsis. By following up on *flr* that had initially been described over a decade ago, the mutant phenotypes analogous to *phan* were observed. Similar to *phan* [36], these phenotypes include radialized organs with abaxial features, various degrees of leaf defects, single recessive inheritance and the enhancement of leaf polarity defect at low temperature. Identification of the mutation reveals the *FLR/AtBT1* gene whose function had not previously been implicated in leaf polarity establishment. Nevertheless, gene expression analysis revealed that there were no changes in the expression levels of the *KNOX* genes tested, including *KNAT1, KNAT2* and *STM,* in *flr* apices, compared to wild type. In contrast, *PHAN* and *AS1* have been proposed to function in the inhibition of expression of *KNOX* genes [4, 37]. This result suggests *FLR/AtBT1* may exert its influence on leaf polarity through a different regulatory

pathway from *PHAN*.

Ectopic abaxialization and shoot meristem defects in *flr*

The co-occurrence of leaf polarity and shoot meristem defects in *flr* is consistent with the proposed intimate link between leaf polarity and shoot meristems [15, 27, 35]. This connection was originally observed in a microsurgical study of potato shoot tips that demonstrated separation of incipient leaf primordia from adjacent shoot meristem results in the formation of radialized leaves exhibiting abaxial features [35]. This experiment was elaborated fifty years later in a more precise laser-ablation analysis in tomato shoots [27]. Partial removal of a single row of cells in the L1 layer of the SAM triggers the formation of radialized leaves, indicating the importance of the L1 layer in communicating leaf polarity signals. In contrast, disturbance of *flr* meristem anatomy was mainly found in the L2 and L3 layers. This suggests contributions from cells in the L2 and L3 layers in promoting proper leaf polarity establishment. Alternatively, the mutation in *FLR/AtBT1* may disrupt communication in all three layers of the SAM.

Several leaf polarity genes have been implicated in the maintenance of shoot apical meristem. Mutations in *HD-ZIP III* genes dramatically affect shoot meristem integrity. *phb phv rev* triple mutants fail to establish functional shoot apical meristems in addition to abaxialization in cotyledons [8]. *phb phv cna* triple mutants displayed a number of meristem defects including enlarged shoot meristems, stem fasciation, extra floral organs and reduced fertility [26]. The gain-of-function *phb-1d* allele displays an enlargement of embryonic shoot meristem and the formation of ectopic buds underneath the proximal region of radialized organs [25]. In contrast, *KAN1*-overexpressing plants fail to establish the shoot apical meristem, indicating the termination of progenitor cells that give rise to

the shoot apical meristem [15]. Together, the formation and maintenance of shoot apical meristem may be promoted by adaxialization and antagonized by abaxialization. Despite evidence of this interconnection between leaf polarity and shoot apical meristems, mutations of *WUS, CLV3* and *STM* did not produce the strong leaf-polarity defects as demonstrated in *flr* or other leaf-polarity mutants [2, 5, 20]. The presence of both leaf polarity and shoot apical meristem defects in *flr* could be explained in two ways. The adaxialization function of *FLR/AtBT1* may also contribute to a shoot meristem maintenance pathway that is distinct from those of conventional shoot apical meristem determinants. Alternatively, the reduction in *WUS* expression in *flr* results in the shoot meristem defects, and *FLR*/AtBT1 functions in leaf polarity and shoot meristem maintenance are independent from each other.

Plastid roles in plant growth and development

The previous biochemical and protein localization study indicated that FLR/AtBT1 is involved in the transport of adenine nucleotides across the plastid membranes [17]. The characterization of *flr* mutants revealed morphological defects in shoot meristems and leaves. Taken together, these results suggest proper plastid functions are required for normal plant growth and development. An emerging line of evidence indicates that plastids are more than merely photosynthetic organelles [1, 18, 28, 29]. A mutation in *CRUMPLED LEAVES (CRL),* which encodes a plastid membrane protein, causes distortion of cell division planes in various organs including shoot meristems, root tips and embryos as well as disturbance of cell differentiation in inflorescence stems and root endodermis [1]. Other studies have shown that unknown secondary messengers generated from impaired plastids trigger the retrograde signaling pathway to suppress expression of

photosynthesis-associated nuclear genes (PhANG) [18, 28, 29]. GENOME UNCOUPLED (GUN) 1, a plastid-targeted pentatricopeptide protein, has been proposed to be involved in this signaling pathway [18]. In the presence of plastid-biogenesis inhibitors, PhANG expression is dramatically down-regulated in wild type and is derepressed in *gun1* mutants [18]. Although the identity of the secondary messengers still remains elusive, several stimuli triggering the signaling pathway have been shown. These include the accumulation of the chlorophyll precursor Mg-protoporphyrin IX, the inhibition of chloroplast genome expression, high glucose concentration, and high light intensities [18, 28]. Remarkably, *flr* was hypersensitive to high-concentration glucose and strong light intensities. This overlap between plastid-nucleus signaling and modifiers of *flr* phenotypes indicates the plastid functions conferred by FLR/AtBT1 may contribute directly to leaf morphogenesis and environmental responses.

Adenine nucleotides AMP, ADP and ATP have been demonstrated to be the substrates of FLR/AtBT1 [17]. ADP and ATP are known precursors for the production of cytokinin, a phytohormone controlling various processes of plant growth and development [30]. Plastids to which several cytokinin-bisosynthesis enzymes are targeted have been proposed as a major site for cytokinin production [14, 30]. Previous studies have demonstrated an interconnection between cytokinin and the regulators of shoot meristem maintenance. Expression of cytokinin-biosynthesis genes is induced by ectopic expression of *STM*, required for the initiation and maintenance of shoot apical meristems [13]. *WUS* has been found to promote cytokinin signaling by repressing expression of *ARR5* and *ARR7,* negative regulators for cytokinin-signaling pathways [21]. Conversely, over-expression of consitutively-active, engineered *ARR7* produces phenotypes similar to

wus mutants suggesting a requirement for cytokinin to maintain shoot apical meristem activities [21]. Furthermore, *LONELY GUY (LOG)*, encoding a cytokinin-activating enzyme in rice, is expressed on the tip of the shoot apical meristem, indicating the meristem as a source of active cytokinin [19]. Additionally, a recent study has demonstrated an up-regulation of *WUS* expression by exogenous cytokinin and overlapping expression patterns of a cytokinin-receptor and *WUS [11]*. Together, a model has been proposed in which active cytokinin is generated in the meristem and signifies an up-regulation of *WUS* expression only in underlying cells where cytokinin-receptors proteins are expressed [11]. Subsequently, *WUS* promotes stem cell formation, completing a regulatory feedback loop [19]. Based on these previous studies and the down-regulation of *WUS* in *flr*, I propose *FLR/AtBT1* may function as a plastid cytokinin transporter. However, structural variation among different active cytokinins may indicate roles for multiple cytokinin transporters regarding FLR/AtBT1 functions. It would be of great interest to determine whether the transport of a specific subset of cytokinins is disrupted in *flr*. Thus, further biochemical characterization of FLR/AtBT1 is crucial to determine how FLR/AtBT1 and plastids specifically contribute to leaf polarity and shoot apical meristem maintenance at a molecular level.

Materials and Methods

Plant Materials and Growth Conditions

flr mutants in the En-2 background were derived from the CS325 line obtained from the Arabidopsis Stock Center (TAIR). Unless specifically noted otherwise, all plants were grown on Promix (Premier Horticulture Inc., Canada) under long-day conditions (16hr/8hr light/dark), 150 μmol.m^{-2}.s^{-1}, 22 ^{o}C. For sugar hypersensitivity test, wild-type and mutant seeds were surface-sterilized and germinated on 1/2X MS medium (Research Product Internationals Corp., USA.) containing 7% agar and 200 mM of glucose, sucrose or mannitol under the same light and temperature conditions.

The genetic study was conducted by crossing *as1-1* and *as1-2* as the maternal parents to *flr* single mutants. F1 seeds were grown and allowed for self-fertilization to obtain the F2 population. *as1-1* and *as2-1*-like F2 plants segregating for the *flr* mutation were self-fertilized, and F3 seeds were collected for the analysis of *flr as1-1* and *flr as2-1* double mutant phenotypes. Double mutants were confirmed for the mutation in *flr* by a cleavage amplified polymorphism marker. DNA fragments containing the mutation were amplified by using primers FLR-CAPF (5'-AAGGTGGGCTCACACTGAAG-3') and FLR-CAPR (5'-TTTTCACAGGTAAAGAGTCAACG-3'). The amplified fragments were then digested with *Mme*I (Biolabs) according to the manufacturer's instruction.

Histology and GUS Staining

Samples including leaves and seedlings were fixed in FAA fixative solution (50% ethanol, 5% (v/v) acetic acid, 3.7% (v/v) formaldehyde). Subsequently, samples were dehydrated through the ethanol series (50%, 70%, 85%, 95%, and 100%) and Histoclear (National Diagnostics), and infiltrated with paraplast (Fisher). For sectioning, infiltrated

samples were embedded in the paraplast and sectioned by the rotary microtome (Richert Inc.). Sections were stained with 0.1% toluidine blue and permanently fixed to microscope slides with permount (Fisher). Sectioning analysis of leaf vasculature system was performed on the middle area of the leaves.

For the examination of *WUS, CLV3,* and *KAN1* expression patterns, seedlings were fixed with 80% acetone and stained with GUS-staining solution (50mM sodium phosphate buffer (pH 7.2), 9 mM $K_4[Fe(CN)_6]$, 9 mM $K_4[Fe(CN)_6]$, 1mg/ml X-Gluc) at room temperature until the blue precipitate was visible. Afterward, seedlings were subjected to the ethanol series for dehydration. For p*KAN1:GUS*, cotyledons were removed at the 100% ethanol step. Then, seedlings were rehydrated and mounted on glass slides with 30% glycerol. For p*WUS:GUS* and p*CLV3:GUS*, after dehydration, seedlings were subject to sectioning. For *FLR/AtBT1* promoter analysis, transgenic seedlings were fixed similarly. GUS-washing and staining solutions contained lower concentrations (2mM) of $K_4[Fe(CN)_6]$ and $K_4[Fe(CN)_6]$. Seedlings were incubated at 37^oC until blue precipitates were detected.

qRT-PCR

For expression analysis of leaf polarity and SAM maintenance genes, three batches of wild-type and *flr* seedlings were germinated on 1/2X MS medium (Research Product Internationals Corp., USA.) for 4 days. 100 apices were collected from each batch after cotyledons and hypocotyls were removed. RNA was extracted from each batch separately by using RNeasy Plant Mini Kit (QIAGEN). 400 μg of total RNA from each extraction were combined and 300 μg of pooled RNA were reverse-transcribed using Superscript III Reverse Transcriptase and oligo-dT primers according to the

manufacturer's instructions (Invitrogen). qPCR was subsequently performed in three replicates with 10-times-diluted cDNA in iCycler-MyiQ detection system (BIORAD). SYBR-Green was used to quantify the reaction products. Primer sequences are provided in Appendix I. For expression analysis of *FLR,* whole mutant and wild-type seedlings were collected for RNA preparation and qRT-PCR reactions were also performed in triplicate with FLR-F/FLR-R primers (Appendix I). Expression levels of the tested genes were normalized against *ACTIN2* (Appendix I).

Map-based Cloning of *FLR/AtBT1*

To locate the *FLR/AtBT1* locus, BAC-specific molecular markers corresponding to Col-0 and L*er* ecotypes sequence polymorphism were used. Additional PCR-based markers were developed for fine-scale mapping using L*er* and Col insertion/deletion (InDel) and single nucleotide (SNP) polymorphism sequence data (http://signal.salk.edu). A recombinant population of 1,492 chromosomes was created. Mapping analysis narrowed the region of *FLR* mutation to 90 kb on the long arm of chromosome 4. Subsequently, T-DNA insertion lines screening and sequencing of candidate genes were employed to isolate the mutation.

Plasmid Construction and Plant Transformation for Complementation Analysis

3,941 bp of an At4g32400 genomic fragment including 1.3 kb upstream, the coding region and 795 bp downstream was amplified from wild-type genomic DNA using Hecules II Fusion enzyme (Stratagene) with primer FLR-genF and FLR-genR (Appendix I). The amplified fragment was then cloned into pENTR/D-TOPO (Invitrogen) and verified by sequencing. The fragment was introduced to pMDC99 [7] by using Gateway LR Clonase® Enzyme mix (Invitrogen). The construct was transformed

into *Agrobacterium tumefaciens* strain GV3101 (pMP90). Flowering 45-day-old *flr* plants were then transformed with this construct by the floral dip method [6]. T1 seeds were surface-sterilized and sowed on 1/2X MS solid medium containing 30 μg/ml Hygromycin (Calbiochem) for selection of transgenic seedlings.

For promoter activity analysis, a 1.7 kb promoter fragment of At4g32400 was amplified by using FLR-promF and FLR-promR primers (Appendix I) with Hercules II Fusion enzyme (Stratagene). The promoter was cloned into pDONR221 (Invitrogen) by using Gateway BP clonase (Invitrogen) and subsequently transferred to pMDC164 containing the *GUS* reporter gene [7]. The promoter-reporter gene fusion was transformed into plants by using the floral dip method. Seeds obtained from the transformation were selected on 1/2X MS solid medium containing 30 μg/ml Hygromycin (Calbiochem). T1 transgenic plants were allowed to self-fertilize. Seeds of 14 independent T2 lines were used for GUS activity analysis as described above.

References

1. Asano T, Yoshioka Y, Kurei S, Sakamoto W, Machida Y: A mutation of the CRUMPLED LEAF gene that encodes a protein localized in the outer envelope membrane of plastids affects the pattern of cell division, cell differentiation, and plastid division in Arabidopsis. Plant J 38: 448-59 (2004).
2. Barton K, Poethig S: Formation of the shoot apical meristem in *Arabidopsis thaliana*: an analysis of development in the wild type and in the *shoot meristemless* mutant. Development 119: 823-831 (1993).
3. Brand U, Fletcher JC, Hobe M, Meyerowitz EM, Simon R: Dependence of stem cell fate in Arabidopsis on a feedback loop regulated by CLV3 activity. Science 289: 617-9 (2000).
4. Byrne ME, Barley R, Curtis M, Arroyo JM, Dunham M, Hudson A, Martienssen RA: Asymmetric leaves1 mediates leaf patterning and stem cell function in Arabidopsis. Nature 408: 967-71 (2000).
5. Clark S, Running M, Meyerowitz E: *CLAVATA3* is a speicfic regulator of shoot and floral meristem development affecting the same processes as *CLAVATA1*. Development 121: 2057-2067 (1995).
6. Clough SJ, Bent AF: Floral dip: a simplified method for Agrobacterium-mediated transformation of Arabidopsis thaliana. Plant J 16: 735-43 (1998).
7. Curtis MD, Grossniklaus U: A gateway cloning vector set for high-throughput functional analysis of genes in planta. Plant Physiol 133: 462-9 (2003).
8. Emery JF, Floyd SK, Alvarez J, Eshed Y, Hawker NP, Izhaki A, Baum SF, Bowman JL: Radial patterning of Arabidopsis shoots by class III HD-ZIP and KANADI genes. Curr Biol 13: 1768-74 (2003).
9. Endrizzi K, Moussian B, Haecker A, Levin JZ, Laux T: The SHOOT MERISTEMLESS gene is required for maintenance of undifferentiated cells in Arabidopsis shoot and floral meristems and acts at a different regulatory level than the meristem genes WUSCHEL and ZWILLE. Plant J 10: 967-79 (1996).
10. Fletcher JC, Brand U, Running MP, Simon R, Meyerowitz EM: Signaling of cell fate decisions by CLAVATA3 in Arabidopsis shoot meristems. Science 283: 1911-4 (1999).
11. Gordon SP, Chickarmane VS, Ohno C, Meyerowitz EM: Multiple feedback loops through cytokinin signaling control stem cell number within the Arabidopsis shoot meristem. Proc Natl Acad Sci U S A 106: 16529-34 (2009).
12. Inan G, Goto F, Jin JB, Rosado A, Koiwa H, Shi H, Hasegawa PM, Bressan RA, Maggio A, Li X: Isolation and characterization of shs1, a sugar-hypersensitive and ABA-insensitive mutant with multiple stress responses. Plant Mol Biol 65: 295-309 (2007).
13. Jasinski S, Piazza P, Craft J, Hay A, Woolley L, Rieu I, Phillips A, Hedden P, Tsiantis M: KNOX action in Arabidopsis is mediated by coordinate regulation of cytokinin and gibberellin activities. Curr Biol 15: 1560-5 (2005).
14. Kasahara H, Takei K, Ueda N, Hishiyama S, Yamaya T, Kamiya Y, Yamaguchi S, Sakakibara H: Distinct isoprenoid origins of cis- and trans-zeatin biosyntheses in Arabidopsis. J Biol Chem 279: 14049-54 (2004).

15. Kerstetter RA, Bollman K, Taylor RA, Bomblies K, Poethig RS: KANADI regulates organ polarity in Arabidopsis. Nature 411: 706-9 (2001).
16. Kirchberger S, Leroch M, Huynen MA, Wahl M, Neuhaus HE, Tjaden J: Molecular and biochemical analysis of the plastidic ADP-glucose transporter (ZmBT1) from Zea mays. J Biol Chem 282: 22481-91 (2007).
17. Kirchberger S, Tjaden J, Ekkehard Neuhaus H: Characterization of the Arabidopsis Brittle1 transport protein and impact of reduced activity on plant metabolism. Plant J (2008).
18. Koussevitzky S, Nott A, Mockler TC, Hong F, Sachetto-Martins G, Surpin M, Lim J, Mittler R, Chory J: Signals from chloroplasts converge to regulate nuclear gene expression. Science 316: 715-9 (2007).
19. Kurakawa T, Ueda N, Maekawa M, Kobayashi K, Kojima M, Nagato Y, Sakakibara H, Kyozuka J: Direct control of shoot meristem activity by a cytokinin-activating enzyme. Nature 445: 652-5 (2007).
20. Laux T, Mayer KF, Berger J, Jurgens G: The WUSCHEL gene is required for shoot and floral meristem integrity in Arabidopsis. Development 122: 87-96 (1996).
21. Leibfried A, To JP, Busch W, Stehling S, Kehle A, Demar M, Kieber JJ, Lohmann JU: WUSCHEL controls meristem function by direct regulation of cytokinin-inducible response regulators. Nature 438: 1172-5 (2005).
22. Leroch M, Kirchberger S, Haferkamp I, Wahl M, Neuhaus HE, Tjaden J: Identification and characterization of a novel plastidic adenine nucleotide uniporter from Solanum tuberosum. J Biol Chem 280: 17992-8000 (2005).
23. Mangelsdorf PC, Jones DF: The Expression of Mendelian Factors in the Gametophyte of Maize. Genetics 11: 423-55 (1926).
24. Mayer KF, Schoof H, Haecker A, Lenhard M, Jurgens G, Laux T: Role of WUSCHEL in regulating stem cell fate in the Arabidopsis shoot meristem. Cell 95: 805-15 (1998).
25. McConnell JR, Barton MK: Leaf polarity and meristem formation in Arabidopsis. Development 125: 2935-42 (1998).
26. Prigge MJ, Otsuga D, Alonso JM, Ecker JR, Drews GN, Clark SE: Class III homeodomain-leucine zipper gene family members have overlapping, antagonistic, and distinct roles in Arabidopsis development. Plant Cell 17: 61-76 (2005).
27. Reinhardt D, Frenz M, Mandel T, Kuhlemeier C: Microsurgical and laser ablation analysis of leaf positioning and dorsoventral patterning in tomato. Development 132: 15-26 (2005).
28. Ruckle ME, DeMarco SM, Larkin RM: Plastid signals remodel light signaling networks and are essential for efficient chloroplast biogenesis in Arabidopsis. Plant Cell 19: 3944-60 (2007).
29. Ruckle ME, Larkin RM: Plastid signals that affect photomorphogenesis in Arabidopsis thaliana are dependent on GENOMES UNCOUPLED 1 and cryptochrome 1. New Phytol 182: 367-79 (2009).
30. Sakakibara H: Cytokinins: activity, biosynthesis, and translocation. Annu Rev Plant Biol 57: 431-49 (2006).

31. Schoof H, Lenhard M, Haecker A, Mayer KF, Jurgens G, Laux T: The stem cell population of Arabidopsis shoot meristems in maintained by a regulatory loop between the CLAVATA and WUSCHEL genes. Cell 100: 635-44 (2000).
32. Semiarti E, Ueno Y, Tsukaya H, Iwakawa H, Machida C, Machida Y: The ASYMMETRIC LEAVES2 gene of Arabidopsis thaliana regulates formation of a symmetric lamina, establishment of venation and repression of meristem-related homeobox genes in leaves. Development 128: 1771-83 (2001).
33. Serrano-Cartagena J, Robles P, Ponce MR, Micol JL: Genetic analysis of leaf form mutants from the Arabidopsis Information Service collection. Mol Gen Genet 261: 725-39 (1999).
34. Sullivan TD, Kaneko Y: The maize brittle 1 gene encodes amyloplast membrane polypeptides. Planta 196: 477-84 (1995).
35. Sussex IM: Morphogenesis in Solanum tuberosum L.: experimental investigation of leaf dorsiventrality and orientation in the juvenile shoot. Phytomorphology 5: 286-300 (1955).
36. Waites R, Hudson A: *phantastica*: a gene required for dorsoventrality of leaves in *Antirrhinum majus*. Development 121: 2143-2154 (1995).
37. Waites R, Selvadurai HR, Oliver IR, Hudson A: The PHANTASTICA gene encodes a MYB transcription factor involved in growth and dorsoventrality of lateral organs in Antirrhinum. Cell 93: 779-89 (1998).
38. Wu G, Lin WC, Huang T, Poethig RS, Springer PS, Kerstetter RA: KANADI1 regulates adaxial-abaxial polarity in Arabidopsis by directly repressing the transcription of ASYMMETRIC LEAVES2. Proc Natl Acad Sci U S A 105: 16392-7 (2008).
39. Xu L, Xu Y, Dong A, Sun Y, Pi L, Huang H: Novel as1 and as2 defects in leaf adaxial-abaxial polarity reveal the requirement for ASYMMETRIC LEAVES1 and 2 and ERECTA functions in specifying leaf adaxial identity. Development 130: 4097-107 (2003).

Chapter 2

A novel regulator of leaf blade expansion and its potential connection with the translational regulation in leaf morphogenesis

Introduction

Proper leaf morphogenesis determines the success of plants as photosynthetic organisms. It depends on correctly establishing asymmetry along three developmental axes. Leaf polarity is determined along the adaxial (dorsal) – abaxial (ventral) axis and leaf blade expansion along the medial-lateral and proximal distal axes. Several regulatory genes have been shown to be critical for determining different aspects of leaf blade expansion [10]. However, internal regulators are not the only source of cues determining proper leaf morphogenesis. External factors, especially light, are significant contributors as well. Low-light conditions have been shown to promote the elongation of petioles and inhibit leaf blade expansion in Arabidopsis [11]. Palisade cells of these leaves are round and form one mesophyll layer. In contrast, leaves of the plants grown under high-intensity light (>200 μmol m^{-2} s^{-1}) can develop two to three layers of elongated palisade cells, resulting in an increase of the leaf thickness [11]. In this chapter, I describe an Arabidopsis mutant *blade expansion defective (bed) 1* that displays a reduction in leaf blade expansion, compared to wild type. This phenotype was dramatically exacerbated by continuous, high-intensity light conditions. Map-based cloning revealed that *bed1* contained a single-base substitution mutation in the second exon of At5g59560*,* which

had previously been described as a circadian clock regulator *Sensitive to Red Light Reduced (SRR) 1* [8]. Hereafter, *bed1* is referred to as *srr1-2.* Genetic analysis present here uncovered the interactions between *SRR1* and the translational machinery. Additionally, additive effects of *srr1-2* on leaf polarity mutant backgrounds indicated *SRR1* functions independently from leaf polarity to complete proper leaf blade expansion. These results demonstrate a novel interconnection between *SRR1* and translational regulation during leaf morphogenesis.

Results

srr1-2 mutants exhibited defects in leaf morphogenesis

When grown under the optimal conditions (16hr/8hr light/dark, 150 μmol.m^{-2}.s^{-1}, 22 ^{o}C), wild-type leaves were slightly downward-curling, rounded and well-expanded and associated with clear boundaries between leaf blades and petioles (Fig. 2-1A and C). In contrast, *srr1-2* mutants were primarily recognized by the formation of flattened, narrow, elongated leaves with more gradual distinction between leaf blade and petiole (Fig. 2-1B and D). Reduction of leaf blade expansion in *srr1-2* was subtle in the first pair of true rosette leaves and became more pronounced in subsequent leaves. The *srr1-2* leaf-blade-expansion defect was reflected on leaf indices, the ratio between leaf length and leaf width (Fig. 2-1E). The first leaf pair of wild type and mutant displayed relatively similar average leaf indices. However, in the second leaf pair, the average mutant indices became significantly higher than wild type. To determine the type of inheritance of the mutation, *srr1-2* was back-crossed to WS wild type plants.

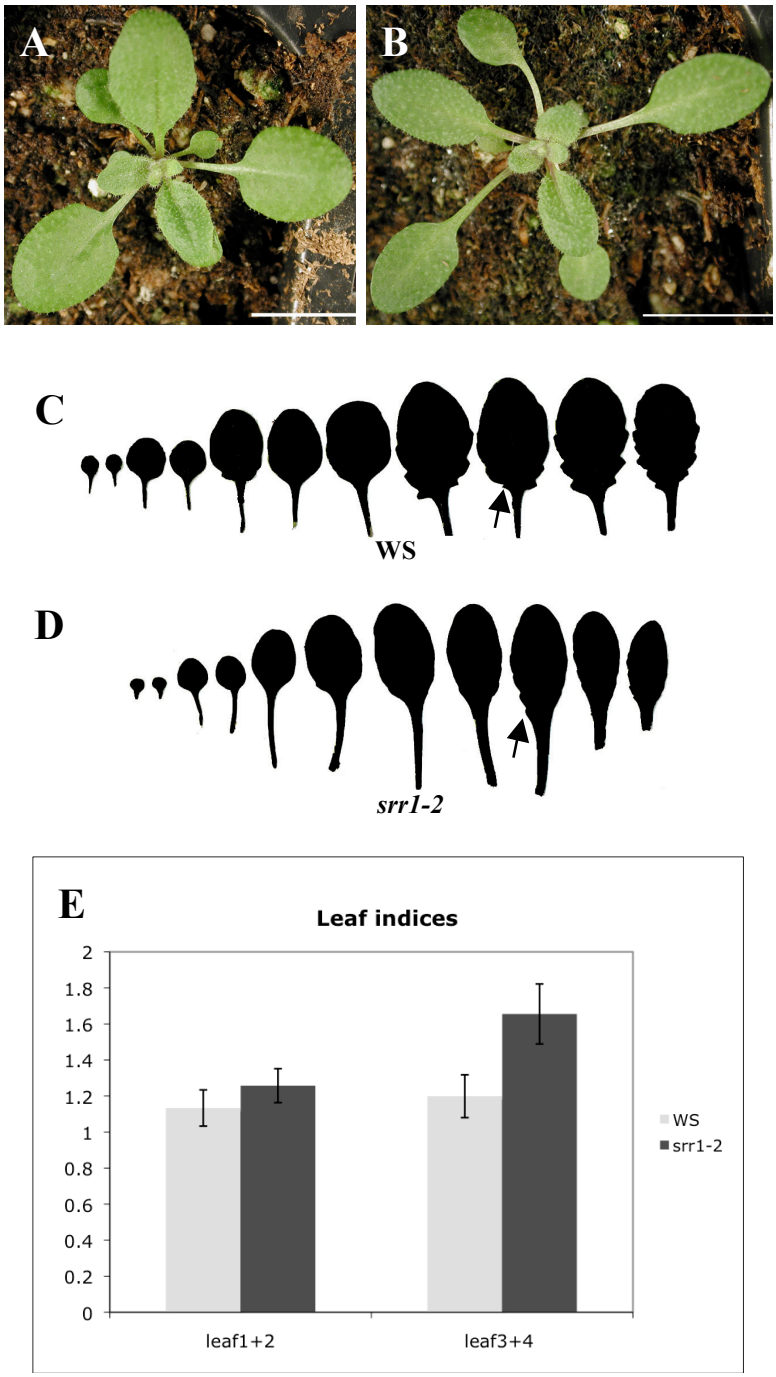

Fig. 2-1 Phenotypic characterization of *srr1-2*. (A) 19-days-after-germination WS produced expanded, oval-shaped leaves, in contrast to the flattened, narrow, elongated leaves formed in *srr1-2* (B). Outlines displayed overall shapes of WS wild-type (C) and *srr1-2* (D) rosette leaves. Note reduced distinction between leaf blades and petioles in *srr1-2*, compared to wild type (arrows). (E) The average leaf indices of wild type (grey bars) and *srr1-2* (dark grey bars) showed the leaf blade expansion defect in mutants was relatively subtle in the first leaf pair (leaf1+2) and more prominent in the second pair (leaf 3+4). (Bars = 1cm)

Light conditions have been shown to influence various developmental processes in plants, especially leaf photomorphogenesis [5, 11]; for example, the formation of sun leaves with several layers of palisade mesophyll cells are easily distinguished from shade leaves with one layer of palisade mesophyll cells [11]. Functional photoreceptors and regulators allow plants to perceive and respond to their environments with specific modifications to leaf morphogenesis [5]. Mutations in *phyB* cause a reduction in leaf length, suggesting the importance of light perception in leaf morphogenesis [5]. In order to examine the effects of light conditions on *srr1-2* leaf phenotypes, wild-type and mutant plants were grown under continuous, high-intensity light conditions (24-hr light, 220 μmol m^{-2} s^{-1}, 22 ^{o}C). As shown in Fig. 2-2A and C, wild-type leaves were dark green and well expanded. In contrast, leaf blade expansion and blade-petiole distinction in *srr1-2* was dramatically reduced under these conditions, and mutant leaves became strap-like (Fig. 2-2B, D). Furthermore, *srr1-2* leaves were distinctly pale green compared to wild type (Fig. 2-2A-B).

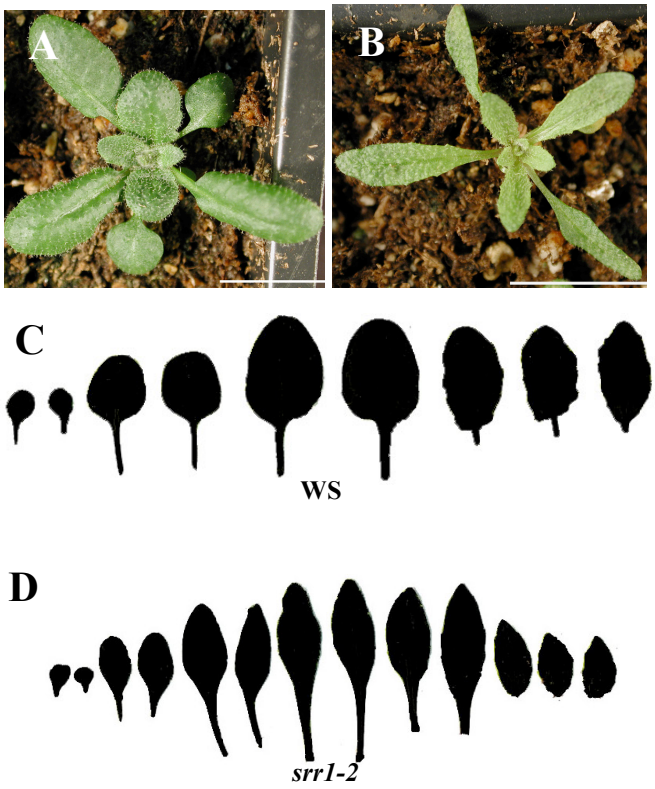

Fig. 2-2 *srr1-2* leaf phenotypes were exacerbated by constant, high-intensity light. Under constant, high-intensity light conditions (24-hr light, 220 μmol m^{-2} s^{-1}, 22 ^{o}C), WS wild type (A) displayed well expanded, dark-green leaves, whereas *srr1-2* mutants (B) produced dramatically narrow, pale-green leaves. Outlines showed the differences in the overall leaf shapes between WS wild type (C) and *srr1-2* (D).

SRR1 is a novel protein involved in the circadian clock regulation

Fine-scaled mapping suggested that the mutation in *srr1-2* occurred in a 170-kilo-base (kb) region on the long arm of chromosome five. This area is composed of 56 genes. Direct sequencing of the coding region of several candidate genes revealed a single base 'G' to 'A' substitution on the second exon of the At5g59560 coding region. This base transition resulted in the conversion of the tryptophan-encoding TGG codon to the premature TGA stop codon (Fig. 2-3A). To confirm the mutation was responsible for the

leaf developmental defects in *srr1-2,* the wild-type genomic fragment of At5g59560 encompassing the promoter, coding region and terminator was isolated and transformed into *srr1-2* mutant plants. Fifteen T1 transgenic plants showed leaf phenotypes as well as the leaf indices of the first and second leaf pairs similar to wild type (Fig. 2-3B and D). The light hypersensitivity of *srr1-2* was also rescued by the transformation (Fig. 2-3C). These results confirmed that the isolated mutation caused *srr1-2* leaf phenotypes. Additionally, a 1.7-kb promoter of At5g59560 was fused to a GUS-reporter gene and transformed into wild-type plants to examine the expression pattern of At5g59560 in Arabidopsis seedlings. GUS staining assays showed that At5g59560 was predominantly expressed in primary roots, vasculature of cotyledons, true leaves, inflorescence stems, cualine leaves and flowers (Fig. 2-3E-G).

At5g59560 was previously described in the *sensitivity to red light reduced (srr) 1-1* mutant [8]. *srr1-1* was primarily identified by hypocotyl and petiole elongation and a reduction in the chloroplast accumulation under the monochromatic red light. The protein encoded by *SRR1* contain no recognizable functional domain and an SRR1 domain that is conserved among different eukaryotes [8]. A protein localization assay reveals that SRR1 is found in both cytoplasm and nuclei [8]. Although a molecular function of SRR1 is unknown, gene expression analysis has demonstrated that rhythmic expression of several circadian clock regulators was disturbed [8]. This suggests the involvement of *SRR1* in the circadian clock regulation. However, distinct from other circadian clock regulators, expression of *SRR1* is arrhythmic but inducible by light [8]. To confirm that *srr1-2* was allelic to *srr1-1,* an allelism test was conducted by crossing *srr1-2* to *srr1-1.* The leaf indices of *srr1-1* and the *srr1-2* x *srr1-1* individuals were compared to Columbia (Col)

wild type. Resembling *srr1-2,* the mutants and the F1 individuals displayed average leaf indices similar to wild type in the first leaf pair and the higher average indices than wild type in the second leaf pair (Fig. 2-3D). Additionally, WS wild-type and *srr1-2* mutant seedlings were entrained under the diurnal conditions (12 hr: 12hr, light/22^{o}C: dark/12^{o}C) and released to the continuous light, 22^{o}C conditions. As shown in Fig. 2-4, the expression of circadian clock regulators including *TIMING of CAB EXPRESSION (TOC) 1, CIRCADIAN CLOCK ASSOCIATED (CCA) 1, LATE ELONGATED HYPOCOTYL (LHY) 1* in the *srr1-2* seedlings displayed a more rapid accumulation, compared to those of WS wild-type seedlings. On the other hand, the oscillation of *GIGANTEA (GI)* became shorter in *srr1-2* as opposed to the 24-hour cycling in wild type (Fig. 2-4). These results validated that *srr1-2* was indeed a novel allele of the *srr1-1* mutant.

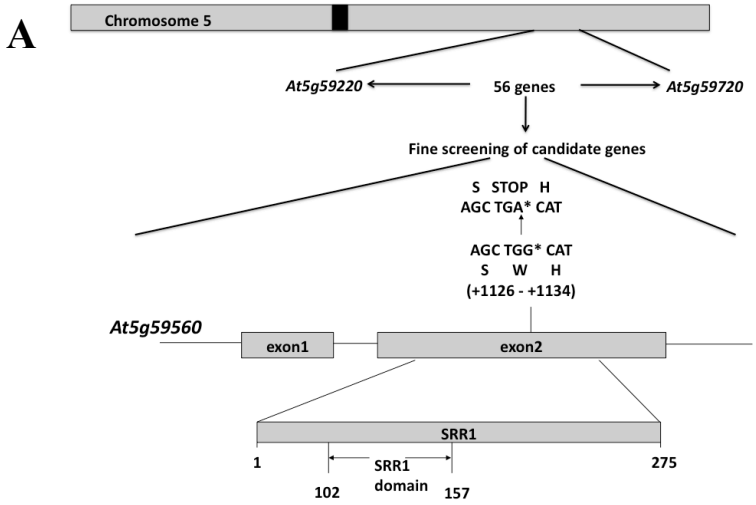
A
Chromosome 5
At5g59220
56 genes
At5g59720
Fine screening of candidate genes
S STOP H
AGC TGA* CAT
AGC TGG* CAT
S W H
(+1126 - +1134)
At5g59560
exon1
exon2
SRR1
1
102
SRR1
domain
157
275

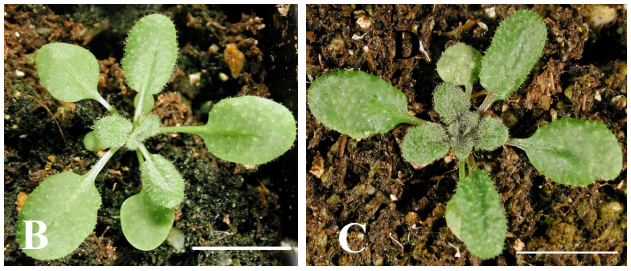
B
C

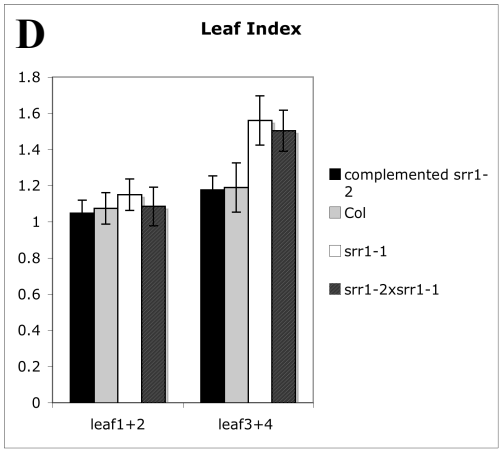
D
Leaf Index
1.8
1.6
1.4
1.2
1
0.8
0.6
0.4
0.2
0
leaf1+2
leaf3+4
complemented srr1-2
Col
srr1-1
srr1-2xsrr1-1

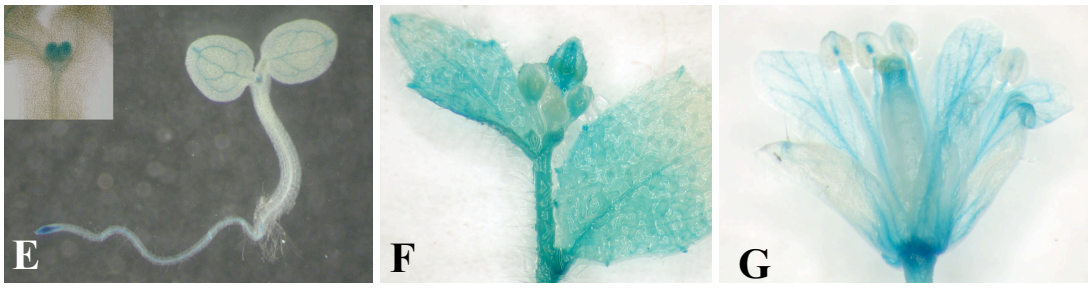
E
F
G

Fig. 2-3 Molecular characterization of *SRR1*. Map-based cloning revealed a non-sense mutation causing a premature stop codon on the second exon of At5g59560 encoding a novel protein with an SRR1 domain (A). Transgenic *srr1-2* harboring wild-type At5g50560 displayed phenotypes similar to wild type under long-day (B, 16-hr/8-hr light/dark, 150 μmol m^{-2} s^{-1}, 22 ^{o}C) and constant, high-intensity light (C, 24-hr light, 220 μmol m^{-2} s^{-1}, 22 ^{o}C) conditions. Leaf indices confirmed the rescued phenotypes of transgenic *srr1-2* (black bars) (D). (D) *srr1-1* (light-grey bars) and *srr1-2*x*srr1-1* F1 plants (dark-grey bars) also displayed increases in leaf indices, compared to Col wild type (white bars). Expression of *SRR1* was detected in primary roots (E), vasculature of cotyledons (E), true leaves (inset in E), cauline leaves (F), and flowers (F). (Bars in B-C = 1cm)

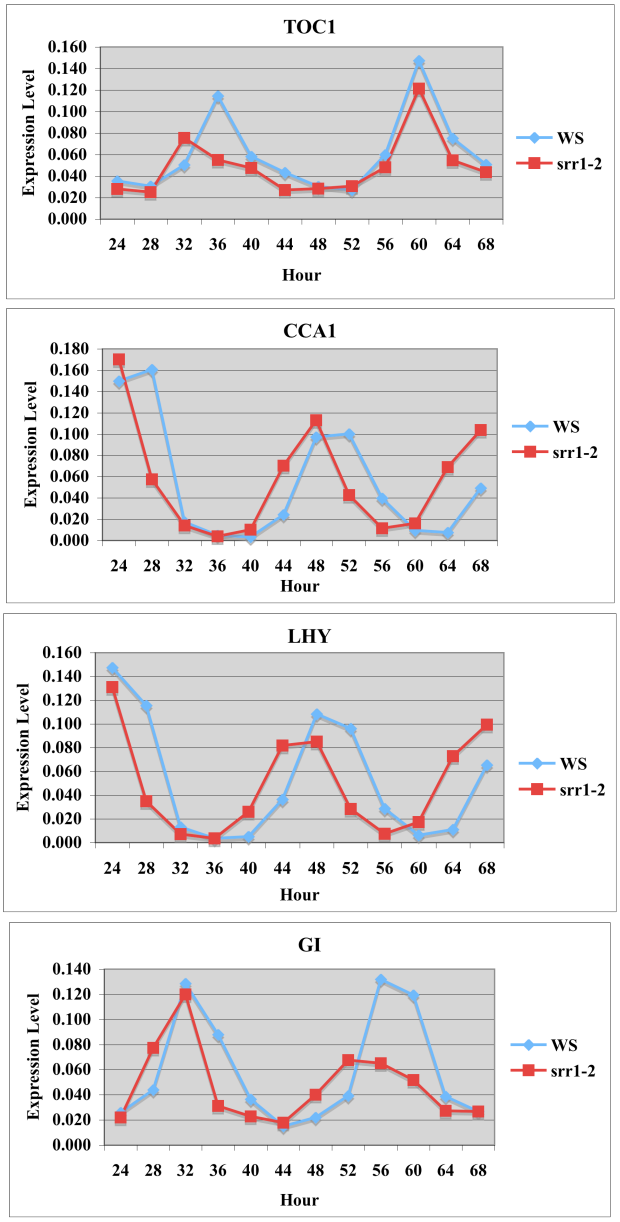

Fig. 2-4 Expression patterns of circadian clock regulatory genes in *srr1-2.* Similar to *srr1-1* mutants, *srr1-2* (red) displayed early peaks in *TOC1, CCA1, LHY* and a shorter oscillatory period in GI, compare to wild type (blue).

Genetic relationships between *srr1-2* and leaf developmental mutants

There are several leaf developmental mutants previously described in Arabidopsis. Among these are mutants containing mutations in genes encoding tranlastional machineries [4, 6, 12, 15]. They are particularly of interest due to their abilities to dramatically enhance leaf polarity defects in various mutants including *as1, as2, rev* single and *kan1 kan2* double mutants [12]. This indicates the existence of the regulation at the translational level in leaf morphogenesis. In this study, *arrow (arw)1-1* and *pointed-first-leaves (pfl) 2-2* were crossed to *srr1-2* single mutants.

The effects of the mutation in *arw1-1* single mutants included the formation of pointed, elliptical, flat leaves with pale green on the adaxial side (Fig. 2-5A). A single base mutation disrupting the splice site of intron 5 of At1g72320 has previously been identified [4]. This gene encodes a protein containing Pumilio/PUF RNA-binding domains. A molecular study has shown that the protein is involved in the cleavage of pre-rRNA during the bisosynthesis of 18S rRNA . *srr1-2* was crossed to *arw1-1* and its progeny was allowed for self-fertilization in order to obtain the F2 generation. However, F2 generation individual plants displayed only either *srr1-2* or *arw1-1* single mutant phenotypes. Seeds of *arw1-1*-like F2 plants were sowed and screened for potential *srr1-2 arw1-1* double mutants. Unexpectedly, a number of individual plants in these F3 families exhibited the leaf phenotypes similar to *srr1-2* single mutants (Fig. 2-5B). The ratio of *arw1-1*-like to *srr1-2*-like plants in this population was 2.5:1, suggesting the segregation of the *srr1-2* mutation and an epistatic effect of *srr1-2* over *arw1-1.* In order to test this speculation, a DNA-based marker was applied and confirmed that these plants were homozygous for the *arw1-1* mutation. These results indicate the common leaf-

developmental pathway between the two genes with *SRR1* positioned upstream of *ARW1*. Due to the relationship of the two genes and *SRR1* involvement in circadian clock regulation, expression of the circadian clock regulators in *arw1* was examined. Different from *srr1-2,* the expression patterns of *TOC1, CCA1, LHY* and *GI* in *arw1* were relatively similar to those of Col wild type (Fig. 2-6).

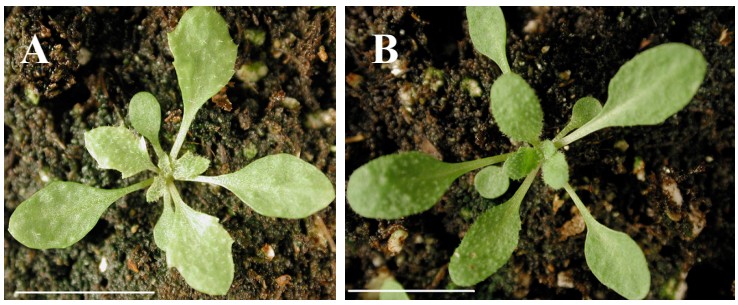

Fig. 2-5 Epistatic interaction of *srr1-2* over *arw1-1.* (A) Pointed-tip and pale-green phenotypes were observed in *arw1-1* single mutants. However, the leaf phenotypes of *srr1-2 arw1-1* double mutants (B) were similar to those of *srr1-2* single mutants suggesting an epistatic effect of *srr1-2* over *arw1-1.* (Bars = 1cm)

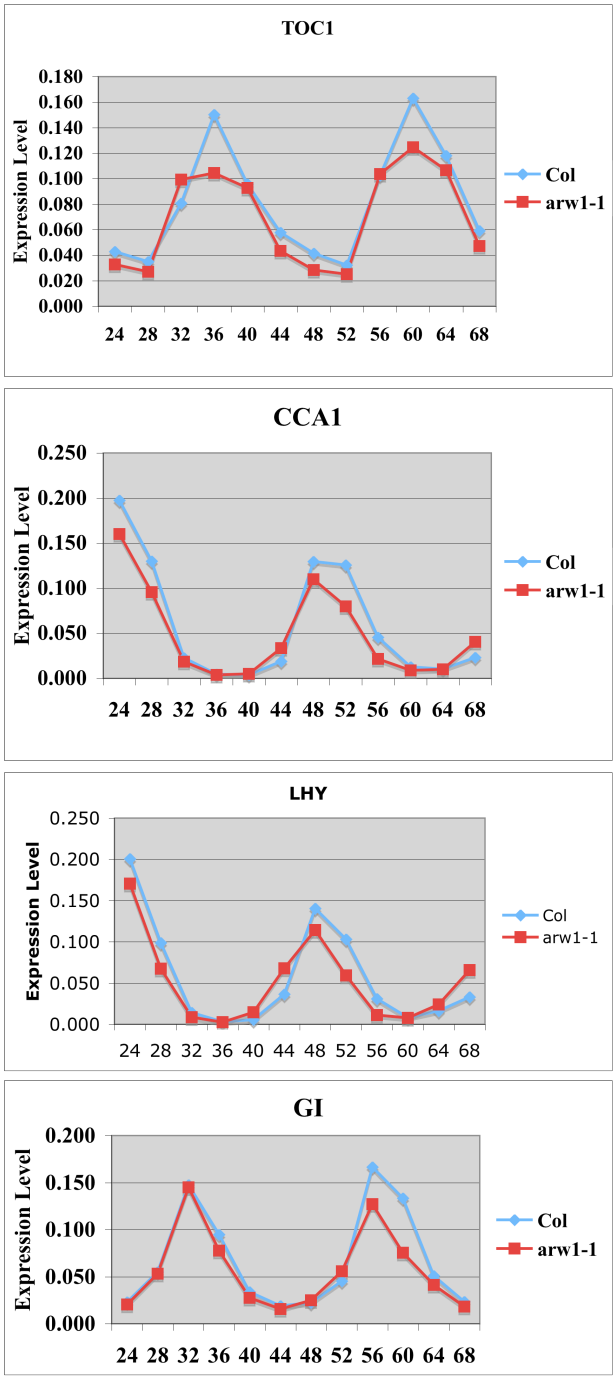

Fig. 2-6 Expression patterns of circadian clock regulatory genes in *arw1-1*mutants. Although *ARW1* potentially functions downstream of *SRR1* in the same pathway, expression patterns of circadian clock regulatory genes including *TOC1, CCA1, LHY* and *GI* in *arw1-1* (red) were relatively similar to wild type Col (blue).

pfl2-2 mutants produced leaves with pointed tips resembling an arrow shape similar to those of *arw1-1* single mutants. These leave were associated with the pale-green color on the upper side of the leaves compared to wild type (Fig. 2-7A). The causative mutation of *pfl2-2* is a T-DNA insertion in the At4g00100 gene that encodes the ribosomal protein S13 (RPS13) of the 40S ribosomal small subunit (Chapter 3). When *srr1-2* was present in the *pfl2-2* background, a synergistic interaction was observed. *srr1-2 pfl2-2* double mutants displayed the small stature phenotype compared to the parental single mutants (Fig. 2-7B). Furthermore, leaf blade expansion of the first leaf pair was dramatically reduced and shoot apical meristems were enlarged (Fig. 2-7B-C). These phenotypes were not seen in either *srr1-2* or *pfl2-2* single mutants. A close relationship between leaf morphogenesis and shoot apical meristems has been previously described [7, 9]. Briefly, shoot apical meristems may be involved in the determination of adaxial cell identity. Separation of leaf primordia results in the formation of radialized lateral organs exhibiting ectopic abaxialization [9]. Despite the enlarged shoot apical meristems and the extremely narrow leaves, the midvein of *srr1-2 pfl2-2* double mutant first leaf pair still displayed xylem adaxial to phloem (Fig. 2-7D). This result suggests *SRR1* and *RPS13* may belong to two independent pathways that interact with each other to promote leaf blade expansion.

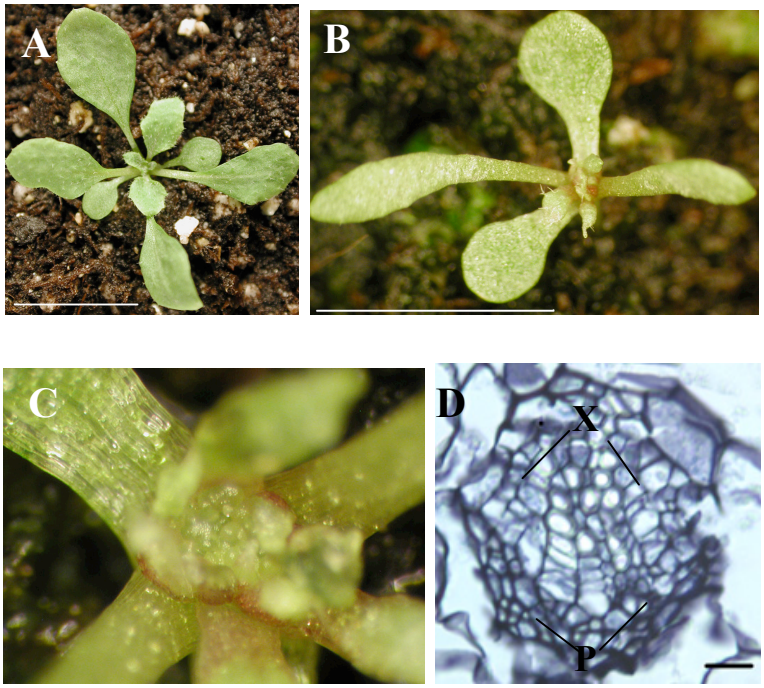

Fig. 2-7 Synergistic interaction between *srr1-2* and *pfl2-2*. (A) *pfl2-2* mutants exhibited pointed leaves relatively similar to *arw1-1*. (B) The leaf-blade-expansion defect of *srr1-2* mutants was dramatically enhanced in *srr1-2 pfl2-2* double mutants. (C) Enlarged shoot apices were also observed in double mutants. In spite of an extreme reduction in leaf blade expansion, double mutants displayed normal patterning of the vascular system in the first leaf pair forming xylem adaxial to phloem in the midvein (D). (Bars in A-B = 1cm; Bar in D = 0.1μm) (X = xylem, P = phloem)

Additive effects between *srr1-2* and leaf polarity mutants

An intimate link between leaf polarity establishment and leaf blade expansion stems from the study of a number of mutants with severe leaf polarity defects [1, 2, 13, 14]. These mutants produce radialized lateral organs associated with the loss of blade growth indicating the requirement of leaf polarity for leaf blade expansion. In order to investigate the relationships between *SRR1* and other leaf polarity regulators, a genetic study was conducted. Among various leaf polarity mutants, *as1-1, as2-1* single and *kan1 kan2* double mutants were relatively sensitive to additional mutations. *as1-1* and *as2-1*

single mutants similarly produced downward-curling, triangular shaped, asymmetric leaves with the wavy surface, whereas *kan1 kan2* double mutants exhibited narrow, pointed leaves with ectopic abaxial outgrowths (Fig. 2-8A, C, E). The examination of leaf phenotypes of the combinatorial double and triple mutants displayed the presence of additive effects between *srr1-2* and the other leaf polarity mutants. Leaf phenotypes of *srr1-2 as1-1* and *srr1-2 as2-1* double were composed of the pale-green phenotype of *srr1-2* and the triangular, asymmetric shapes similar to those of *as1-1* and *as2-1* single mutants (Fig. 2-8B, D). A reduction of the downward-curling phenotype in both double mutants was observed and likely reflected the decrease of leaf blade expansion caused by the *srr1-2* mutant background. Leaves of *srr1-2 kan1 kan2* triple mutants were narrow with pointed tips and ectopic abaxial outgrowths resembling to those of *kan1 kan2* double mutants (Fig. 2-8F). Additionally, they appeared pale-green showing the effect of the *srr1-2* single mutant background (Fig. 2-8F). These results suggest *SRR1* may exert its function on a leaf developmental pathway that is independent to those of the leaf polarity regulators.

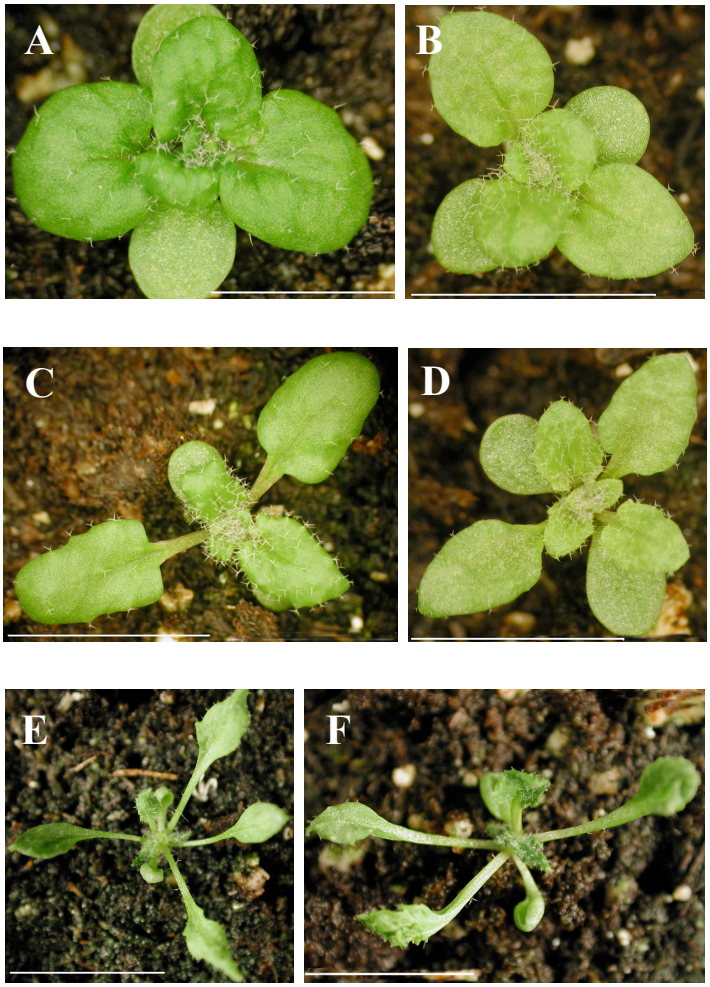

Fig. 2-8 Genetic interactions between *srr1-2* and leaf polarity mutants. *as1-1* (A) and *as2-1* (C) single mutants similarly produced lobed, asymmetric leaves with mild defects in petioles. (E) *kan1 kan2* double mutants displayed severe leaf-morphological defects including narrow, pointed leaves with ectopic abaxial outgrowths. Although leaf polarity establishment has been proposed as a requirement for leaf blade expansion, only additive effects were observed in *srr1-2 as1-1* (B), *srr1-2 as2-1* (D) double and *srr1-2 kan1 kan2* (F) triple mutants (see text). (Bars = 1cm)

Discussion

The data present here is obtained from the study of *srr1-2* mutants in which leaf blade expansion is reduced. The identification of the mutation reveals that *SRR1* is involved in this developmental process. *SRR1* encodes for a novel protein with an unknown function due mainly to the absence of recognizable functional domains [8]. However, it contains an SRR1 domain that is conserved among other proteins found in other eukaryotes including rice, yeast, Drosophila, mouse and human [8]. Disruption of *BERNOMYL RESISTANCE (BER) 1,* encoding a yeast ortholog of SRR1, resulted in the resistance to bernomyl and nocodazole, microtubule-depolymerizing drugs [3]. This suggests BER1 either directly or indirectly is involved in the stability of microtubules [3]. Although synthetic lethal screens of the *ber1Δ* knock-out yeast strain yielded several BER1 potential protein partners [3], molecular functions of these proteins are relatively diverse, rendering it difficult to predict the SRR1 molecular activities through its yeast orthologous counterpart.

Rhythmic expression of several genes that are involved in and regulated by the circadian clock is perturbed in *srr1-1* [8]. Whether *SRR1* participates in this regulation directly or indirectly still remains unclear. The epistatic interaction between *srr1-2* and *arw1-1* indicates that *SRR1* and *ARW1* may reside in the same pathway that promotes proper formation of the leaf shape. Different from *srr1-2,* rhythmic expression of the tested genes in *arw1-1* mutants was relatively unchanged. There are two possible explanations for this observation. *SRR1* regulates the rhythm of circadian clock regulators at the transcriptional level, whereas *ARW1* may act downstream of this interaction in the translational level since the protein facilitates the generation of 18S rRNA [4].

Alternatively, *SRR1* and *ARW1* may commonly belong to a leaf developmental pathway that is independent from the role of *SRR1* in the circadian clock regulation. Further characterization of *SRR1* molecular functions will enable us to better understand the control of leaf morphogenesis and its interconnection with circadian clock and translational regulation.

Genetic relationships between *srr1-2* and other leaf polarity mutants are particularly remarkable in terms of leaf morphogenesis study. Mutations in several ribosmomal proteins have been previously shown to result in the enhancement of leaf polarity defects in the background of *as1, as2, rev* single and *kan1 kan2* double mutants [6, 15]. These results suggest an existence of a translational regulation that interacts with those of conventional leaf polarity determinants to promote leaf polarity establishment. *SRR1* potentially belongs to the same pathway as *ARW1* and synergistically interacts with *RPS13.* Mutations in *ARW1* and *RPS13* dramatically enhance the polarity defects of *as1,as2, rev* single and *kan1 kan2* double mutants {[4] and Chapter3}. However, the additive effects of *srr1-2* in the leaf polarity mutant backgrounds suggest their separate, non-interacting contributions in leaf morphogenesis. These additive effects indicate that leaf polarity establishment, although indispensable, may be unable to solely determine proper leaf blade expansion. Based on the data present in this study, a proposed model of leaf morphogenesis involving *SRR1*, the translational machineries and the leaf polarity genes is shown in Fig. 2-9. Expression of *SRR1* is induced by light [8]. Subsequently, *SRR1* exerts its function upstream of *ARW1* in a pathway that interacts with *RPS13* and mainly contributes to leaf blade expansion. In parallel, *ARW1* and *RPS13* cooperate with

leaf polarity genes to promote leaf polarity establishment through another distinct pathway. Together, these components lead to the formation of functional mature leaves.

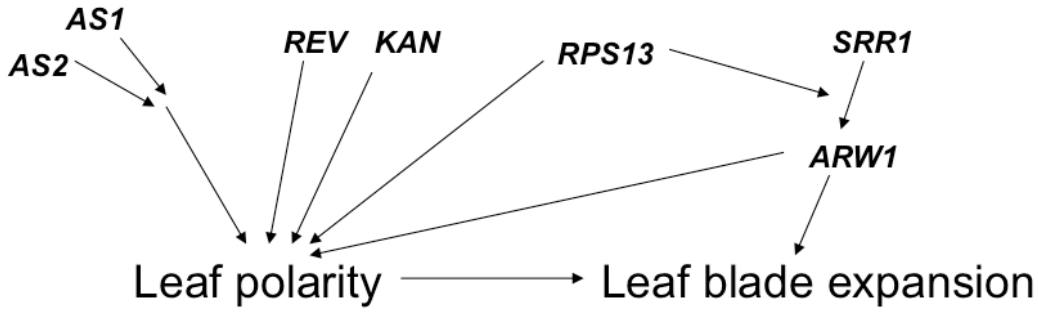

Fig. 2-9 A proposed model of the key determinants of leaf morphogenesis. *SRR1* expression is inducible by light. *ARW1* acts downstream to *SRR1* in the same developmental pathway that synergistically interacts with *RPS13* to promote leaf blade expansion. *ARW1* and *RPS13* also function in other pathways that are independent from *SRR1* and interact with those of *AS1, AS2, KAN1* and *KAN2* to promote leaf polarity establishment.

Materials and Methods

Plants and growth conditions

The *srr1-2* mutant line used in this research was initially isolated from an ethy-methanesulfonate (EMS)- mutagenized population. The mutation was present in the WS wild-type background. Unless specified otherwise, wild-type and mutant seeds were germinated on Promix (Premier Horticulture Inc., Canada) under long-day conditions (16hr/8hr light/dark), 150 $\mu mol.m^{-2}.s^{-1}$, 22 ^{o}C.

Genetic analysis between *srr1-2* and other mutants

To obtain combinatorial double mutants, *srr1-2* single mutants were used as the maternal parent and crossed out to other single mutants including *arw1-1, pfl2-2, as1-1* and *as2-1*. The F1 progeny was allowed for self-fertilization to create the F2 population. The analysis of the double mutants was performed in the F3 generation obtained from *arw1-1-, as1-1-* and *as2-1-* like F2 plants segregating for the *srr1-2* mutation. *srr1-2 pfl2-2* double mutant plants were obtained from the F2 population.

For the analysis of *srr1-2 kan1 kan2* triple mutants, maternal *SRR1/srr1-2 kan1/kan1* plants were crossed to *kan1/kan1 KAN2/kan2* mutants to obtain *SRR1/srr1-2 kan1/kan1 KAN2/kan2* plants. These plants were allowed to self-fertilize to create *srr1-2/srr1-2 kan1/kan1 KAN2/kan2* plants in which self-progeny segregate for *srr1-2 kan1 kan2* triple mutants.

Plasmid construction and plant transformation

A 3.4 kb genomic fragment of *SRR1* encompassing the promoter, coding region and terminator was isolated from the transformation-competent bacterial artificial chromosome (TAC) JAtY58P01 (http://www.jicgenomelab.co.uk) by using *SpeI* digestion. The fragment was cloned into the *XbaI* site in pCAMBIA1300 containing hygromycin resistance gene (www.cambia.org). The plasmid was transformed into *Agrobacterium tumefaciens* strain GV3101 (pMP90). 45-days old *srr1-2* plants were then transformed with this construct by the floral dip method. T1 seeds were sowed on 1/2X MS solid medium containing 30 μg/ml hygromycin (Calbiochem) for selection of transgenic seedlings. The promoter of *SRR1* was amplified from the same plasmid used for the complementation analysis with high-fidelity Hercules polymerase enzymes (Stratagene) with SRR1-promF/ SRR1-promR primers. The promoter was subsequently cloned into pMDC163 containing the GUS reporter gene by using Gateway LR Clonase® Enzyme mix (Invitrogen). The plasmid was then transformed into *A. tumefaciens* and WS wild-type plants by the floral dip method. Ten independent T2 lines were used in GUS staining. Briefly, transgenic seedlings were fixed with 80% acetone and rinsed with GUS-rinsing solution (50mM sodium phosphate buffer (pH 7.2), 2 mM $K_4[Fe(CN)_6]$, 2 mM $K_4[Fe(CN)_6]$). The rinsing solution was removed, and the seedlings were incubated in a new rinsing solution with 1mg/ml X-Gluc at room temperature until the blue precipitate was visible. Afterward, seedlings were subject to the ethanol series for dehydration and chloroplast removal to facilitate visualization.

Circadian clock entraining and RNA preparation

WS, Col, *srr1-2,* and *arw1-1* seeds were surface-sterilized by soaking in washing solution (70% ethanol and 0.05% TritonX-100) for 10 minutes. Subsequently, washing

solution was removed and replaced by 100% ethanol for 5 minutes. 100% ethanol was removed and replaced with new 100% ethanol. Seeds were spread on filter paper, allowed to air-dry, and germinated on 1/2X Murashige& Skoog media. Seedlings were entrained under 12-hr/12-hr: light (22^{o}C)/dark (12^{o}C) conditions with 150 μmol.m^{-2}.s^{-1} illumination for 7 days and subsequently released to constant-light and temperature conditions (150 μmol.m^{-2}.s^{-1}, 22^{o}C) for one day. Afterwards, sample seedlings were collected every four hours.

RNA extraction of samples at each time point was performed by using RNeasy Plant Mini Kit (QIAGEN). Two-μg of total RNA of each time point was used for reverse-transctiption reactions with Superscript III Reverse Transcriptase and oligo-dT primers according to the manufacturer's instructions (Invitrogen). Standard curves were constructed by pooling cDNA of each sample to create a dilution series and used for normalization of the samples. cDNA of each sample was diluted 20 times and used for cDNA quantification with iCycler-MyiQ detection system (BIORAD). Sequences of the primers are listed in appendix 1.

Histology

To examine the arrangement of vascular tissues, leaves were subjected to paraplast infiltration for sectioning. Briefly, leaf samples were fixed in FAA fixative solution (50% ethanol, 5% (v/v) acetic acid, 3.7% (v/v) formaldehyde). Subsequently, samples were dehydrated through the ethanol series (50%, 70%, 85%, 95%, and 100%) and Histoclear (National Diagnostics), and infiltrated with paraplast (Fisher). For sectioning, infiltrated samples were embedded in the paraplast and sectioned by the

rotary microtome (Richert Inc.). Sections were stained with 0.1% toluidine blue and permanently fixed with permount (Fisher).

References

1. Emery JF, Floyd SK, Alvarez J, Eshed Y, Hawker NP, Izhaki A, Baum SF, Bowman JL: Radial patterning of Arabidopsis shoots by class III HD-ZIP and KANADI genes. Curr Biol 13: 1768-74 (2003).
2. Eshed Y, Izhaki A, Baum SF, Floyd SK, Bowman JL: Asymmetric leaf development and blade expansion in Arabidopsis are mediated by KANADI and YABBY activities. Development 131: 2997-3006 (2004).
3. Fiechter V, Cameroni E, Cerutti L, De Virgilio C, Barral Y, Fankhauser C: The evolutionary conserved BER1 gene is involved in microtubule stability in yeast. Curr Genet 53: 107-15 (2008).
4. Huang T: Transcriptional and translational regulation of leaf polarity, pp. 131p. Rutgers, the State University of New Jersey, New Brunswick (2009).
5. Kozuka T, Horiguchi G, Kim GT, Ohgishi M, Sakai T, Tsukaya H: The different growth responses of the Arabidopsis thaliana leaf blade and the petiole during shade avoidance are regulated by photoreceptors and sugar. Plant Cell Physiol 46: 213-23 (2005).
6. Pinon V, Etchells JP, Rossignol P, Collier SA, Arroyo JM, Martienssen RA, Byrne ME: Three PIGGYBACK genes that specifically influence leaf patterning encode ribosomal proteins. Development 135: 1315-24 (2008).
7. Reinhardt D, Frenz M, Mandel T, Kuhlemeier C: Microsurgical and laser ablation analysis of leaf positioning and dorsoventral patterning in tomato. Development 132: 15-26 (2005).
8. Staiger D, Allenbach L, Salathia N, Fiechter V, Davis SJ, Millar AJ, Chory J, Fankhauser C: The Arabidopsis SRR1 gene mediates phyB signaling and is required for normal circadian clock function. Genes Dev 17: 256-68 (2003).
9. Sussex IM: Morphogenesis in Solanum tuberosum L.: experimental investigation of leaf dorsiventrality and orientation in the juvenile shoot. Phytomorphology 5: 286-300 (1955).
10. Tsuge T, Tsukaya H, Uchimiya H: Two independent and polarized processes of cell elongation regulate leaf blade expansion in Arabidopsis thaliana (L.) Heynh. Development 122: 1589-600 (1996).
11. Tsukaya H: Leaf shape: genetic controls and environmental factors. Int J Dev Biol 49: 547-55 (2005).
12. Van Lijsebettens M, Vanderhaeghen R, De Block M, Bauw G, Villarroel R, Van Montagu M: An S18 ribosomal protein gene copy at the Arabidopsis PFL locus affects plant development by its specific expression in meristems. Embo J 13: 3378-88 (1994).
13. Waites R, Hudson A: *phantastica*: a gene required for dorsoventrality of leaves in *Antirrhinum majus*. Development 121: 2143-2154 (1995).
14. Williams L, Grigg SP, Xie M, Christensen S, Fletcher JC: Regulation of Arabidopsis shoot apical meristem and lateral organ formation by microRNA miR166g and its AtHD-ZIP target genes. Development 132: 3657-68 (2005).
15. Yao Y, Ling Q, Wang H, Huang H: Ribosomal proteins promote leaf adaxial identity. Development 135: 1325-34 (2008).

Chapter 3

Ribosomal proteins RPS13 and its role in leaf polarity establishment

Abstract

Introduction

The regulation of leaf morphogenesis occurs at different levels including transcription, post-transcription, translation and post-translation [1, 12, 13, 23]. Described in this chapter is phenotypic characterization of *pointed-first-leaves (pfl) 2-2,* in which the ribosomal protein *RPS13* gene is disrupted by a T-DNA insertion. *plf2-2* exhibited the pointed-leaf phenotype similar to other ribosomal protein mutants [13, 17, 23]. The examination of the paradermal layers showed the disturbance in adaxially and abaxially anatomical structures. Genetic interactions between *pfl2-2* and other leaf polarity mutants revealed synergistic contribution between *RPS13* and the leaf polarity genes in leaf polarity establishment. These results emphasize the involvement of RPS13 in a translational regulation of leaf morphogenesis.

Result

pfl2-2 mutants exhibited various leaf morphological defects

The *pfl2-2* mutant line was derived from the SAIL_747_B10 T-DNA insertion line [15]. The mutant was primarily recognized by its formation of flattened, narrow, pale-green leaves with pointed tips, as opposed to round, well-expanded, dark-green Columbia (Col) wild-type leaves (Fig. 3-1A-D). In order to examine the effects of the mutation on the mesophyll layer structures, wild-type and mutant leaves were subject to the chloral hydrate treatment. As shown in Fig. 3-1F, in wild type, the adaxial mesophyll layer was composed of round-shaped cells that were densely packed to facilitate light capture, and the abaxial mesophyll layer contained irregular-shaped cells associated with large intercellular spaces promoting gas exchange. Both adaxial and abaxial mesophyll layers of *pfl2-2* were disturbed. *pfl2-2* adaxial mesophyll cells were loosely packed and accompanied with large intercellular spaces, while the abaxial mesophyll layer contained smaller, less irregular-shaped cells (Fig. 3-1F). Additionally, the venation complexity was highly reduced in mutant first leaves as opposed to highly branching vasculature in the same leaves of wild type (Fig 3-1F-G). Despite these changes in leaf morphology, the midvein of mutant leaves was similar to wild type and composed of xylem on the adaxial side and phloem on the abaxial side (Fig. 3-1H-I).

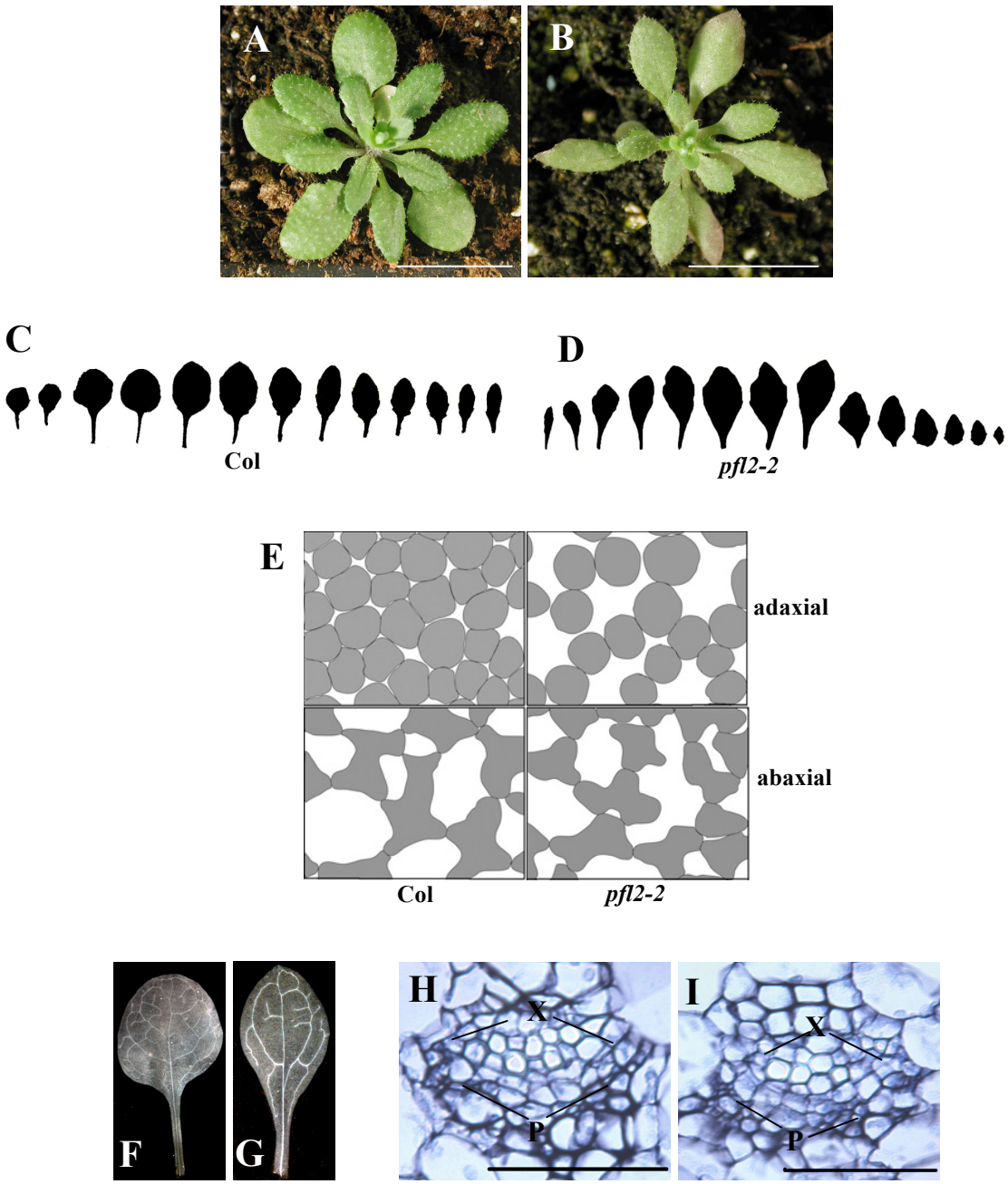

Fig. 3-1 Phenotypic characterization of *pfl2-2* compared to Col wild type. Twenty-seven day-after-germination Col wild type (A) and *pfl2-2* (B) displayed distinct leaf phenotypes (see text). Diagrams of leaf outlines show the rounded, well-expanded shape of wild type leaves (C) and pointed, narrow *pfl2-2* leaves (D). (E) Camera-lucida drawings of the adaxial and abaxial mesophyll layers demonstrated the disturbance in *pfl2-2,* compared to wild type. Venation complexity of the first leaves was higher in Col (F) than *pfl2-2* (G). Col (H) and *pfl2-2* (I) display normal vasculature patterning with xylem forming adaxial to phloem in the midvein of the first leaf pair. (Bars in A-B = 1cm, Bars in G-H = 0.5μm) (X = xylem, P = Phloem)

An F2 population generated from a test-cross produced 1,553 wild-type and 360 mutant plants. The ratio was 4.3:1 and relatively close to the 3:1 segregation ratio suggesting the mutation is transmitted as a single, recessive trait. The T-DNA insertion in the promoter of the *KAN3* gene was initially identified and considered the cause of the leaf phenotypes present in *pfl2-2.* However, a number of heterozygous *KAN3::*T-DNA-inserted plants also exhibited the mutant phenotypes, rejecting *KAN3::*T-DNA as the cause of the mutant phenotypes . To test whether an additional T-DNA insertion was present in the mutant genome, an inverse PCR (IPCR) analysis was employed. A DNA fragment was amplified by using the primers complimentary to the T-DNA sequence of the pDAP101 plasmid used for the generation of this mutant line [15]. Sequencing of this DNA fragment revealed a 40-bp border region matching the sequence of the 5'-untranslated region (UTR) of At4g00100 that encodes ribosomal protein RPS13 (Fig 3-2A). Another mutation in *RPS13* has been previously reported in the *pointed first leaves (pfl) 2* mutant [9]. Genotyping of Col, *pfl2-2* and Col/*pfl2-2* heterozygote with T-DNA and gene specific primers confirmed the presence of the T-DNA insertion (Fig. 3-2B). To verify that this T-DNA is responsible for the mutant leaf phenotypes, a genomic fragment of *RPS13* was amplified from wild type and transformed into the mutants. The transgenic mutants exhibited leaf phenotypes comparable to those of wild type, thus confirming the mutant phenotypes are caused by the disruption of the *RPS13* gene (Fig. 3-2C).

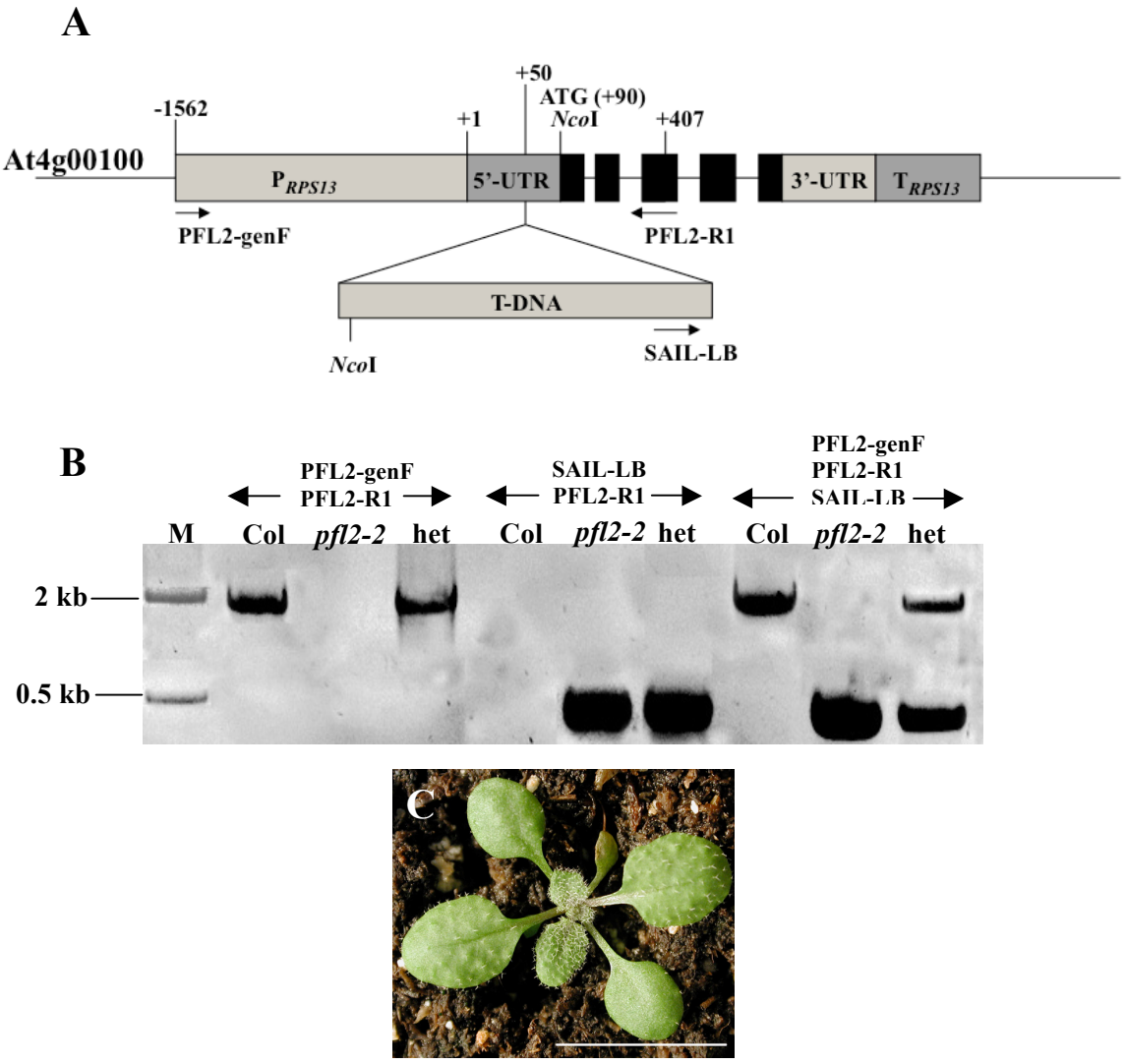

Fig.3-2 Isolation of the T-DNA insertion in *pfl2-2*. (A) A T-DNA insertion was identified on the 5'-UTR of the *RPS13* gene. (B) Genotyping of Col, *pfl2-2* and Col/*pfl2-2* heterozygote with pfl2promF/pfl2RTR1, sail-LB/pfl2RTR1 and pfl2promF/pfl2RTR1/sail-LB primer pairs validated the presence of the T-DNA insertion in At4g00100. (C) Transgenic *pfl2-2* (15-day-after-germination) harboring the wild-type genomic fragment of *RPS13* displayed leaf phenotypes comparable to wild type confirming the T-DNA insertion is responsible for the *pfl2-2* leaf phenotypes (Bar = 1cm).

Synergistic interactions between *pfl2-2* and leaf polarity mutants

The perturbation in the mesophyll layers of *pfl2-2* suggests the contribution of RPS13 to the determination of adaxial and abaxial cell fates (Fig. 3-1E). There are several key determinants required for adaxializaiton. *AS1* is an ortholog of *PHANTASTICA,* the first leaf polarity gene isolated from *Antirrhinum majus* [4, 19, 20]. The *as1-1* mutant exhibits the formation of lobed, triangular-shaped, asymmetric leaves with a wavy surface (Fig. 3-3A). Similarly, *as2-1* displays leaf phenotypes resembling those of *as1-1,* except the petioles of *as2-1* were relatively longer than those of *as1-1* (Fig. 3-3D). Both *as1-1* and *as2-1* exhibit mild defects of leaf polarity in the petioles [4, 11]. The mutation in *RPS13* enhanced the polarity defects of *as1-1* and *as2-1* as observed in the *pfl2-2 as1-1* and *pfl2-2 as2-1* double mutants (Fig. 3-3B, E). *pfl2-1 as1-1* double mutants produced extreme narrow leaves, and the most striking phenotype was the formation of radialized leaves that indicated a complete loss of leaf polarity (Fig. 3-3B-C). Similar to *pfl2-2 as1-1* double mutants, early leaves of *pfl2-2 as2-1* double mutants were relatively narrow, and subsequent leaves became radialized. *pfl2-2 as2-1* double mutants also produced lotus-leaf-like organs that are usually found in the stronger allele *as2-101* in the Landsber *erecta* (L*er)* background [22] (Fig. 3-3E). Additionally, ectopic abaxialization occurred in midveins of *pfl2-2 as1-1* and *pfl2-2 as2-1* radialized leaves as shown by xylem surrounded by phloem (Fig. 3-3H, J). This was in contrast to the arrangement of xylem and phloem situated on the adaxial and abaxial sides, respectively, in the parental single mutants (Fig 3-1I, 3-3G, I).

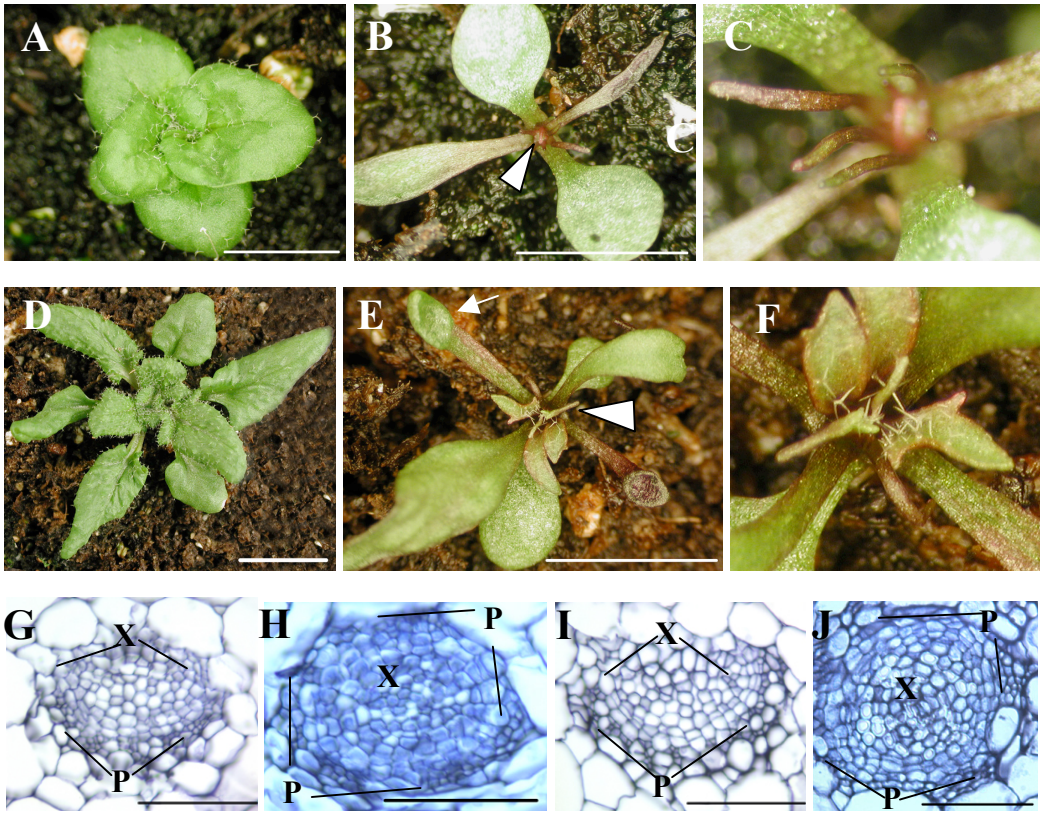

Fig. 3-3 Synergistic interactions between *pfl2-2* and *as1-1* and *as2-1* single mutants. *as1-1* (A) and *as2-1* (D) single mutants exhibited triangular-shaped, asymmetric leaves. Leaf polarity defects of *as1-1* and *as2-1* single mutants were dramatically enhanced in *pfl2-2 as1-1* (B) and *pfl2-2 as2-1* (E) double mutants as demonstrated by the formation of radialized structures (arrowheads in B and E). Lotus-leaf-like organs (arrow in E) were observed in *pfl2-2 as2-1* double mutants. Magnified views of radialized structures found in *pfl2-2 as1-1* (C) and *pfl2-2 as2-1* (F). Midveins of *as1-1* (G) and *as2-1* (I) single mutants displayed normal vasculature patterning as opposed to abaxialized midveins of *pfl2-2 as1-1* (H) and *pfl2-2 as2-1* (J) double mutants with xylem surrounded by phloem in the midvein. (Bars in A, B, D, E = 1cm, Bars in G-J = 0.5µm) (X = xylem, P = Phloem)

HD-ZIPIII genes, including *PHB, PHV,* and *REV,* have been demonstrated to determine the adaxial cell identity [7]. Their expression domains are confined to the adaxial side of leaf primordia [7]. *phb* and *phv* single mutants are aphenotypic, whereas *rev* single mutants produces only defective lateral and floral meristems and aberrant stem vasculature [14, 16]. As shown in Fig. 3-4A, *rev* rosette leaves were well expanded and relatively resembled those of wild type. In contrast, *pfl2-2 rev* double mutants produced pointed, pale-green leaves resembling those of *pfl2-2* single mutants during the early vegetative stage (Fig. 3-4B). Subsequently, several radialized leaves were formed (Fig. 3-4C). These radialized organs were abaxialized as demonstrated by xylem surrounded by phloem in their midveins (Fig. 3-4E), whereas *rev* single mutants displayed normal vasculature patterning (Fig. 3-4D). During the reproductive stage, while floral meristems in *pfl2-2* generated fertile flowers with no obvious defects (Fig. 3-4F), a number of flowers in *rev* single mutants were sterile due to the lack of pistils or stamens [16] (Fig. 3-4G). Furthermore, a greater degree of defects in floral meristems caused the formation of filamentous structures in *rev* (Fig. 3-4G). The floral meristem defects of *rev* single mutants were greatly enhanced in *pfl2-2 rev* double mutants. The development of floral organs was aborted in all of the meristems. This resulted in the sole formation of filamentous structures in double mutants.

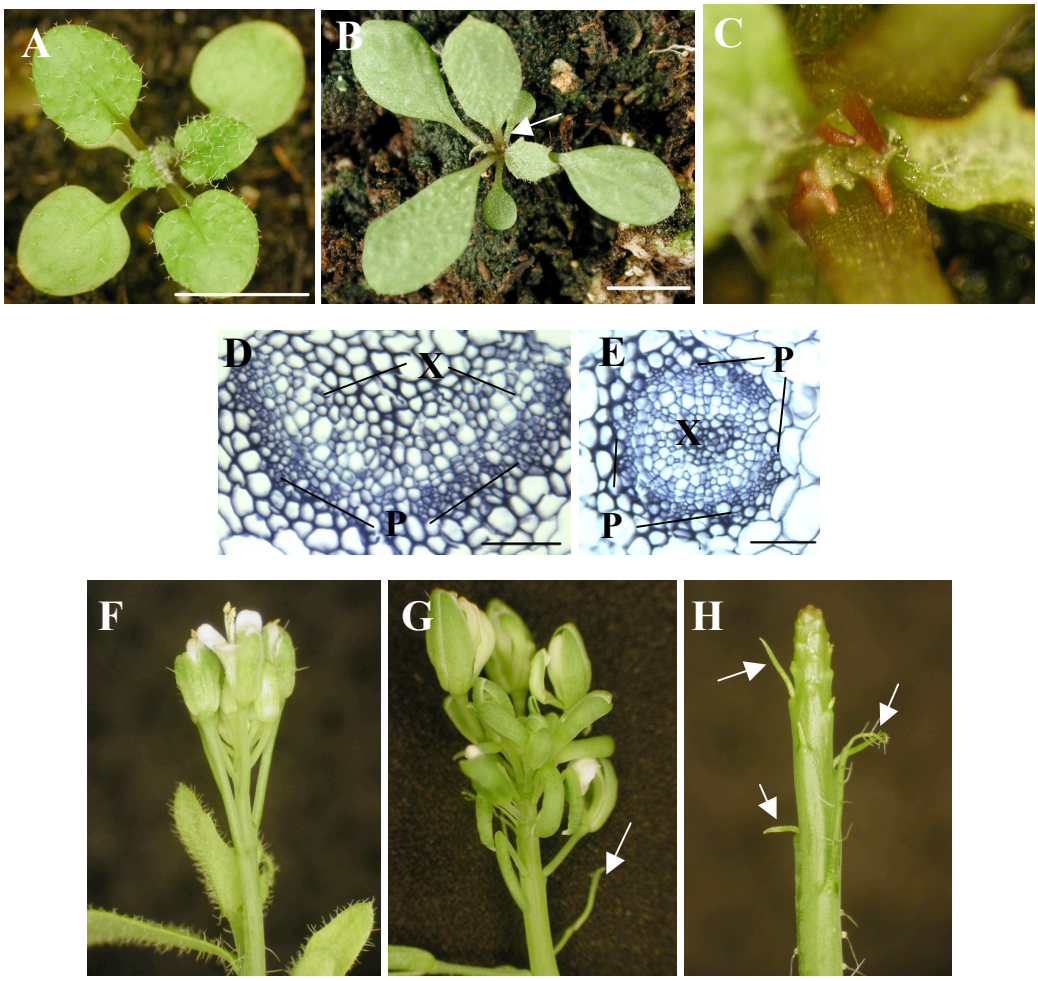

Fig. 3-4 Synergistic interaction between *pfl2-2* and *rev*. (A) *rev* single mutants displayed relatively normal leaf morphology. During early vegetative stage, *pfl2-2 rev* double mutants (B) produced early leaves similar to *pfl2-2* single mutants, and subsequent leaves became radialized (arrow). (C) Magnified views of radialized organs found in *pfl2-2 rev* double mutants. The midvein of *rev* single mutant leaves displayed xylem adaxial to phloem (D), whereas xylem was surrounded by phloem in the midvein of the radialized organs of *pfl2-2 rev* double mutants (E). Floral meristems developed into functional flowers in *pfl2-2* (F). *rev* single mutants occasionally formed filamentous structures (arrow) (G). Floral meristem defects of *rev* single mutants were enhanced in *pfl2-2 rev* double mutants (H) where only filamentous structures (arrows) were developed. (Bars in A-B = 1cm, Bars in D-E = 0.5μm) (X = xylem, P = Phloem)

KAN genes have been demonstrated as the regulators signifying abaxialization [8, 10]. There are four gene members that belong to this family, *KAN1, KAN2, KAN3* and *KAN4.* A single mutation in *KAN1* only results in subtle leaf phenotypes, due mainly to the genetic redundancy [10]. However, *kan1 kan2* double mutants exhibit dramatic leaf defects including a reduction in leaf blade expansion, pointed leaves and ectopic abaxial outgrowths (Fig. 3-5A, C). The leaf defects of *kan1 kan2* double mutants were enhanced in *pfl2-2 kan1 kan2* triple mutants (Fig. 3-5B, D). Leaf blades of triple mutants were greatly reduced and lacked the ectopic abaxial outgrowths observed in the double mutants. Leaf blade growth has been proposed as a result of the juxtaposition of adaxial and abaxial domains [19]. Based on the synergistic interaction shown here, *RPS13* may also promote the determination of abaxial cell identity by *KAN* genes. The loss of its function leads to the complete disruption of the adaxial-abaxial boundary that in turn inhibits the formation of the outgrowths.

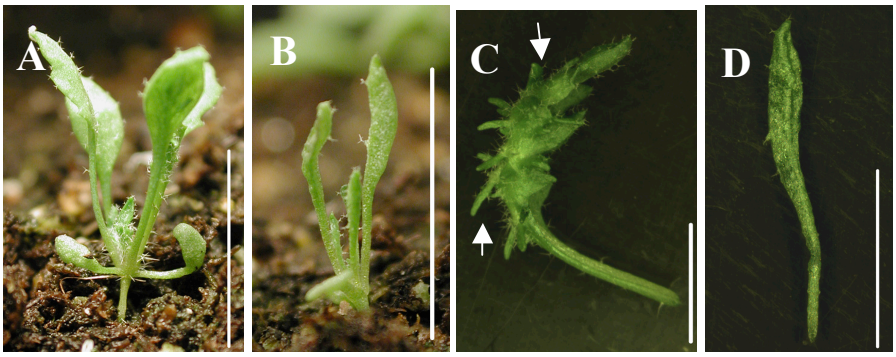

Fig. 3-5 Synergistic interaction between *pfl2-2* single and *kan1 kan2* double mutants. (A) *kan1 kan2* double mutants displayed narrow leaves with pointed tips and ectopic abaxial outgrowths on leaf 5 (C) (arrows). The leaf morphological defects of the double mutants were enhanced in *pfl2-2 kan1 kan2* triple mutants (B). Leaf 5 of *kan1 kan2* double mutants displayed numerous ectopic abaxial outgrowths (C), while the same leaf of *pfl2-2 kan1 kan2* triple mutants is extrememly narrow and did not form the abaxial outgrowths (D). (Bars in A-B = 1cm, Bars in C-D = 5mm)

Discussion

Ribosomes are composed of several components including various protein subunits and rRNA [2]. Although only one copy of each ribosomal protein is incorporated into the ribosome, plant ribosomal proteins are present in multi-gene families [3]. Each paralog of plant ribosomal protein families is actively expressed but may accumulate at different levels. For example, *RPS18A, RPS18B,* and *RPS18C* account for 27%, 16% and 57 % of the total pool of *RPS18* transcripts, respectively [18]. Furthermore, variations in phenotypes of the mutants of each paralog have been shown. *rpl23aA* knockdown mutants exhibited growth delay, leaf and root morphology defects as well as a reduction in the venation complexity [6]. Conversely, a knockdown of *RPL23aB* resulted in mutants with phenotypes relatively comparable to wild type [6]. Based on Arabidopsis genome database, two copies of the ribosomal protein RPS13 are present in the genome, At4g00100 and At3g60770 (http://www.arabidopsis.org). The two paralogs are different by one single amino acid. This difference may imply the two copies are spatiotemporally distinct or accumulate at different levels. Further detailed analysis and comparison of the two paralogs and their corresponding mutants will enable us to understand the biological significance of gene dublication in plant ribosomal protein genes.

The isolation of the T-DNA insertion in *pfl2-2* in this study suggests that *RPS13* is required for proper leaf morphological and anatomical structures. Recent studies have demonstrated leaf mutant phenotypes similar to *pfl2-2* are observed in other ribosomal protein mutants as well. These include *short valve (stv) 1, piggyback (pgy) 1,*and *asymmetric leaves1/2 enhancer (ae) 5* [13, 23]. *pgy1* and *ae5* mutants have been shown

to enhance leaf polarity defects in *as1, as2* and *rev* single mutants [13, 21, 23]. Additive effects are observed only in *pgy1 kan1 kan2* triple mutants, whereas *ae5 kan1 kan2* triple mutants display a synergistic interaction similar to what was observed in *pfl2-2 kan1 kan2* triple mutants [13, 23]. These results suggest the distinct degrees of contributions between different ribosomal proteins regarding leaf morphogenesis. Another question also still remained unanswered. Although required for the determination of both adaxial and abaxial identities, do ribosomal proteins function equally in the two domains? Abaxially and adaxially restricted expression of ribosomal proteins in their corresponding mutant backgrounds will help us to gain more insight in the roles of the translational machineries in leaf morphogenesis.

Materials and Methods

Plant materials and growth conditions

pfl2-2 mutant was originally derived from the Arabidopsis SAIL_747_B10 line. All Arabidopsis seedlings were germinated on Promix (Premier Horticulture Inc., Canada) under long-day conditions (16hr/8hr light/dark), 150 $\mu mol.m^{-2}.s^{-1}$, 22 ^{o}C.

To obtain *pfl2-2 as1-1* and *pfl2-2 as2-1* double mutants, *pfl2-2* was used as a maternal parent. When crossed to *as2-1, pfl2-2* was used as a paternal parent. The F2 individuals exhibiting phenotypes resembling *as1-1, as2-1* and *rev* single mutants were allowed to self-fertilize. Double mutants were recovered in the obtained F3 generation.

pfl2-2 kan1 kan2 triple mutants were created by crossing *pfl2-2* as a maternal parent to *kan1/kan1 KAN2/kan2* plants. F1 plants were self-fertilized to generate F2 population segregating for the triple mutant plants.

Chloral hydrate treatment

To examine the paradermal layers and the venation complexity, leaves were subject to chloral hydrate treatment. Briefly, leaves were fixed in ethanol/acetic acid mixture (6:1) at room temperature overnight. The mixture was removed and replaced with 100% ethanol for 30 minutes. Subsequently, leaves were incubated in 70% ethanol for 30 minutes and changed to chloral hydrate/glycerol/water mixture (8 g: 1 ml: 1 ml). After an overnight incubation, leaf samples were mounted on slides for visualization under the microscope.

IPCR analysis for T-DNA border regions

Genomic DNA of *pfl2-2* was extracted from the mutant leaves and used for iPCR analysis. Briefly, 10 μl digestion reaction was set up with 200 ng genomic DNA and *Nco*I Digested DNA was self-ligated for circularization by using 0.2 unit of T4-DNA ligase (NEB Biolabs) in a 40 μl reaction. Subsequently, 4 μl of circularlized DNA was used for the inverse PCR reaction with PAQ5000 polymerase (Stratagene) and IPFL2-L/ IPFL2-R. The sequences of the primers are listed in Appendix I. Amplified fragments were run on 0.8% Agarose gel and isolated by using Gel Extraction kits (QIAGEN). The fragments were sequenced and the obtained sequences were blast against whole genome Arabidopsis database.

Plasmid construction and complementation analysis

The 3.4 kb genomic fragment of At4g00100 encompassing the promoter, coding region and terminator was amplified from wild-type DNA with the PFL2-genF and PFL2-genR primers (Appendix I). The amplified fragment was cloned into pDONR221 by using Gateway BP recombinase enzyme (Invitrogen). To create the transformation construct, pDONR221::AROG was recombined with pMDC99 [5] by using LR recombinase enzyme (Invitrogen). The complementation construct was transformed into *Agrobacterium tumefaciens* stain GV3101 (pMP90) for Arabidopsis transformation with the floral-dip method. Seeds obtained from the transformed plants were germinated on the 1/2X MS medium containing 30 μg/ml hygromycin. Transgenic plants were subsequently transferred to soil for observation of the phenotypes.

References

1. Allen E, Xie Z, Gustafson AM, Carrington JC: microRNA-directed phasing during trans-acting siRNA biogenesis in plants. Cell 121: 207-21 (2005).
2. Bailey-Serres J: Cytoplasmic ribosomes of higher plants. In: Bailey-Serres J, Gallie DR (eds) A Look Beyond Transcription: Mechanisms Determining mRNA Stability and Translation in Plants., pp. 125-144. American Society of Plant Physiologists, Rockville (1998).
3. Barakat A, Szick-Miranda K, Chang IF, Guyot R, Blanc G, Cooke R, Delseny M, Bailey-Serres J: The organization of cytoplasmic ribosomal protein genes in the Arabidopsis genome. Plant Physiol 127: 398-415 (2001).
4. Byrne ME, Barley R, Curtis M, Arroyo JM, Dunham M, Hudson A, Martienssen RA: Asymmetric leaves1 mediates leaf patterning and stem cell function in Arabidopsis. Nature 408: 967-71 (2000).
5. Curtis MD, Grossniklaus U: A gateway cloning vector set for high-throughput functional analysis of genes in planta. Plant Physiol 133: 462-9 (2003).
6. Degenhardt RF, Bonham-Smith PC: Arabidopsis ribosomal proteins RPL23aA and RPL23aB are differentially targeted to the nucleolus and are desperately required for normal development. Plant Physiol 147: 128-42 (2008).
7. Emery JF, Floyd SK, Alvarez J, Eshed Y, Hawker NP, Izhaki A, Baum SF, Bowman JL: Radial patterning of Arabidopsis shoots by class III HD-ZIP and KANADI genes. Curr Biol 13: 1768-74 (2003).
8. Eshed Y, Izhaki A, Baum SF, Floyd SK, Bowman JL: Asymmetric leaf development and blade expansion in Arabidopsis are mediated by KANADI and YABBY activities. Development 131: 2997-3006 (2004).
9. Ito T, Kim GT, Shinozaki K: Disruption of an Arabidopsis cytoplasmic ribosomal protein S13-homologous gene by transposon-mediated mutagenesis causes aberrant growth and development. Plant J 22: 257-64 (2000).
10. Kerstetter RA, Bollman K, Taylor RA, Bomblies K, Poethig RS: KANADI regulates organ polarity in Arabidopsis. Nature 411: 706-9 (2001).
11. Lin WC, Shuai B, Springer PS: The Arabidopsis LATERAL ORGAN BOUNDARIES-domain gene ASYMMETRIC LEAVES2 functions in the repression of KNOX gene expression and in adaxial-abaxial patterning. Plant Cell 15: 2241-52 (2003).
12. Mallory AC, Reinhart BJ, Jones-Rhoades MW, Tang G, Zamore PD, Barton MK, Bartel DP: MicroRNA control of PHABULOSA in leaf development: importance of pairing to the microRNA 5' region. Embo J 23: 3356-64 (2004).
13. Pinon V, Etchells JP, Rossignol P, Collier SA, Arroyo JM, Martienssen RA, Byrne ME: Three PIGGYBACK genes that specifically influence leaf patterning encode ribosomal proteins. Development 135: 1315-24 (2008).
14. Prigge MJ, Otsuga D, Alonso JM, Ecker JR, Drews GN, Clark SE: Class III homeodomain-leucine zipper gene family members have overlapping, antagonistic, and distinct roles in Arabidopsis development. Plant Cell 17: 61-76 (2005).
15. Sessions A, Burke E, Presting G, Aux G, McElver J, Patton D, Dietrich B, Ho P, Bacwaden J, Ko C, Clarke JD, Cotton D, Bullis D, Snell J, Miguel T, Hutchison

D, Kimmerly B, Mitzel T, Katagiri F, Glazebrook J, Law M, Goff SA: A high-throughput Arabidopsis reverse genetics system. Plant Cell 14: 2985-94 (2002).
16. Talbert PB, Adler HT, Parks DW, Comai L: The REVOLUTA gene is necessary for apical meristem development and for limiting cell divisions in the leaves and stems of Arabidopsis thaliana. Development 121: 2723-35 (1995).
17. Van Lijsebettens M, Vanderhaeghen R, De Block M, Bauw G, Villarroel R, Van Montagu M: An S18 ribosomal protein gene copy at the Arabidopsis PFL locus affects plant development by its specific expression in meristems. Embo J 13: 3378-88 (1994).
18. Vanderhaeghen R, De Clercq R, Karimi M, Van Montagu M, Hilson P, Van Lijsebettens M: Leader sequence of a plant ribosomal protein gene with complementarity to the 18S rRNA triggers in vitro cap-independent translation. FEBS Lett 580: 2630-6 (2006).
19. Waites R, Hudson A: *phantastica*: a gene required for dorsoventrality of leaves in *Antirrhinum majus*. Development 121: 2143-2154 (1995).
20. Waites R, Selvadurai HR, Oliver IR, Hudson A: The PHANTASTICA gene encodes a MYB transcription factor involved in growth and dorsoventrality of lateral organs in Antirrhinum. Cell 93: 779-89 (1998).
21. Wenkel S, Emery J, Hou BH, Evans MM, Barton MK: A feedback regulatory module formed by LITTLE ZIPPER and HD-ZIPIII genes. Plant Cell 19: 3379-90 (2007).
22. Xu L, Xu Y, Dong A, Sun Y, Pi L, Huang H: Novel as1 and as2 defects in leaf adaxial-abaxial polarity reveal the requirement for ASYMMETRIC LEAVES1 and 2 and ERECTA functions in specifying leaf adaxial identity. Development 130: 4097-107 (2003).
23. Yao Y, Ling Q, Wang H, Huang H: Ribosomal proteins promote leaf adaxial identity. Development 135: 1325-34 (2008).

Chapter 4

Research Significance of the Dissertation

Leaf morphogenesis is a crucial process in plant growth and development and involves multiple regulatory determinants. Although various regulators controlling proper leaf dorsoventrality and leaf blade expansion have been identified, other aspects of leaf morphogenesis still await to be discovered. Unexpected involvement of plastids in leaf morphogenesis is underlined by the identification of *FLR/AtBT1* functions in leaf adaxialization and plastid adenine-nucleotide transport. *FLR*/*AtBT1* and other key regulators contribute to a regulatory network promoting leaf polarity establishment that has long been implicated in leaf blade expansion [1].

Characterization of *srr1-2* suggests a novel involvement of the circadian clock in leaf blade expansion. The genetic study of *srr1-2* also indicates that, although initiated by the formation of adaxial/abaxial domain boundaries [1], leaf blade expansion may be completed by a distinct set of regulators. Additionally, the genetic study of the translational machinery mutant *pfl2-2* reveals a potential contribution of the translational regulation in the two processes. Based on data present in this dissertation, a tentative model of the regulatory network involving *FLR, SRR1, RPS13* and other regulators is shown in Fig. 4-1.

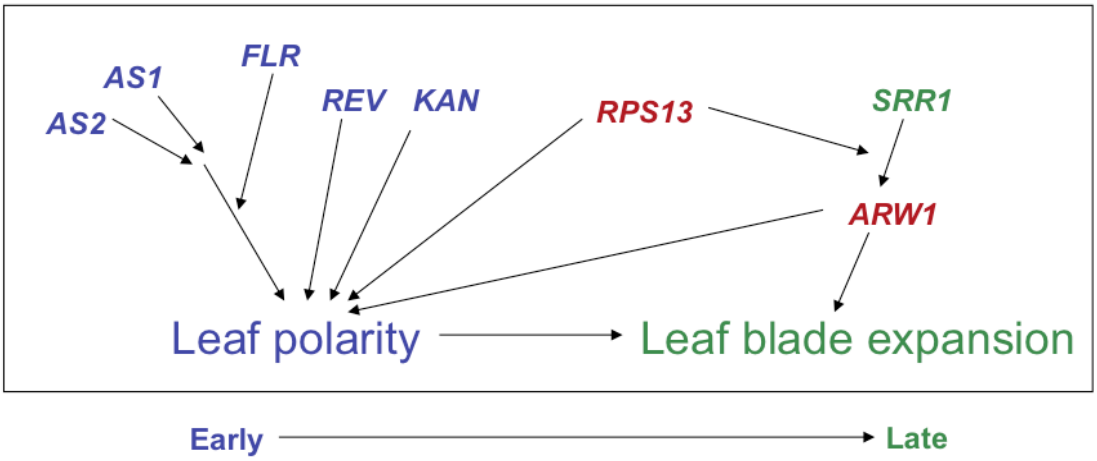

Fig. 4-1 A tentative model regarding *FLR/AtBT1*, *SRR1* and *RPS13* functions in leaf morphogenesis. *FLR* and other leaf polarity genes are involved in the determination of leaf polarity during the early stage of leaf development. The establishment of leaf polarity leads to the subsequent expansion of leaf blades. *SRR1* exerts its effect upstream of *ARW1* and contributes to the blade growth along the width axis. The translational machineries *RPS13* and *ARW1* are also implicated in both developmental processes. Blue indicates genes mainly involved in leaf polarity establishment during early development, while green designates the gene specifically contribute to subsequent leaf blade expansion. Red represents the genes that potentially play roles in the two developmental processes.

Reference

1. Waites R, Hudson A: *phantastica*: a gene required for dorsoventrality of leaves in *Antirrhinum majus*. Development 121: 2143-2154 (1995).

Appendices

Introduction

Appendix 1 includes all of the sequences of primers used in experiments described in this dissertation. The following appendix 2 is the manuscript that has been published in journal Plant Molecular Biology in February 2007. The manuscript describes the application of Integrase, phiC31 phage site-specific recombinase, for removal of the plastid selectable marker gene. As shown by DNA-blot analysis, the *aadA* gene, conferring spectinomysin resistance, was successfully excised from the plastid genomes by nuclear-encoded Integrase enzymes. This represents an alternative to the Cre/*lox* system in which fault recombination between introduced *loxP* and plastid pseudo-*lox* sites occurs.

Appendix 1

Table A1-1: Sequences primer used for qRT-PCR analysis

Gene	Primer	Sequence (5'-3')
At5g16560	KAN1-F	CGGTTTGTTCACGCTGTTGAGC
At5g16560	KAN1-R	TGAGCTCAAGAACCGACTTTGG
At1g32240	KAN2-F	GGTCTCTTTCATGGAGCTGTTTCC
At1g32240	KAN2-R	GATCTTCTTCTCTGCCATGTCG
At1g08465	YAB2-F	CATCTGAGCGTGTTTGCTATGTCC
At1g08465	YAB2-R	TGGTACAATGGCCACATCTCAC
At4g00180	YAB3-F	TACACTTTGGACTCATGGCTGACC
At4g00180	YAB3-R	CAGCTGAACCGTAAAACCCTTCTC
At2g33860	ARF3-F	GGTGGAGCCGGTGCCAGGAGA
At2g33860	ARF3-R	ACCCGTGCTGCTGCCGATGA
At5g60450	ARF4-F	GGCATGATTTCTGCAATGTGGTGTGG
At5g60450	ARF4-R	GGAGAAGAATCAGGCTGGCTCACAGAA
At2g37630	AS1-F	GCTGCGCCTCAACCGCCAATCC
At2g37630	AS1-R	TGCCCAAGCTCGGTGCCCTTCC
At1g65620	AS2-F	ACGAGCTTCACCCTTCACAACG
At1g65620	AS2-R	AGGCGCATGTCGGCTTCATAGG
At2g34710	PHB-F	AACCAGCACAGCGGGTGGAACG
At2g34710	PHB-R	TGGTAGTGGCGTGCTTTGTGCC
At1g30490	PHV-F	ACCGAATCAATACAAGGGGTGG
At1g30490	PHV-R	TGGAAGTGGTGTCCTCTGTGCC
At5g60690	REV-F	TGCAATGGCGATCTCACCGTCTGG
At5g60690	REV-R	ACCGAGTCGTCGCTTCCAAGTGAAT
At2g17950	WUS-F	CGCCATCATAACCGAGTTGG
At2g17950	WUS-R	AACCATAAGGCTCGTGAGCG
At2g27250	CLV3-F	AACCATAAGGCTCGTGAGCG
At2g27250	CLV3-R	GTGGGTTCACATGATGGTGC
At1g62360	STM-F	CATGAACTCTTGCTTGAGGC
At1g62360	STM-R	ACAAGCTGAGGATAGAGAGC
At4g08150	KNAT1-F	TAAAGAAGCACGGCAGAAGC
At4g08150	KNAT1-R	TTGATTCCGCCAACGCTACC
At1g70510	KNAT2-F	GGTCCAGCGTCTGCTACAGC
At1g70510	KNAT2-R	TCTTTGTTGGCTGTCATCCG
At3g18780	ACT2-F	GGATCGGTGGTTCCATTCTTGC
At3g18780	ACT2-R	TCATACTCGGCCTTGGAGATCC
At4g32400	FLR-F	GTTGCACCTGCTCGAGCCGTCG
At4g32400	FLR-R	AGCTTCTTCGATCTTCCTCC
At5g59560	SRR1-F	GTTTCTACTCAATGCAATGATTCC
At5g59560	SRR1-R	AGCTTCTTCGATCTTCCTCC
At5g61380	TOC1-F	AATAGTAATCCAGCGCAATTT TCTTC
At5g31380	TOC1-R	CTTCAATCTACTTTTCTTCGGTGCT

Table A1-1 (Continued): Sequences of primers used for qRT-PCR analysis

Gene	Primer	Sequence (5'-3')
At2g46830	CCA1-F	CAGCTCCAATATAACCGATCCAT
At2g46830	CCA1-R	CAATTCGACCCTCGTCAGACA
At1g01060	LHY-F	CAATGCAACTACTGATTCGTGGAA
At1g01060	LHY-R	GCTATACGACCCTCTTCGGAGAC
At1g22770	GI-F	ACTAGCAGTGGTCGACGGTTTATC
At1g22770	GI-R	GCTGGTAGACGACACTTCAATAGAT

Table A1-2: Sequences of primers used for plasmid construction

Gene	Primer	Sequence (5'-3')
At4g32400	FLR-genF	CACCAAGACCTCGGCTTTAACAAT
At4g32400	FLR-genR	TTATGCTGTAAACAGTGGCTA
At4g32400	FLR-promF	GGGGACAAGTTTGTACAAAAAAGCAGG CTGTTATGCTTCAGCTTGGTGC
At4g32400	FLR-promR	GGGGACCACTTTGTACAAGAAAGCTGGG TCCCCATGACCAATCGTCGAAC
At5g59560	SRR1-promF	GGGGACAAGTTTGTACAAAAAAGCAGG CTCAAAAGGCACGACGGTTTAGGC
At5g59560	SRR1-promR	GGGGACCACTTTGTACAAGAAAGCTGGG TCAGTCGTTTCCATTGAAGCTTCC
At4g00100	PFL2-genF	GGGGACAAGTTTGTACAAAAAAGCAGGC TCAGCTGCAGCATTTACTGC
At4g00100	PFL2-genR	GGGGACCACTTTGTACAAGAAAGCTGGG TATGAAGTTGCCGAGGAACGG

Table A1-3: Sequences of primers used for IPCR and genotyping of *pfl2-2*

Primer	Sequence (5'-3')
IPFL2-L	GCAAGAACGGAATGCGCGTGACC
IPFL2-R	AGTGAGCGAGGAAGCGGAAGAGCG
PFL2-R1	ATCACACCAATCTGGGAAGG
SAIL-LB	TTCATAACCAATCTCGATACAC

Appendix 2

Plastid marker gene excision by the phiC31 phage site-specific recombinase

Chokchai Kittiwongwattana[1], Kerry Lutz[1], Mark Clark[1] and Pal Maliga[1,*]

(1) Waksman Institute, Rutgers, The State University of New Jersey, 190 Frelinghuysen Road, Piscataway, NJ 08854-8020, USA

Abstract

Marker genes are essential for selective amplification of rare transformed plastid genome copies to obtain genetically stable transplastomic plants. However, the marker gene becomes dispensable when homoplastomic plants are obtained. Here we report excision of plastid marker genes by the phiC31 phage site-specific integrase (Int) that mediates recombination between bacterial (*attB*) and phage (*attP*) attachment sites. We tested marker gene excision in a two-step process. First we transformed the tobacco plastid genome with the pCK2 vector in which the spectinomycin resistance (*aadA*) marker gene is flanked with suitably oriented *attB* and *attP* sites. The transformed plastid genomes were stable in the absence of Int. We then transformed the nucleus with a gene encoding a plastid-targeted Int that led to efficient marker gene excision. The *aadA* marker free Nt-pCK2-Int plants were resistant to phosphinothricin herbicides since the pCK2 plastid vector also carried a bar herbicide resistance gene that, due to the choice of its promoter, causes a yellowish-golden (aurea) phenotype. Int-mediated marker excision reported here is an alternative to the currently used CRE/loxP plastid marker excision system and expands the repertoire of the tools available for the manipulation of the plastid genome.

Keywords: Nicotiana tabacum - phiC31 phage recombinase - Plastid marker excision - Plastid transformation

Abbreviations: *aadA* Gene encoding aminoglycoside 3″-adenylytransferase - *attB* Bacterial attachment site - *attP* Phage attachment site - bar Gene conferring resistance to the herbicide bialaphos - Cre P1 phage site-specific recombinases - Int Integrase or phiC31 phage site-specific recombinase - *int* Gene encoding Int - ptDNA Plastid genome - PP–*Bam*HI Fusion promoter containing the promoter of the plastid rrn operon and the plastid *clpP* gene - Prrn Promoter of the plastid *rrn* operon - *rrn* Plastid rRNA operon - TpsbA *psbA* gene 3′-UTR - *clpP, trnI, trnV, rrn16* and 3′-*rps12/7* Plastid genes

Contributions

Pal Maliga and Kerry Lutz wrote the manuscript. Kerry Lutz and Mark Clark constructed pPRV111A*att* and pPRV111B*att* plasmids. Chokchai Kittiwongwattana contributed to the construction of the pCK2 plasmid, plastid transformation, the confirmation of transplastomic plants with DNA-blot analysis, Agrobacterium co-cultivation, the investigation of Int-mediated marker gene excision, and antibiotic and herbicide resistance tests.

Introduction

Plastids are plant cellular organelles with a ~120–150-kb genome present in 1,000–10,000 copies per cell [2]. The plastid genome (ptDNA) has become an attractive alternative to nuclear gene transformation due to the obtainable high recombinant protein levels, the lack of pollen transmission of the transgene and the opportunity to express multiple genes in operons. Plastid transformation has been extensively used to probe plastid gene function, plastid transcription and mRNA editing. Exploratory research has shown that plastids are also suitable for biotechnological applications, including expression of genes that confer insect and herbicide resistance, and for the expression of recombinant proteins. Although plastid transformation has been achieved in many species, it is routine only in tobacco. For references see reviews in [3, 8, 24].

Plastid transformation vectors are *E. coli* plasmids that contain ptDNA flanking the marker gene and the gene of interest. The transforming DNA is introduced into plastids by the biolistic process, where it integrates into the ptDNA by homologous recombination via the flanking targeting sequences. Since ptDNA is present in many copies, selectable marker genes are critically important to achieve uniform transformation of all genome copies during an enrichment process that involves gradual sorting out of non-transformed plastids on a selective medium [24]. However, when all genome copies are transformed and a homoplastomic plant is obtained, the marker gene is no longer necessary. There are multiple reasons for post-transformation removal of plastid marker genes. First, a highly expressed marker gene may impose a metabolic burden on the plant. An example for a highly expressed marker gene is FLARE, which accumulates to 18% of the total soluble cellular protein [17]. Secondly, there are only two efficient

selective markers available for plastid transformation: resistance to the antibiotics spectinomycin [9, 27] and kanamycin [5, 14]. Thus, multiple engineering steps depend on removal of the marker gene before a new cycle of engineering may be initiated. Thirdly, the marker gene would not be acceptable in any commercial crop.

There are three approaches to obtain marker free transplastomic plants. The first system relies on deletion of marker genes by homologous recombination via direct repeats flanking the marker gene [15, 19]. The second approach utilizes transient cointegration vectors combined with visually aided complementation of knockout mutants [13, 18]. The third approach relies on marker excision by the Cre–*loxP* site-specific recombination system. According to this approach, *loxP* sites in the transformation vector flank the marker gene. The marker gene is stable in the absence of Cre. When excision of the marker gene is required, a plastid-targeted cre gene is expressed in the nucleus and the Cre protein is imported into chloroplasts where it excises the plastid marker gene [7, 12, 23]. Problems encountered with Cre-mediated marker excision were recombination of *loxP* sequences with fortuitous pseudo lox sites in the plastid genome [7], and enhanced homologous recombination adjacent to *loxP* sites that resulted in the loss of ptDNA segments between directly repeated sequences [6, 31]

Complex engineering requires the use of multiple site-specific recombinases that promote excision and integration of target sequences [26]. Thus far in higher plant plastids ptDNA manipulation was carried out with two phage recombinases. The Cre/*loxP* system derived from the P1 phage was shown to be useful for the excision of marker genes (see above). Int, the phiC31 phage integrase [29, 30], has been employed for the insertion of transforming DNA [22]. Here we report a different use of Int, efficient

excision of marker genes. Since the *attB* and *attP* sequences are not homologous, plastid genomes carrying *att*-flanked marker genes are predicted to be more stable than those with marker genes flanked by identical *loxP* sequences.

Materials and methods

Construction of the pCK2 plastid vector

The pPRV111A*att* (GenBank Accession no. EF416277) and pPRV111B*att* (GenBank Accession no. EF416276) excision vectors are pPRV100A and pPRV100B vector derivatives [32] in which the spectinomycin resistance (aadA) marker gene is flanked by 215 bp *attP* and 54 bp *attB* sites. Plasmid pCK2 is based on a progenitor of pPRV100Aatt that carries an herbicide resistance (*bar*) gene [23] expressed in a cassette with the PP-*Bam*HI promoter (a variant of the rRNA (*rrn*) operon PEP promoter and clpP-53 NEP promoter fusion described earlier (Kuroda and Maliga 2002)) and TrbcL, the plastid *rbcL* gene 3′ untranslated region. The DNA sequence of the PP-*Bam*HI promoter is deposited in GenBank (accession no. EF416278).

Plastid transformation and testing of resistance phenotype

Plastid transformation was carried out by the biolistic protocol, as previously described [21, 27]. Briefly, 1 μm gold particles were coated with pCK2 vector DNA for bombardment of sterile Nicotiana tabacum cv Petit Havana leaves with the PDS-1000 biolistic gun (Bio-Rad, Hercules, CA, USA). Transplastomic clones were selected by spectinomycin resistance manifested as formation of green shoots on RMOP medium containing 500 mg/l spectinomycin dihydrochloride. Leaf peaces from the shoots were transferred for a second cycle of shoot regeneration on a selective RMOP plant regeneration medium containing 500 mg/l spectinomycin dihydrochloride and 4 mg/l phosphinotricin. The shoots were rooted on RM plant maintenance medium in sterile culture. Transformation of the plastid genome was confirmed by DNA gel blot analysis

of total leaf DNA. The transplastomic plants are designated by the plasmid name, a serial number to identify independent transformation events, and letters identifying shoots derived from the same event. The number of letters indicates the number of regeneration cycles on selective medium.

To test the resistance phenotypes, leaves of greenhouse-grown plants were sterilized by rinsing in 70% ethanol, soaking in 10-fold diluted Clorox (0.5% sodium hypochloride) for 5 min and rinsing in sterile water three times. Small (5 mm × 5 mm) leaf pieces were cultured on RMOP medium containing no drugs, 500 mg/l spectinomycin dihydrochloride, 100 mg/l gentamycin or 4 mg/l phosphinothricin. Sensitive leaf pieces bleached whereas formation of green callus indicated resistance.

Transformation of the plant nucleus with the int gene

An integrase gene (*int*) engineered for expression in the plant nucleus in plasmid pKO117 is available in a binary plasmid in the EHA101 Agrobacterium strain [22]. To provide Int activity for marker gene excision, leaf pieces of the Nt-pCK2-30CA transplastomic plant were co-cultivated with Agrobacterium carrying binary plasmid pKO117 for two days, then transferred onto RMOP medium containing 100 mg/l gentamycin and 500 mg/l carbenicillin. On this medium shoots formed only if transformed with the aacC1 gentamycin resistance gene carried in the pKO117 plasmid as the plant marker linked to the *int* gene. Carbenicillin was provided to kill the Agrobacterium. For a more detailed protocol see [11]. Plants regenerated on the selective medium are designated as Nt-pCK2-Int and a serial number.

DNA gel blot analysis of ptDNA

DNA gel blot analysis was carried out as described [27]. Briefly, total leaf cellular DNA was digested with the appropriate restriction endonucleases. The DNA fragments were separated by electrophoresis in 0.8% agarose gels and transferred to Hybond-N membranes (GE Healthcare, Piscataway, NJ) using the PosiBlot Transfer apparatus (Stratagene, La Jolla, CA). Hybridization with the probes was carried out in Rapid Hybridization Buffer (GE Healthcare, Piscataway, NJ) overnight at 65°C. A double-stranded DNA probe was prepared by random-primed 32P-labeling. The templates for probing were prepared from the targeting region (*rrn16-I* probe, 2.0 kb *Apa*I–*Eco*RV fragment; rrn16-II probe, 1.0 kb *Apa*I–*Stu*I fragment), *aadA* (*Spe*I–*Spe*I fragment) and *bar* (*Nco*I–*Bgl*II fragment).

Results

Construction of transplastomic tobacco to test Int-mediated marker gene excision

We designed the experiment as a two-stage process. First we constructed transplastomic tester tobacco in which the marker gene is flanked with *attB* and *attP* sites. When the homoplastomic tester was obtained, we introduced Int into the chloroplasts to test excision of the marker gene. As part of the project, we constructed pPRV111Aatt and pPRV111Batt plastid transformation vectors (Fig. 1) where the spectinomycin resistance (*aadA*) genes are flanked by directly oriented non-identical phage *attP* (215 bp) and bacterial *attB* (54 bp) attachment sites targeting insertions in the *3'-rps12-trnV* intergenic region. To facilitate cloning, a multiple cloning site was inserted adjacent to the *aadA* gene cassette. The pCK2 plastid transformation vector derives from a progenitor of vector ppRV111A*att* in which a bar herbicide resistance gene is cloned divergent to the *aadA* gene (Fig. 2).

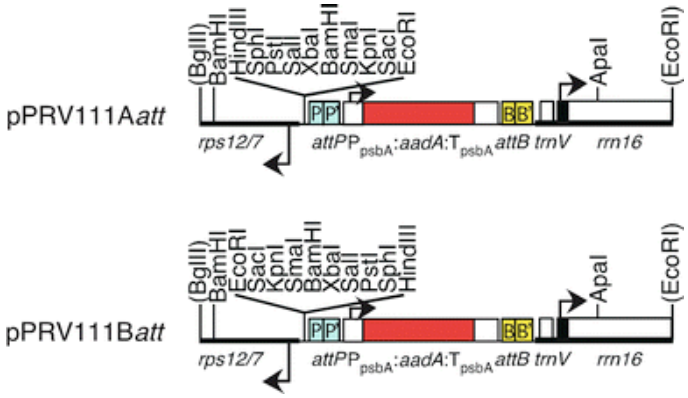

Fig. A2-1 Plastid vectors pPRV111A*att* and pPRV111B*att*. Plastid targeting regions (heavy lines) target insertions in the *rps12/7* and *trnV* intergenic region; *rrn16* is a plastid gene (Shinozaki et al. 1986). The spectinomycin resistance marker gene (*aadA*) expressed in the PpsbA and TpsbA cassette, the *attB* (BB′) and *attP* (PP′) sequences and multiple cloning sites are marked. Restriction sites in brackets have been removed during construction. Site of transcription initiation is marked with horizontal arrow

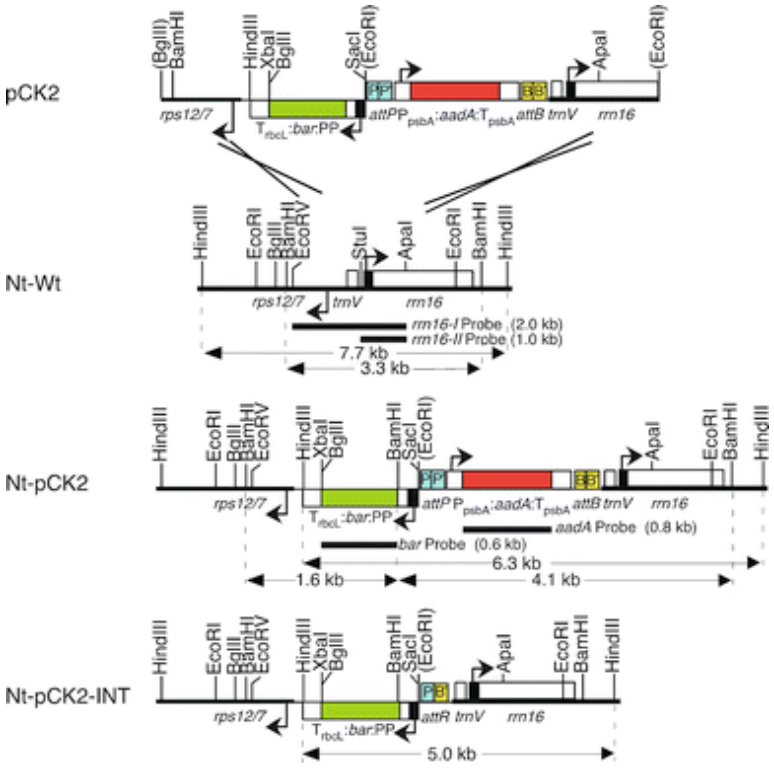

Fig. A2-2 Plastid DNA maps to show Int-mediated marker excision. Plastid targeting region of vector pCK2, the cognate wild-type ptDNA (Nt-Wt), the region of ptDNA transformed with vector pCK2 (Nt-pCK2) and its derivative with *aadA* excised (Nt-pCK2-Int) are shown. Position and size of DNA probes and fragment sizes are also shown. Note bar herbicide resistance gene adjacent to *aadA* flanked with *attB* (BB′) and *attP* (PP′) sites. For further details see caption to Fig. 1.

The pCK2 plasmid DNA was introduced into tobacco plastids by the biolistic process and transformed transplastomic plants were obtained by selection for spectinomycin resistance then by selection for both spectinomycin and phosphinothricin resistance. Uniform transformation of the plastid genomes was confirmed by DNA gel blot analysis and probing with the *rrn16-I* probe. This probe in *Bam*HI digested total leaf DNA detected only the transplastomic 4.1 kb and 1.6 kb fragments in lines Nt-pCK2-4BB, Nt-pCK2-4BC, Nt-pCK2-20AA, Nt-pCK2-30CA and Nt-pCK2-30CC instead of the 3.3 kb wild type fragment, indicating that these transformed plants are homoplastomic (Fig. 3A). Subsequent experiments were carried out with one transplastomic line, Nt-

pCK2-30CA, which will be referred to as the Nt-pCK2 line. The presence of the bar and *aadA* genes was also confirmed in the Nt-pCK2 line in *Hind*III digested leaf DNA that yielded a 6.3 kb fragment with the targeting sequence (*rrn16-II*), bar and *aadA* probes (lane CK2-30CA in the left of Fig. 3B). The homoplastomic Nt-pCK2 plants were used as testers for Int-mediated plastid marker excision.

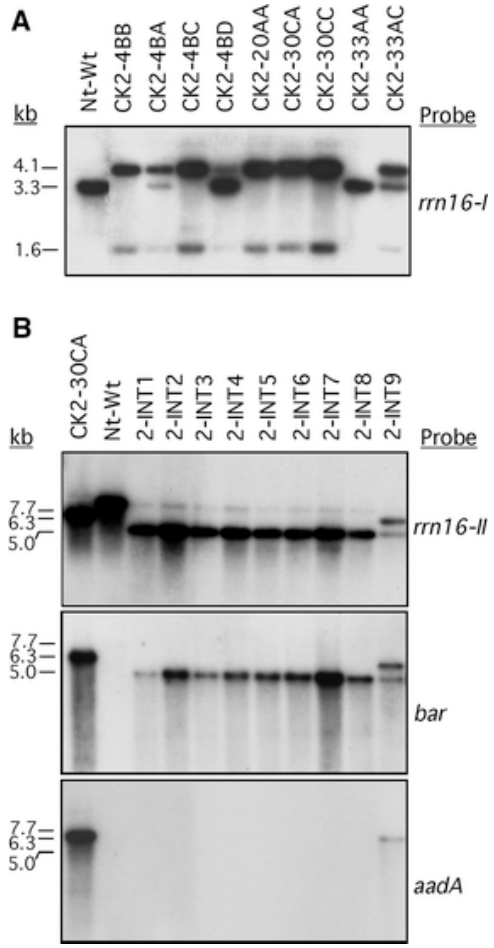

Fig. A2-3 DNA gel blot analyses to detect Int-mediated *aadA* excision in Nt-pCK2 plants. (A) Identification of homoplastomic Nt-pCK2 lines. The *Bam*HI-digested total cellular DNA was probed with a 2.0-kb *Eco*RV–*Apa*I targeting region (*rrn16-I*). (B) Verification of Int-mediated excision of *aadA* gene. *Hind*III-digested total cellular DNA was probed with 1.0-kb *Apa*I-*Stu*I targeting region (rrn16-II), 960-bp *aadA* coding region, and 600-bp bar coding region

Int mediated *aadA* gene excision

To test Int-mediated marker gene excision, Nt-pCK2 leaf pieces were cocultivated with Agrobacterium harboring pKO117, a binary nuclear transformation vector. Plasmid pKO117 encodes a plastid-targeted Int. Plastid targeting of Int is ensured by a translational fusion with the rubisco small subunit transit peptide [22]. Transgenic lines were selected for gentamycin resistance, the plant marker that is linked to the *int* gene in the binary vector. Altogether 32 independently transformed gentamycin resistant lines were obtained. The shoots were excised from the cocultivation plates, transferred to rooting medium, and immediately tested for *aadA* excision. Complete excision was obtained in 27 lines, indicated by hybridization to a 5 kb fragment with the rrn16-II and bar probes and the absence of a signal when probing with *aadA* (Fig. 3B). In three clones *aadA* excision was incomplete. An example in Fig. 3B is the Nt-pCK2-Int9 line, in which the unexcised 6.3 kb fragment is detected by all three probes, including *aadA*. Partial excision in the three lines is probably due to low level Int expression and testing excision relatively early after nuclear gene transformation. In the Int lines a weak □7.7 kb fragment is also visible above the 5.0 kb transgenic fragment with the rrn16-II targeting region probe. We believe that this signal derives from ptDNA integrated in the nucleus [1], since this fragment does not hybridize with the bar or *aadA* probes and no wild-type ptDNA is detected with the sensitive phenotypic assay (see below).

Phenotypes of the marker free plants

Wild type, Nt-pCK2 and *aadA*-free Nt-pCK2-Int plants have similar phenotypes in culture. However, when they are transferred to greenhouse, the rapidly growing young

leaves of Nt-pCK2 and *aadA*-free Nt-pCK2-Int plants have a distinct yellowish-golden (aurea) phenotype (Fig. 4A). Sectors with wild-type plastids, or with plastids lacking bar at this growth stage are readily recognized by their normal green color (data not shown). Leaves of older flowering Nt-pCK2 and Nt-pCK2-Int plants are normal green that is indistinguishable from the wild type (data not shown). A variant of the PP-*Bam*HI promoter that drives bar expression in the pCK2 construct has already been shown to cause a chlorotic phenotype due to interference with maturation of the intron-containing clpP1 mRNA [20]. The promoter used in this study is slightly different from the one earlier described: it contains a shorter *clpP* sequence and drives expression of bar and not the *neo* (kanamycin resistance) gene.

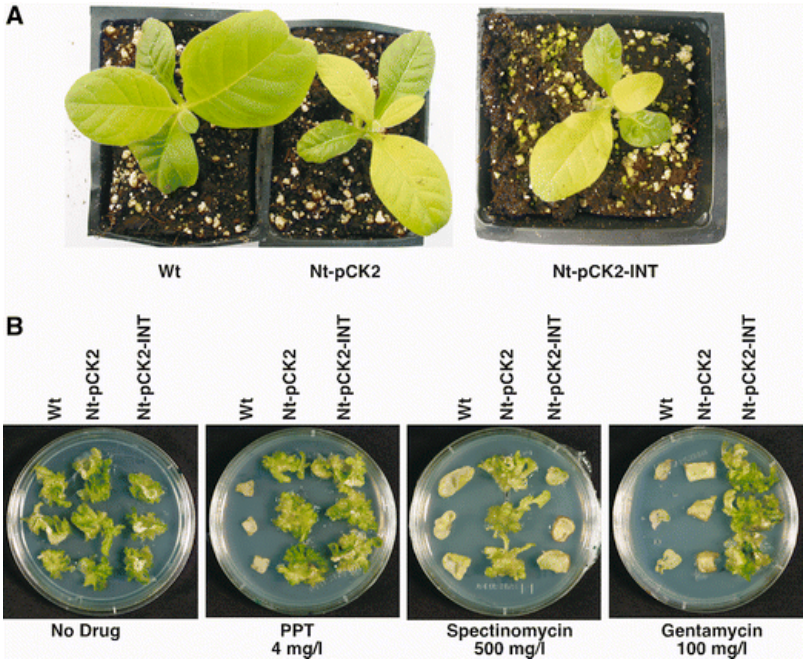

Fig. A2-4 Phenotypes of wild type, Nt-pCK2, and *aadA*-free Nt-pCK2-Int plants. (A) Young dark green wild type and aurea Nt-pCK2 and Nt-pCK2-Int22 plants in the greenhouse. (B) Testing of leaves for antibiotic resistance confirms excision of *aadA* gene in Nt-pCK2-Int22 plant. Note, that the Nt-pCK2-Int22 plant is resistant to gentamycin, the plant marker linked to *int*

Leaves of greenhouse grown wild type, Nt-pCK2 and Nt-pCK2-Int plants were tested for spectinomycin, phosphinothricin and gentamycin resistance. As expected, Nt-pCK2 leaves are resistant to spectinomycin and phosphinothricin due to expression of aadA and bar (Fig. 4B). Nt-pCK2-Int plants are resistant to phosphinothricin conferred by bar expression and to gentamycin due to expression of the plant marker in the Agrobacterium pKO117 binary vector, but sensitive to spectinomycin due to excision *aadA* by Int (Fig. 4B).

Discussion

We report here efficient excision of the *aadA* marker gene by the Streptomyces phage phiC31 integrase. Efficient excision is indicated by absence of the *aadA* target sequence in 27 out of the 32 lines transformed with the Int construct. The phiC31 integrase is the second site-specific recombinase after Cre that has been shown to excise plastid marker genes. There are several different prokaryotic site-specific recombinases used for engineering the nucleus of plants and animals [4, 10, 16, 26, 28], many of which may be adaptable for marker gene excision in plastids.

Testing Cre-mediated marker gene excision revealed fortuitous ptDNA sequences or pseudo lox sites in the plastid genome that are recognized by the Cre. As the consequence, when a *loxP* site is present, Cre mediates deletions between *loxP* and lox-rps12 or *loxP* and *lox-psbA* sequences [7]. In this study no deletions were found on DNA blots that would be indicative of recombination between *attP* or *attB* sequences and fortuitous ptDNA sequences that function as pseudo-*attP* or pseudo-*attB* sites. When Int was used for plastid transformation with a vector carrying an *attP* site, the vector always inserted into the bacterial *attB* sequence that was incorporated in the plastid genome [22]. Thus no fortuitous sequences appear to be present in the plastid genome that would be recognized by the Int.

A second problem observed during Cre-mediated marker excision was deletion of ptDNA sequences by recombination via directly repeated non-*loxP* sequences that resulted in the loss of the *trnV* gene [6, 12]. The observation was explained by enhanced homologous recombination of the native plastid recombination machinery in the presence

of Cre. Deletion of sequences via direct (and inverted) repeats adjacent to *loxP* sites has also been observed in Cre-expressing *E. coli* [25]. Deletions in plastids were dependent on the presence of direct repeats, such as the rRNA operon promoter (Prrn), adjacent to the *loxP* sites. By altering the vector design we could avoid deletions via repeated ptDNA sequences in the presence of Int. Although the pCK2 plasmid also carries duplicated Prrn sequences (as part of the PP promoter), these are now in an inverted orientation and apparently are not prone to deletion by the homologous recombination machinery in the presence of Int. However, when the Prrn promoters are in a direct orientation adjacent to *attB* and *attP* sites, Int also enhances homologous recombination via the Prrn repeats (data not shown). Thus, deletions detected in □40% of the clones in the presence of Cre [31] could also be avoided by omitting directly repeated ptDNA sequences adjacent to *loxP* sites.

Deletion of plastid marker genes by homologous recombination via relatively long, 200-bp to 400-bp direct repeats is one of the approaches to obtain marker-free plants [15, 19]. The frequency of deletion is proportionate with the length of the repeat. Although the *loxP* sequences are relatively short, 34 bp in length, we expect that they still may cause infrequent loss of the marker gene in the absence of Cre. Since the *attB* and *attP* sequences are not homologous, plastid genomes carrying *att*-flanked marker genes are predicted to be more stable than those with marker genes flanked by identical *loxP* sequences. The absence of homology between the *attB* and *attP* sites and the absence of pseudo-*att* sites in ptDNA make Int a preferred alternative to Cre for plastid marker excision.

Acknowledgements

This research was supported by the USDA Biotechnology Risk Assessment Research Grant Program Award No. 2005-33120-16524 to PM. Chokchai Kittiwongwattana is the recipient of a Ph.D. scholarship of the Thailand Commission on Higher Education. Mark Clark contributed to this project while supported by a Summer Undergraduate Research Fellowship.

Reference

1. Ayliffe MA, Timmi JN: Tobacco nuclear DNA contains long tracts of homology to chloroplast DNA. TAG Theoretical and Applied Genetics 85: 229-238 (1992).
2. Bendich AJ: Why do chloroplasts and mitochondria contain so many copies of their genome? Bioessays 6: 279-82 (1987).
3. Bock R: Plant biotechnology: resistance management, metabolic engineering and molecular farming. Current Opinion in Biotechnology (in press) 18: doi:10.1016/j.copbio.2006.12.001 (2007).
4. Branda CS, Dymecki SM: Talking about a revolution: The impact of site-specific recombinases on genetic analyses in mice. Dev Cell 6: 7-28 (2004).
5. Carrer H, Hockenberry TN, Svab Z, Maliga P: Kanamycin resistance as a selectable marker for plastid transformation in tobacco. Mol Gen Genet 241: 49-56 (1993).
6. Corneille S, Lutz K, Svab Z, Maliga P: Efficient elimination of selectable marker genes from the plastid genome by the Cre-*lox* site-specific recombination system. The Plant Journal 72: 171-178 (2001).
7. Corneille S, Lutz KA, Azhagiri AK, Maliga P: Identification of functional lox sites in the plastid genome. Plant J 35: 753-62 (2003).
8. Daniell H, Chebolu S, Kumar S, Singleton M, Falconer R: Chloroplast-derived vaccine antigens and other therapeutic proteins. Vaccine 23: 1779-83 (2005).
9. Goldschmidt-Clermont M: Transgenic expression of aminoglycoside adenine transferase in the chloroplast: a selectable marker of site-directed transformation of chlamydomonas. Nucleic Acids Res 19: 4083-9 (1991).
10. Groth AC, Calos MP: Phage integrases: biology and applications. J Mol Biol 335: 667-78 (2004).
11. Hajdukiewicz P, Svab Z, Maliga P: The small, versatile pPZP family of Agrobacterium binary vectors for plant transformation. Plant Mol Biol 25: 989-94 (1994).
12. Hajdukiewicz PT, Gilbertson L, Staub JM: Multiple pathways for Cre/lox-mediated recombination in plastids. Plant J 27: 161-70 (2001).
13. Herz S, Fussl M, Steiger S, Koop HU: Development of novel types of plastid transformation vectors and evaluation of factors controlling expression. Transgenic Res 14: 969-82 (2005).
14. Huang FC, Klaus SM, Herz S, Zou Z, Koop HU, Golds TJ: Efficient plastid transformation in tobacco using the aphA-6 gene and kanamycin selection. Mol Genet Genomics 268: 19-27 (2002).
15. Iamtham S, Day A: Removal of antibiotic resistance genes from transgenic tobacco plastids. Nat Biotechnol 18: 1172-6 (2000).
16. Keravala A, Groth AC, Jarrahian S, Thyagarajan B, Hoyt JJ, Kirby PJ, Calos MP: A diversity of serine phage integrases mediate site-specific recombination in mammalian cells. Mol Genet Genomics 276: 135-46 (2006).
17. Khan MS, Maliga P: Fluorescent antibiotic resistance marker for tracking plastid transformation in higher plants. Nat Biotechnol 17: 910-5 (1999).

18. Klaus SM, Huang FC, Golds TJ, Koop HU: Generation of marker-free plastid transformants using a transiently cointegrated selection gene. Nat Biotechnol 22: 225-9 (2004).
19. Kode V, Mudd EA, Iamtham S, Day A: Isolation of precise plastid deletion mutants by homology-based excision: a resource for site-directed mutagenesis, multi-gene changes and high-throughput plastid transformation. Plant J 46: 901-9 (2006).
20. Kuroda H, Maliga P: Overexpression of the clpP 5'-untranslated region in a chimeric context causes a mutant phenotype, suggesting competition for a clpP-specific RNA maturation factor in tobacco chloroplasts. Plant Physiol 129: 1600-6 (2002).
21. Lutz KA, Bosacchi MH, Maliga P: Plastid marker-gene excision by transiently expressed CRE recombinase. Plant J 45: 447-56 (2006).
22. Lutz KA, Corneille S, Azhagiri AK, Svab Z, Maliga P: A novel approach to plastid transformation utilizes the phiC31 phage integrase. Plant J 37: 906-13 (2004).
23. Lutz KA, Knapp JE, Maliga P: Expression of bar in the plastid genome confers herbicide resistance. Plant Physiol 125: 1585-90 (2001).
24. Maliga P: Plastid transformation in higher plants. Annu Rev Plant Biol 55: 289-313 (2004).
25. Mlynarova L, Libantova J, Vrba L, Nap JP: The promiscuity of heterospecific lox sites increases dramatically in the presence of palindromic DNA. Gene 296: 129-37 (2002).
26. Ow DW: Recombinase-directed plant transformation for the post-genomic era. Plant Mol Biol 48: 183-200 (2002).
27. Svab Z, Maliga P: High-frequency plastid transformation in tobacco by selection for a chimeric aadA gene. Proc Natl Acad Sci U S A 90: 913-7 (1993).
28. Thomson JG, Ow DW: Site-specific recombination systems for the genetic manipulation of eukaryotic genomes. Genesis 44: 465-76 (2006).
29. Thorpe HM, Smith MC: In vitro site-specific integration of bacteriophage DNA catalyzed by a recombinase of the resolvase/invertase family. Proc Natl Acad Sci U S A 95: 5505-10 (1998).
30. Thorpe HM, Wilson SE, Smith MC: Control of directionality in the site-specific recombination system of the Streptomyces phage phiC31. Mol Microbiol 38: 232-41 (2000).
31. Tungsuchat T, Kuroda H, Narangajavana J, Maliga P: Gene activation in plastids by the CRE site-specific recombinase. Plant Mol Biol 61: 711-8 (2006).
32. Zoubenko OV, Allison LA, Svab Z, Maliga P: Efficient targeting of foreign genes into the tobacco plastid genome. Nucleic Acids Res 22: 3819-24 (1994).

CURRICULUM VITAE for Chokchai Kittiwongwattana

Education

Rutgers, the State University of New Jersey, New Brunswick, NJ

2005-2010 Ph.D. in Plant Biology

Thesis Title: Arabidopsis Mutants Revealing Novel Aspects of Leaf Morphogenesis

Kasetsart University, Bangkok, Thailand

2003-2005 M.S. in Genetics

Thesis Title: Expression of a Transgene in Tobacco (*Nicotiana tabaccum* cv. Ottawa) using *AtExp4* Promoter

Kasetsart University, Bangkok, Thailand

1999-2003 B.S. in Biology (Genetics)

Publication

Chokchai Kittiwongwattana, Kerry Lutz, Mark Clark, Pal Maliga (2007), Plastid marker gene excision by the phiC31 phage site-specific recombinase. Plant Mol. Bio. 64: 137-43